Stochastic Resonance in Ferroelectric TGS Crystals

Dissertation

zur Erlangung des akademischen Grades
doctor rerum naturalium (Dr. rer. nat.)

vorgelegt der

Mathematisch-Naturwissenschaftlich-Technischen Fakultät
(mathematisch-naturwissenschaftlicher Bereich)
der Martin-Luther-Universität Halle-Wittenberg

von Konstantin Drozhdin
geb. am 12. Juli 1973 in Woronesh

Gutachter:

1. Prof. Dr. Beige
2. Prof. Dr. Trimper
3. Prof. Dr. Lauterborn

Halle, den 28.11.2001

urn:nbn:de:gbv:3-000003015
[http://nbn-resolving.de/urn/resolver.pl?urn=nbn%3Ade%3Agbv%3A3-000003015]

Table of Contents

List of Abbreviations and Symbols:

A	surface area
A_0	amplitude of periodic modulation
$\widetilde{A}_0 = \frac{A_0}{ax_m}$	scaled amplitude
a,b	parameters of double-well potential
AS	asymptotic
C_0	linear capacitance
C_F	ferroelectric capacitance
c_k	Fourier coefficient
d	sample thickness
D	noise intensity
D_m	noise intensity that maximises system response
$\widetilde{D} = \frac{D}{ax_m^2}$	scaled noise intensity
E	electric field strength
eq.	equation
f	frequency
$f(x) = -V'(x)/m$	scaled first derivative of the potential *V(x)*
g_n	expansion coefficient
$H(t)$	Heaviside step function
i	imaginary unit
k, m, n	indexes
$K_{xx}^{0}(t)$	correlation function

$L_0(t)$	unperturbed Fokker-Planck operator
$L_{ext}(t)$	Fokker-Planck operator of periodic perturbation
$L^*(t)$	adjoint Fokker-Planck operator
m	mass
M_n	complex valued amplitudes of the system response
p	probability density
$\{p_\mu\}$	Floquet modes
$\mathbf{P}$	polarisation
$P(X,t/Y,s)$	transition probability density
P	power
P_1	integrated power of the delta-like peak at the frequency $f=\Omega$
P_A	total power of the modulation signal in the absence of noise
P_n	integrated power of δ-peaks of the n-th frequency component
Q	electric charge
Q_F	electric charge of nonlinear capacitance C_F
r_K	Kramer's rate
R	ohmic resistance
$S(\omega)$	output spectral density
$S_N(\omega)$	spectral density of noise
SNR	signal-to-noise ratio
t, s, τ	time
t_0	initial time
$\tilde{t} = \frac{at}{\gamma}$	scaled time
T	period
T_K	period of Kramer's hopping
T_Ω	period of periodic modulation
TGS	triglycine sulfate
U_{C_0}	voltage drop over C_0
U_{C_F}	voltage drop over C_F
U_G	driving voltage (periodic modulation)
U_R	voltage drop over R

v	velocity
$V(x)$	double-well potential
$\Delta V(x)$	height of the potential barrier
$x(t)$	one-dimensional time-dependent coordinate
$x_0=x(t_0)$	initial condition
x_m	coordinate of the potential minima
$\bar{x}(D)$	periodic component of the system response
$\tilde{x}=\frac{x}{x_m}$	scaled variable x
$\delta x(t)$	system response within linear response approximation
$X(\omega)$	Fourier transform of $x(t)$
$X(t)$, $Y(s)$	state vectors
Z	impedance
$\chi(t)$	response function
$\chi(\omega)$	Fourier transform of $\chi(t)$
δ	delta-function
ϕ	phase shift
γ	viscous friction
η	spectral amplification
φ	phase
λ_n	eigenvalue of Fokker-Planck operator
μ	Floquet eigenvalue
Θ	temperature
$\Delta\Theta$	accuracy of temperature measurement
τ_{smpl}	sample rate
ω_0	angular frequency
ω_k, ω_n	discrete angular frequency
Ω	angular frequency of external periodic modulation
$\tilde{\Omega}=\frac{\gamma\Omega}{a}$	scaled angular frequency
$\xi(t)$	Gaussian white noise

Chapter One

Introduction

1.1 The Phenomenon of the Stochastic Resonance

For the last two decades the phenomenon of the stochastic resonance has undoubtedly served for a boom in nonlinear sciences. Since its introduction in the early 80s merely as a theoretical assumption in the modelling of the recurrence cycles of the Earth's ice ages, it has been attracting an increasing attention from diverse fields of science such as climatology, chemistry, biophysics and physiology, laser physics, solid-state physics, neuroscience, ferromagnetism, superconductivity and even social sciences, being successfully explored theoretically as well as experimentally.

The reason for this growing interest lies unquestionably in the unique nature of the phenomenon. It has been shown in numerous investigations that the action of noise, usually believed to be an unwelcome obstacle feature in most investigations, can nevertheless act as a positive element. In nonlinear systems the influence of noise can under certain conditions lead to the appearance of the ordered functioning regimes through the formation of regular signal structures, increase of coherence degree, signal-to-noise ratio enhancement, etc. therefore *improving* the overall system performance rather than hampering it.

The term "stochastic resonance" characterises new group of effects, whereby this rather paradoxical concept of the enhancement of the order degree of the system by means of random noise is realised [44].

As it is pointed out in [34], there are three following basic requirements for the onset of stochastic resonance, namely: a) a nonlinear system with energetic activation barrier or any

form of threshold, b) a weak coherent input signal and c) a source of random noise coupled to the coherent input or embedded in the system. The main characteristic property of the system demonstrating stochastic resonance behaviour is the increased sensitivity to even vanishingly small perturbations. Granted these features, the response of the system subjected to the feeble external coherent input signal and noise undergoes a resonance-like dependence as a function of noise intensity due to the establishment of global statistic synchronisation between the stochastic processes governed by noise and coherent input, which in its turn results in the maximum enhancement of the coherent component of the system response at some optimum noise level.

Owing to the principal generality of the above mentioned requirements, stochastic resonance might be thought of as a distinctive feature of nonlinear systems rather independent on their physical nature, whereby the characteristic system time scales can be controlled through the use of noise.

Over the last twenty years since its discovery, the effect of stochastic resonance has been studied in numerous theoretical and experimental investigations. After the appearance of the first publications by Benzi [1,2] and Nicolis [3], several theoretical approaches have been developed for the description of stochastic resonance in various dynamical regimes. Since the list of publications on stochastic resonance is exponentially growing, as it is reflected, for instance, in the permanently updated bibliography maintained in the database by Gammaitoni [54], it is scarcely possible to provide a complete digest of all latest areas of study and applications of the stochastic resonance. The core contributions to the understanding of the phenomenon have been made by McNamara and Wiesenfeld [5,7,34], Gammaitoni et al.[11,12,22,34], Jung and Hänggi [13,15,34] and others. The theoretical predictions have been supported by numerous digital [13,14,34] and analogue simulations [34,44], amongst others, the first successful demonstration of the stochastic resonance in Schmitt trigger circuit. Up to date stochastic resonance has been observed in a wide variety of experiments as well, including laser systems, semiconductors, ferromagnetic systems, neurophysiological living systems etc., and there seems to be no end in sight [54].

In spite of the impressing number of works devoted to the experimental investigation of stochastic resonance in divergent systems, the ferroelectrics as a class of materials have not yet been reported to provide the experimental evidence for this effect. Simple consideration of the general properties of ferroelectricity, as given briefly for example in [25], leads to the straightforward conclusion that ferroelectrics in fact may well serve as a bright example of the stochastic resonance phenomenon, owing, first of all, to their peculiar nature. As it is known, at the temperature below the Curie point, i.e., in ferroelectric phase, the ferroelectrics have two (or more) metastable states characterised by different direction of spontaneous polarisation, which are separated by a potential barrier. Being imposed simultaneously to the action of noise and weak (in general, periodic) external signal not sufficient to cause the reversal of polarisation, such a system obviously meets the above mentioned general conditions for stochastic resonance as a fundamental phenomenon, especially when taking

into account the extreme sensitivity of ferroelectric materials to the small perturbations in the vicinity of phase transition. Therefore the appearance of typical resonance-like behaviour of the system response on the noise intensity can be expected.

The idea of obtaining the experimental evidence of stochastic resonance in ferroelectrics is quite tempting. On one hand, the ferroelectrics such as TGS, chosen in the present work to conduct the investigations, claim to represent a comfort model system to study stochastic resonance due to several practical advantages. Apart from easy sample preparation, relative simplicity and convenience of experimental conditions (the existence of reversible spontaneous polarisation at ambient temperatures), which allow to avoid unnecessary measurement complications, profound experimental and theoretical knowledge of material properties has been gained since ferroelectric TGS has been long serving as a model material in the study of ferroelectrics.

On the other hand, despite numerous investigations in the successful history of ferroelectricity, there are various problems not likely to be solved in the framework of conventional theoretical and experimental methods, even when it comes to comparatively uncomplicated crystal structures, (just to mention a few, domain structure behaviour during polarisation reversal, phase transitions etc.). As a new effect for this class of materials, produced directly by alteration of ferroelectric domain structure, stochastic resonance represents a fresh and promising approach for the study of ferroelectrics.

1.2 The Purpose of the Study

Taking into account the above presented considerations, the first task of the present study is to establish experimentally the effect of stochastic resonance in ferroelectric TGS crystal. As a next step it should be proved whether the theoretical conceptions as developed in the framework of generic model for continuos bistable systems can be considered valid when realising stochastic resonance in actual experiment with ferroelectric TGS crystal. The theoretical predictions concerning general effect properties are to be checked experimentally. In order to do this, the stochastic resonance behaviour should be studied over the wide range of experimental parameters. To provide thorough characterisation of the stochastic resonance in ferroelectric TGS crystal, the plan presented below is followed in the course of study:

- ***Experimental set-up design.***

The measurement set-up which makes possible the experimental realisation of stochastic resonance in the course of investigations is described in Chapter 2. The experimental techniques are introduced together with the definition of actual stochastic resonance observables and ways of their estimation in the experiment.

- ***Presentation of theoretical conceptions for stochastic resonance.***

  In Chapter 3 the theoretical considerations concerning stochastic resonance are given. The effect basics and its main characteristics are introduced briefly on the basis of a generic two-state model. The accurate description of the effect applicable in general to the case of ferroelectrics is provided within the framework of the Floquet approach for continuos bistable systems after Jung and Hänggi [13] and Gammaitoni et al. [34]. Brief explanation of the main properties of ferroelectrics which are responsible for the onset of stochastic resonance is sketched in Section 3.

- ***Experimental study of stochastic resonance in ferroelectric TGS.***

  The experimental results obtained in the study of stochastic resonance in TGS crystal are presented in Chapter 4. The validity of theoretical predictions raised in the modelling of stochastic resonance behaviour in continuos bistable system is proved experimentally for the case of a ferroelectric TGS crystal serving as a system to observe the effect. The characterisation of stochastic resonance in actual experiment is provided over the wide range of measurement parameters such as frequency and amplitude of the external modulation signal and temperature of the ferroelectric sample. The specific features of stochastic resonance have been registered, which were not observed in other experimental systems.

Chapter Two

The Experimental Set-up

This chapter describes the nonlinear system used in the experimental study of stochastic resonance in ferroelectric TGS crystal.
First, the electric circuit serving as a core element of the experimental set-up is presented. As a next step the general principles of signal characterisation used in the investigation of the stochastic resonance are outlined. This is followed by the introduction of the stochastic resonance measures involved in the actual experiments and methods of their estimation. Finally the description of the measurement set-up developed for the study of the effect over the wide range of experimental parameters is provided specifying available measurement configurations and regimes.

2.1 The Electric Circuit

The electric circuit described below is configured to satisfy basic requirements of stochastic resonance under conditions of *real experiment*. Ferroelectric crystal chilled below Curie point possesses double-well potential that corresponds to the two metastable states with opposite polarisation direction. Since stochastic resonance is confirmed to be a *fundamental* phenomenon i.e. independent of the nature of the system where it is observed, when exposed to the sum of weak periodic modulation and noise, the presented experimental system should manifest corresponding output signal enhancement as a function of noise. On one hand, the proposed experimental set-up admits the possibility to verify experimentally the general theoretical predictions derived for stochastic resonance behaviour. On the other hand, because

the phenomenon of stochastic resonance in ferroelectric crystal is produced by the polarisation switching at the frequency of the weak periodic modulation established at an appropriate noise level, it provides the opportunity to investigate the behaviour of ferroelectric material within this complicated stochastic process as well as peculiarities of the stochastic resonance itself defined by the properties of ferroelectrics.

2.1.1 Experimental Realisation

The circuit involved in the course of measurement is a well-known Sawyer-Tower bridge which is usually used to register ferroelectric hysteresis. This circuit shown schematically on *Figure 2.1* includes following parts: non-linear ferroelectric capacitance C_F , linear capacitance C_0 and linear ohmic resistance R. The non-linear capacitance C_F is represented in our experiment by ferroelectric TGS crystal plate with electrodes. The ferroelectric axis of the crystal is oriented along the thickness and is normal to the electrode surfaces. Therefore the sample can be considered as bar-shaped condenser filled with ferroelectric dielectric material.

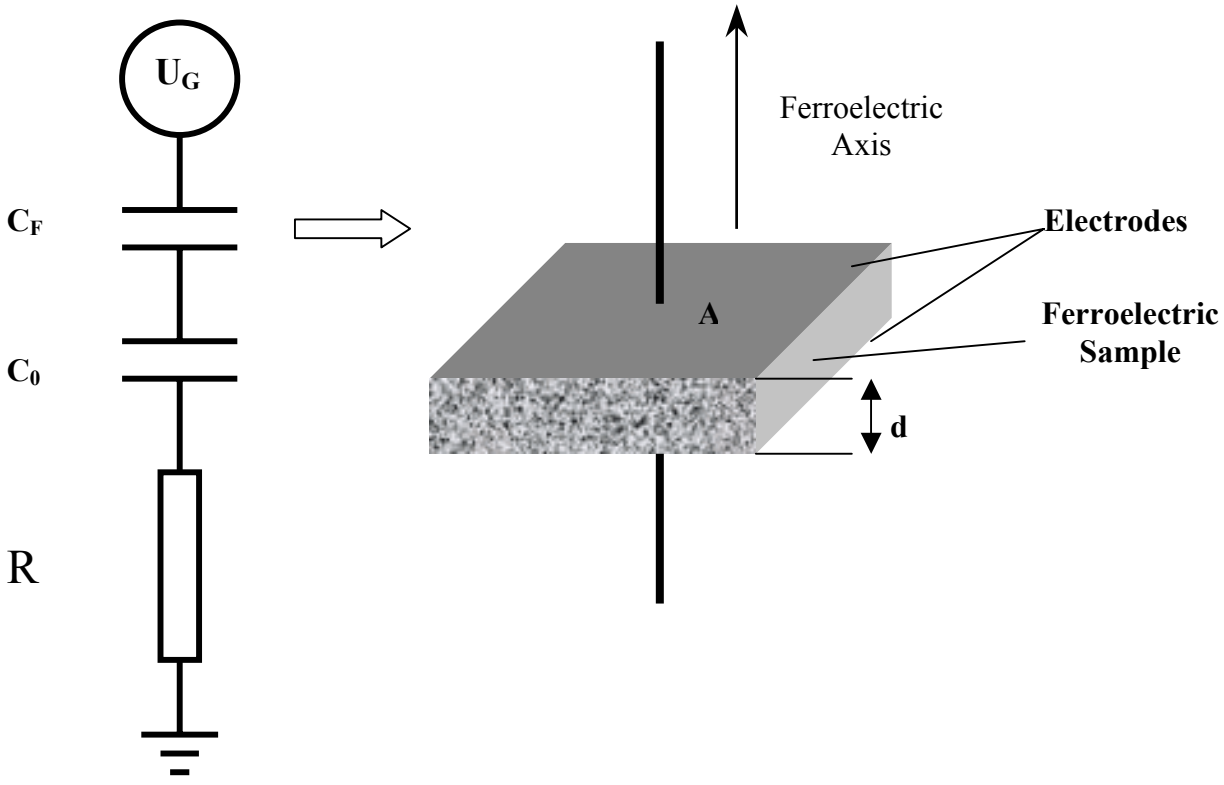

Figure 2.1 *Experimental circuit*

Applying the periodic voltage of appropriate amplitude to the circuit one produces polarisation switching of ferroelectric. This process can be registered by recording hysteresis loops which accompany repolarisation.
The voltage applied to the circuit is split into the sum of voltage drops over every circuit component and can be written as:

$$U_G = U_{C_F} + U_{C0} + U_R . \tag{2.1}$$

Choosing the capacitance C_0 much larger than C_F and thus maintaining the relation

$$R << \frac{1}{\omega_0 C_0} << \frac{1}{\omega_0 C_F} \tag{2.2}$$

assures that most of the driving voltage drops over the ferroelectric capacitance C_F. Because of the serial junction of capacitors C_0 and C_F the charges of both capacitors are equal $Q=Q_F$. Therefore the voltage drop over C_0 yields:

$$U_{C_F} C_F = U_{C_0} C_0 , \tag{2.3}$$

$$U_{C_0} = \frac{Q_F}{C_0} . \tag{2.4}$$

Since the polarisation of ferroelectric is defined as a charge per surface unit, i. e.:

$$\mathbf{P} = \frac{Q_F}{A} , \tag{2.5}$$

by registering the voltage over C_0 versus field strength, which is defined as

$$E = \frac{U_{C_F}}{d} , \tag{2.6}$$

where d stands for sample thickness, one retrieves well known hysteresis loop.

2.2 Methods of Signal Characterisation

In the investigations of stochastic resonance the behaviour of system output signal in the dependence of noise intensity is studied. Most of different experimental techniques are based on the measurements of power spectrum and time series of system output [13, 34]. Before the introduction of the stochastic resonance measures used in the course of investigations, the basic principles concerning signal characterisation in time and frequency range are outlined below.

The arbitrary signal can be represented as either function of time *x(t)* or frequency *X(ω)*. According to Fourier theorem, time-dependent signal *x(t)* can be represented in the following form:

$$x(t) = \frac{1}{2\pi} \int_{-\infty}^{\infty} X(\omega) \exp(i\omega t) d\omega , \tag{2.7}$$

where *X(ω)* is defined as follows

$$X(\omega) = \int_{-\infty}^{\infty} x(t) \exp(-i\omega t) dt . \tag{2.8}$$

Here *X(ω)* stands for so called Fourier transform of *x(t)* and according to definition (2.7), represents time evolution of signal *x(t)* in the form of superposition of oscillations *X(ω)exp(iωt)* over the wide frequency range. In general case the Fourier transform of real function *x(t)* is a complex function

$$X(\omega) = \left| X(\omega) \right| \exp(i\varphi) , \tag{2.9}$$

where $|X(\omega)|$ stands for the amplitude and φ for the phase of the signal with frequency ω. The representation of the amplitude and phase of the signal in dependence on the frequency is named *Fourier-spectrum* of the signal. If the square of the signal amplitude is registered, the spectrum becomes so called *power spectrum*.

If the signal under investigation is periodic in time, i.e. *x(t)=x(t+T)*, its Fourier transform reads

$$x(t) = \sum_{k=-\infty}^{\infty} c_k \exp(ik \frac{2\pi}{T} t) , \tag{2.10}$$

where c_k are corresponding Fourier coefficients defined as follows

$$c_k = \frac{1}{T}\int_0^T x(t)\exp(-ik\frac{2\pi}{T}t)dt\ . \qquad (2.11)$$

Therefore, the periodic signal with frequency $\omega=2\pi/T$ can be represented as a superposition of periodic signals with frequencies $\omega_k = 2\pi k/T$. The corresponding power spectrum consists of discrete δ-like peaks centred at frequencies ω_k.[1]

2.3 Stochastic Resonance Measures

Next the stochastic resonance observables measured in the experiments are introduced. The signal measured over capacitance C_0 is considered to be the output signal of the system. As it has been shown above the voltage drop over this linear capacitor is proportional to the polarisation of ferroelectric sample, therefore registering the power spectrum and time series of this signal provides the opportunity for direct observation of the processes taking place in the ferroelectric during the onset of stochastic resonance.

2.3.1 Spectral Amplification

The spectral amplification is one of the most prominent characteristics used to demonstrate the effect of the amplification of the periodic component of the output signal at the variation of the noise intensity at the system input. In the present work the spectral amplification is defined as a ratio between the power P_S stored the first harmonic measured at a given noise strength D and power P_0 of first harmonic measured in the absence of noise.

$$\eta = \frac{P_S}{P_0}\ . \qquad (2.12)$$

Here both P_S and P_0 are supposed to be measured in linear units (i.e., watts). In actual measurement the absolute peak values in power spectrum are first registered in logarithmic dBm scale and then evaluated according to the definition of absolute peak value given by the following relation (here and further on the indexes "*dBm*" and "*W*" correspond to the logarithmic and linear scale respectively):

[1] Note that in real system there's always some noise present, therefore power spectrum of periodic signal is presented by δ-peaks at frequency harmonics distributed over broadband noise.

$$P_{ABS}^{dBm} = 10lg\left(\frac{P_{ABS}^{W}}{1mW}\right). \qquad (2.13)$$

Since the measurements are performed at some given noise intensity added to the system input, there is always noise power contributions to the value of first harmonic peak of the power spectrum, which must be extracted to get the true value of the periodic component of the output power spectrum.

All of the estimates used are sketched on *Figure 2.2* for reader's convenience. Splitting the absolute peak value P_{S+N} of the first harmonic measured at some noise power P_N into the sum of the noise power and pure periodic component:

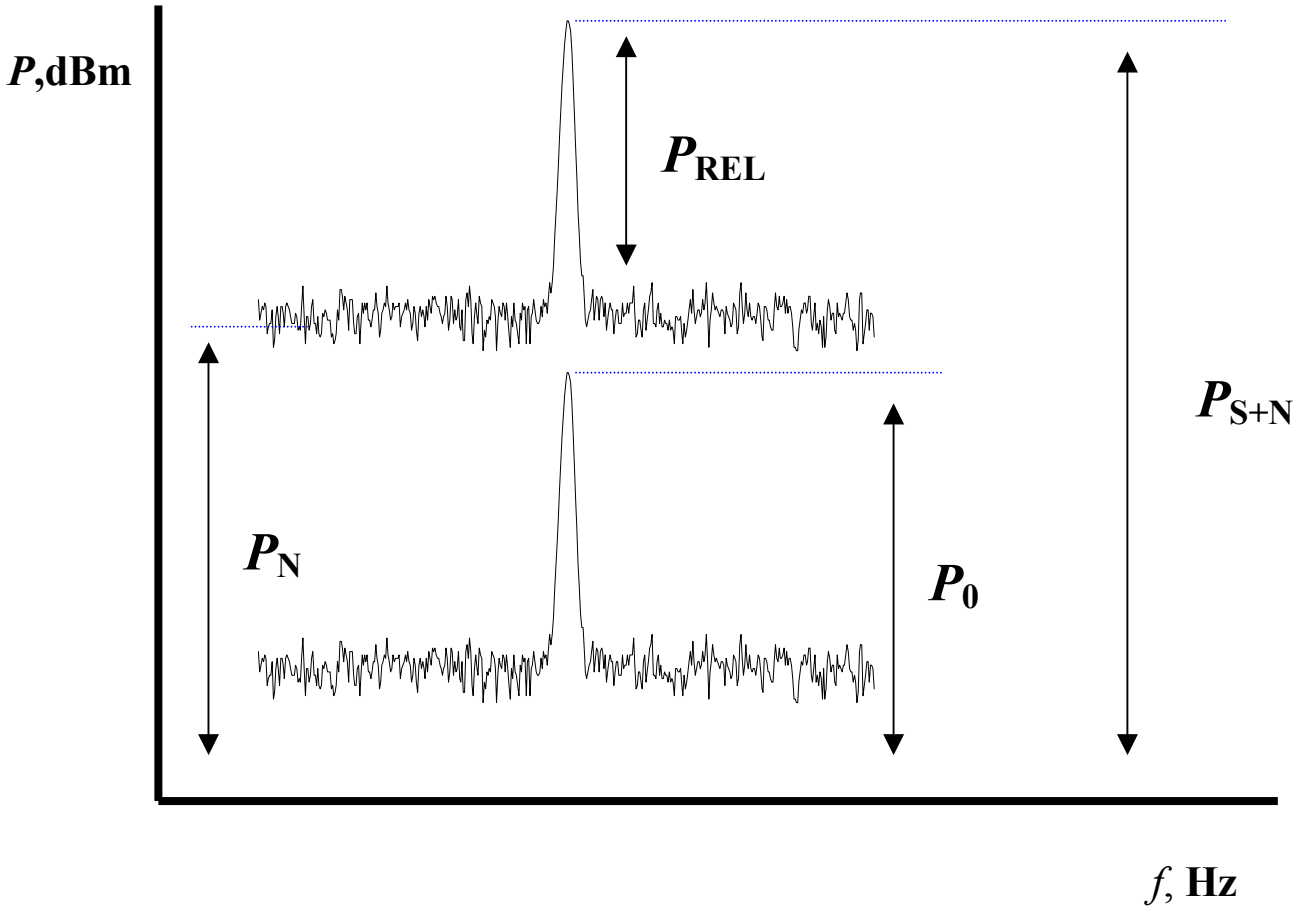

Figure 2.2 *Estimation of stochastic resonance measures from power spectrum*

$$P_{S+N}^{W} = P_{S}^{W} + P_{N}^{W}, \tag{2.14}$$

where noise power is calculated analogously to (2.13), i.e.,

$$P_{N}^{dBm} = 10lg\left(\frac{P_{N}^{W}}{1mW}\right), \tag{2.15}$$

the relative peak value P_{REL} is determined as follows (*see Figure 2.2*)

$$P_{REL}^{dBm} = P_{S+N}^{dBm} - P_{N}^{dBm} = 10lg\left(\frac{P_{S}^{W} + P_{N}^{W}}{P_{N}^{W}}\right). \tag{2.16}$$

Following some unsophisticated estimations the correction formula for the pure periodic signal power P_{S} can be extracted:

$$P_{S}^{W} = P_{S+N}^{W}\left(1 - 10^{-\frac{P_{REL}^{dBm}}{10}}\right). \tag{2.17}$$

Therefore, knowing the absolute value of first harmonic peak, noise power at a signal frequency and relative peak value one can estimate the corrected value of signal power and calculate the spectral amplification according to the formula (2.12).

2.3.2 Signal-to-Noise Ratio

Another frequently used characteristic of stochastic resonance is signal-to-noise ratio (SNR), which is an alternative measure of signal enhancement. Traditionally, this ratio is defined as a ratio between the power of periodic signal and the noise power at a signal frequency, i.e.

$$SNR = \frac{P_{S}^{W}}{P_{N}^{W}}. \tag{2.18}$$

In terms of power spectrum measured in dBm-scale, signal-to-noise ratio corresponds to the value of relative peak at a signal frequency, provided the total power of noise and signal $P_{\mathrm{S+N}}$, which is actually measured in experiment, is replaced by the corrected power of pure periodic signal P_{S}. It is worth to mention that since one has to deal with logarithmic dBm-scale, the difference of 20dB between first harmonic peak and noise background leads to the fact, that

power of periodic component exceeds that of the noise in 100 times. Therefore, if the periodic output is high enough, the estimated power of pure periodic signal differs from the total measured output power of noise and periodic signal in some vanishingly small percentage. Hence the corrections on noise power contribution may become practically neglectable and credible results can be reached by measuring directly the level of first harmonic peak and corresponding relative peak value to obtain the spectral amplification and signal-to-noise ratio values.

2.4 Experimental Set-up

The stochastic resonance behaviour in the proposed experimental system is undeniably governed by a number of experimental parameters. First of all, as the process of stochastic resonance onset is related directly to the polarisation switching of the sample included in the circuit, the choice of the ferroelectric material will affect the whole range of the appropriate measurement parameters. In this work the study of stochastic resonance is restricted to TGS crystals. It is known that the process of ferroelectric switching is a nonequilibrium process strongly influenced by the properties of the actual ferroelectric crystal under investigation, such as defects, their interaction with domain walls, etc., which are determined by the history of the crystal and its geometry. In this sense the choice of TGS crystal as a ferroelectric material to study stochastic resonance is quite evident, alone for two following reasons. Since the TGS crystal has been long serving the role of model ferroelectric in a number of various investigations, the volume of knowledge obtained for its different properties is rather sufficient and covers practically all thinkable parameters of the experiment and crystal itself over an impressing diversity of combinations. This “excessiveness” of experimental data is to some degree provoked by the fact that TGS is quite convenient (but nevertheless not simple!) ferroelectric material to explore, having one axis of polarisation and Curie point within the ambient temperature range.
Apart from the properties of the system determined by the ferroelectric sample and its geometry, the stochastic resonance behaviour is affected by the following experimental parameters provided by the electric circuit itself:

- Circuit parameters, such as capacitance C_0 and resistance R. While holding the relation (2.2) true during the course of investigations, these parameters may require adjustment as, for instance, the frequency of periodic driving signal is set to high or low values thus affecting the reactive resistance of both capacitors.

- Parameters of the external driving signal U_G, such as frequency, amplitude and form of oscillations.

- The temperature of the ferroelectric sample which determines the parameters of the ferroelectric sample such as spontaneous polarisation, dielectric permittivity, etc. by affecting the form and height of potential barrier separating two stationary states with the opposite polarisation directions (below Curie point). In the vicinity of the phase transition the ferroelectric material becomes extremely sensitive to even vanishingly small external perturbations. This sensitivity together with increasing nonlinearity of the ferroelectric may lead to the considerable changes in the system behaviour.

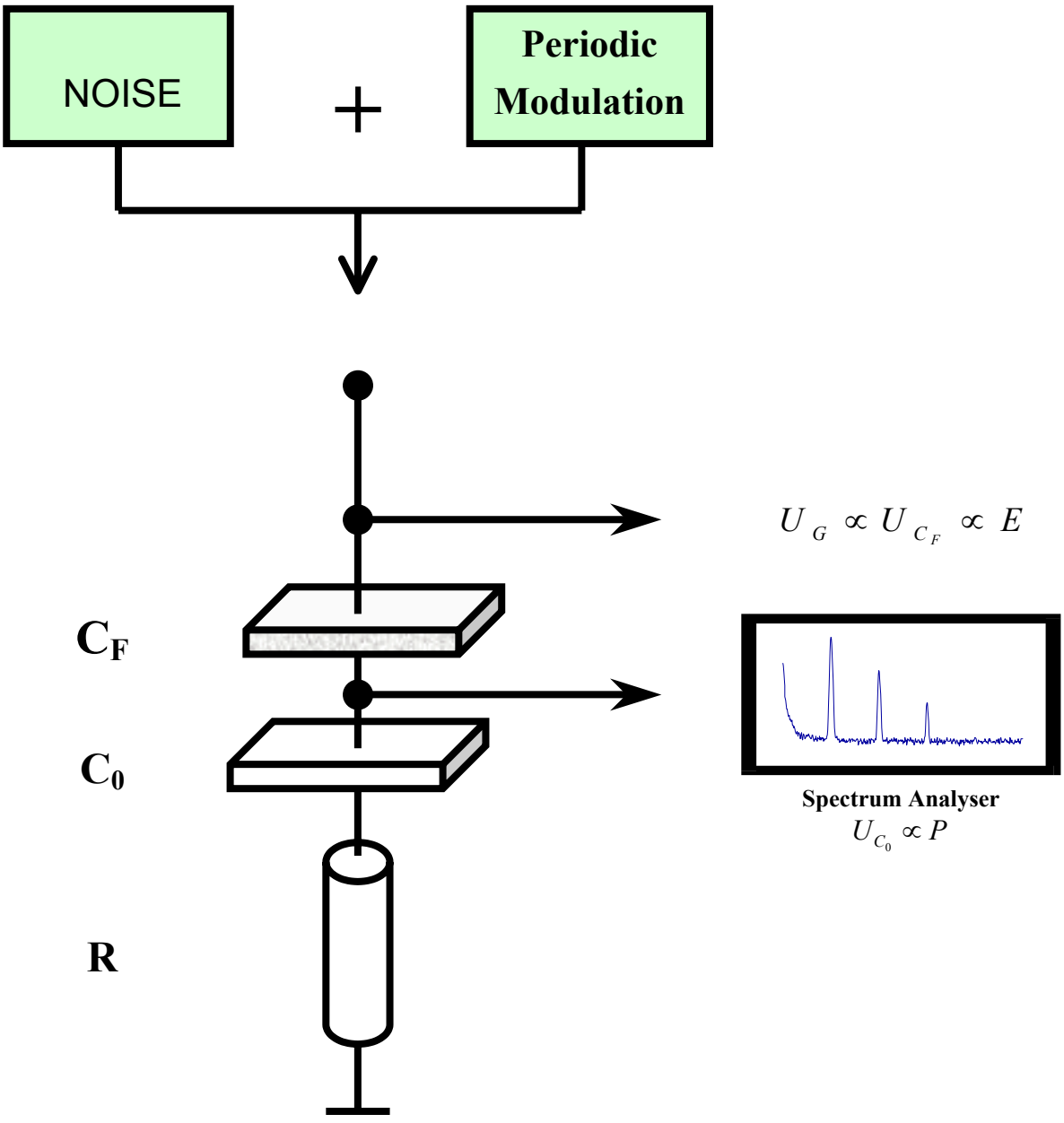

Figure 2.3 *Experimental plug-in*

Pondering on the above said speculations, it is straightforward that the experimental set-up should be constructed to so as to allow to perform measurements of stochastic resonance observables over most wide parameter range available, while keeping along high data acquisition reliability.

To extract the experimental data the Sawyer-Tower circuit driven by the sum of periodic signal and noise is linked via additional connection to the measurement circuit as shown on *Figure 2.3*. This connection allows to measure the voltage over ferroelectric capacitor C_F , which is proportional to the strength of the electric field E between the electrodes and the voltage over linear capacitor C_0 proportional to the instant value of polarisation of ferroelectric sample. The complete scheme of experimental set-up is presented on *Figure 2.4*. As it can be seen, the considerable flexibility is provided within the set-up design achieved through the implementation of two switch units HP3488A. Using this feature it is possible to perform various series of investigations which refer to different aspects of ferroelectricity. The set-up allows to conduct measurements on dielectric properties of ferroelectric sample, ferroelectric hysteresis, chaotic behaviour (by adding the coil and thus transforming the Sawyer-Tower bridge into nonlinear resonance RLC-circuit), etc. without rebuilding the set-up design, which enhances the reliability of the measurements.

The periodic driving signal is applied to the circuit from function generator HP3325B. Its features allow to vary with high accuracy the frequency of the output signal in the range from 1 μHz to 20.999 MHz and the amplitude from 0.3 mV_{RMS} to 3.5 V_{RMS} along with the form of carrier signal. The arbitrary function Generator HP33120A is used in the investigation of stochastic resonance as a source of broadband noise. With the amplitude of noise signal being variable from 6.09 mV_{RMS} to 1.217 V_{RMS}, it has a cut-off frequency of $f = 10\ MHz$ and therefore can be referred to as a white noise source since most of the frequencies used in the course of measurements lie below 100 kHz. After adding up the periodic driving signal and noise the summary input signal is amplified approximately by the factor of 10 with the amplifier. Due to very low internal impedance of $Z \approx 2Ohm$ of the amplifier, the amplitude of the driving signal is considered to be independent from current flow in the circuit. The input signal value is monitored by digital voltmeter RFT G-1006.500.

To characterise the output signal measured over the capacitance C_0 which is proportional to the polarisation of ferroelectric sample in terms of power spectrum over the wide frequency range, the Spectrum- and Network Analyser Wandel-Goltermann SNA-2 is used. The power and amplitude spectrum as well as the phase of the signal can be directly registered. To exclude possible input overload with signals of high amplitudes, two attenuators with damping factors of –20dB and –40 dB are provided.

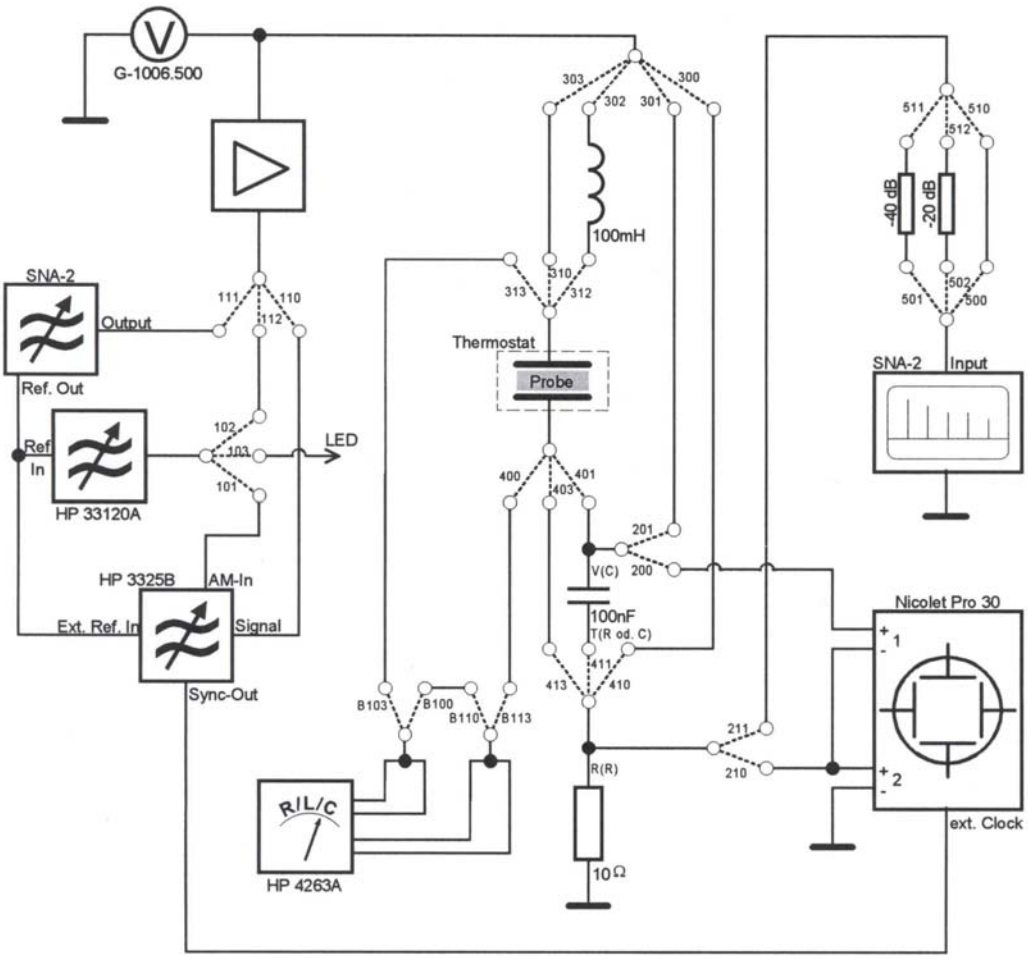

Figure 2.4 *Scheme of experimental set-up*

Simultaneously with power spectrum measurement, the time series reflecting the temporal evolution of the studied signal can be registered by two channel digital oscilloscope Nicolet Pro 30 with 12 Bit resolution and sample rate of $\tau_{smpl} \geq 100$ ns. Apart from time series observation it is possible to display directly the input signals of both channels versus each other thus providing for example, the opportunity to inspect hysteresis loops occurring during the repolarisation of ferroelectric. The possibility of averaging the input signals over many sampling cycles available as signal acquisition option becomes very useful in the investigations of stochastic resonance. It allows to perform *experimentally* the procedure of averaging of the output signal over the ensemble of noise realisations which, as it will be shown below, is core starting point in theoretical modelling [7,34,44,]. Since in the study of stochastic resonance one has to analyse by definition the statistical properties of the signal, the averaging, along with the high-and low-frequency filtering facilitates the extraction of

periodic component of the output signal and thus the registration of synchronisation phenomenon taking place during stochastic resonance. The LCR-meter HP 4263A which is plugged over the ferroelectric sample allows for quick characterisation of the dielectric properties of the material.

The ferroelectric sample is located in the thermostat. The measurement of the temperature is realised by registering the voltage over Ni-NiCr thermoelement with digital PREMA 4000 voltmeter. Correct scaling of the measured values is provided with the help of zero-point cell Zeref 1360. The regulation of temperature is achieved using the built-in heating line driven by the power source HP 6634A. The different regimes of temperature change as well as temperature stabilisation are accomplished with the help of software developed under LABWindows™ [46]. Stabilisation of the temperature, being of great importance especially for the measurements in the vicinity of the phase transition of the ferroelectric is provided with accuracy not less than $\Delta\Theta=0.01\ K$. Apart from temperature monitoring and regulation, the software package admits the possibility to control via IEC-Bus all the measurement equipment included in the experimental set-up. Due to flexibility of the program and set-up design, it is possible to perform complicated measurement regimes involving simultaneous use of different measurement devices at either continuous or discrete pre-set variation of external experimental parameters. Data acquisition features included in the software provide direct instant recording of the experimental measures followed by conversion procedures required for further data processing.

Chapter Three

Theoretical Description of Stochastic Resonance

In the current chapter the theoretical conceptions describing the phenomenon of stochastic resonance are presented. As it has been already mentioned in Introduction, stochastic resonance is a well established *fundamental* phenomenon occurring in nonlinear systems where characteristic time scales determining the system behaviour can be varied by means of noise. The basic requirements for the onset of this effect are general enough to expect the appearance of the typical resonance-like dependence of the system response on the noise intensity in a large diversity of systems in spite of their different physical nature and corresponding underlying mechanisms.

Therefore the accurate theoretical description of the general stochastic resonance properties provided for a particular class of systems yields relevant theoretical predictions which can be proved in *concrete* experimental realisation using the *universal* features of the system under investigation, responsible for the stochastic resonance behaviour. As it will be demonstrated below, such an approach is successfully applicable in the actual study of the effect in ferroelectrics although there is no special theory derivations developed particularly for this class of systems.

The chapter is structured as follows. First, to facilitate the understanding of the underlying physical principles of stochastic resonance and give some historical overview, the effect basics are introduced starting with the brief description of curious initial consideration of the

problem of Earth's periodic climate change, which originated the conception of stochastic resonance. Following the introduction of main characteristics of the effect, the theory of stochastic resonance for the class of continuos bistable systems is given in Sections 3.3 and 3.4. Most theoretical estimations and conclusions, including results of simulations are presented after the works of Jung and Hänggi [13], Gammaitoni et.al. [34] and V. Anishenko et. al. [44] where the stochastic resonance behaviour is modelled with Fokker-Planck equation. The theoretical results derived within this approach cover wide range of parameter variation and thus allow for a possibility to prove the obtained predictions in real experiment (see Chapter 4). In addition, the basic properties of ferroelectric TGS are presented. It is shown that due to the peculiarities of the material, the system with ferroelectric crystal as a core element meets the above outlined requirements for the onset of stochastic resonance and therefore qualifies at least qualitatively for an experimental study. Brief consideration of some possible distinctive features of the stochastic resonance in ferroelectrics, which are determined primarily by the nature of the material and may not be observed in other experimental systems is given as a concluding remark.

3.1 Effect Basics

The term „stochastic resonance" describes the group of effects observed in nonlinear systems, whereby the response of the system to the weak external signal is remarkably amplified by the increase of noise intensity in the system. As a result, integral system characteristics such as signal-to-noise ratio, spectral amplification, etc. undergo pronounced maximum as a function of noise intensity at some optimal noise level[2].

Originally this term was introduced independently by Benzi and co-workers[1,2] and Nicolis [3] in attempt to explain the peculiar phenomenon of periodic recurrence in Earth ice ages. It is known from the results of statistical analysis of continental ice volume variations over 10^6 years that the sequence of glaciation times has an average periodicity of approximately 10^5 years. The only comparable astronomical time scale of Earth dynamics known up to date is the modulation period of Earth's orbital eccentricity caused by planetary gravitational perturbations, which in their turn result in the variations of the solar energy influx, on the Earth's surface, so called solar constant. As these variations attain vanishingly small values of approximately 0.1%, the question arises if the climate sensitivity to such small external periodic perturbations can be amplified, which would lead to periodic climate change.

[2] Exact definition of stochastic resonance measures see below Section 3.2. Famous analogue simulation of the effect in Schmitt trigger circuit, [34] can serve here as a typical example. It has been proved that when the circuit is imposed simultaneously to the external noise source and weak periodic signal at the input, the signal-to-noise ratio at the trigger output first increases with the increase of the noise, then reaches the maximum and then decreases again. Thus periodic component of the output signal attains its maximum value at a certain noise intensity.

In the proposed model the global climate is characterised by the position of particle moving in double-well potential. The corresponding potential minima represent ice ages with low temperatures and normal climate cycles respectively. The potential is subject to small periodic forcing which reflects the modulations of the eccentricity of Earth orbit. Usual short-term climate fluctuations such as the annual variance of solar radiation are implemented through Gaussian white noise. As it has been proved by numerical simulations, by varying the noise intensity in such a system, the interplay of stochastic fluctuations and weak periodic modulation could result in synchronised switching between warm and cold climate thus leading to significant enhancement of the response of the Earth's climate to small perturbations caused by modulations of orbital eccentricity of the Earth [34].

For nearly a decade then the effect of stochastic resonance was left to oblivion, owing not at last to the principal difficulty of precise computations at the time. The renaissance it experiences ever since has eventually resulted in different theoretical approaches treating the problem. The concept of stochastic resonance has been extended to include various mechanisms. The theoretical description has been developed for excitable and threshold systems, quantum stochastic resonance, systems with deterministic chaos and many more.

Despite the vast diversity of systems exhibiting stochastic resonance behaviour, where stochastic resonance is undeniably governed by the forces of sometimes completely different nature, to grasp the idea of the onset of this intuitively contradictable phenomenon, the following principle picture of physical mechanisms that give rise to stochastic resonance will suffice. Qualitatively the effect basics could be explained in a consideration of the motion of over-damped particle in symmetric double-well potential subject to both noise source and periodic driving[3].

3.1.1 System with Double-well Potential

The motion of the over-damped particle in double-well potential coupled to the source of noise and periodic driving is described with the following simple equation:

$$\dot{x}(t) = -V'(x) + A_0 \cos(\Omega t + \varphi) + \xi(t)\,, \tag{3.1}$$

where $V(x)$ represents a double well potential given in the dimensionless form by

[3] Which is the initial model proposed by Benzi [1,2] in the consideration of periodical change of Earth's climate.

$$V(x) = -\frac{1}{2}x^2 + \frac{1}{4}x^4. \qquad (3.2)$$

The potential $V(x)$ is bistable with its minima located at $\pm x_m$, where $x_m = 1$, as shown on *Figure 3.1* which illustrates schematically the process responsible for the onset of stochastic resonance. The height of the potential barrier between the two minima is $\Delta V = \frac{1}{4}$.

The zero-mean Gaussian white noise $\xi(t)$ with intensity D is defined by its auto-correlation function

$$\langle \xi(t)\xi(0) \rangle = 2D\delta(t). \qquad (3.3)$$

In the absence of periodical driving the particle fluctuates around one of its local stable states. The probability for the particle to "hop" between the potential wells is defined through noise-dependent Kramer's rate

$$r_K = \frac{1}{\sqrt{2}\pi}\exp\left(-\frac{\Delta V}{D}\right). \qquad (3.4)$$

Weak periodic forcing of amplitude A_0, which alone is insufficient to make particle switching between the potential wells, leads to the periodic modulation of the potential and, consequently, to that of the probability for the particle to switch. The potential wells are tilted asymmetrically up and down thus periodically raising and lowering the potential barriers as it is shown on *Figure 3.1*. The noise-induced hopping can become then statistically synchronised with periodic driving. If the averaged waiting time between two interwell hopping events, which is given by

$$T_K(D) = \frac{1}{r_K} \qquad (3.5)$$

becomes comparable with the half of the period T_Ω of periodic driving, the system attains the maximum probability to switch, as the Kramer's rate is also varied with the same period, then the synchronisation takes place thus providing simple time scale matching condition for stochastic resonance:

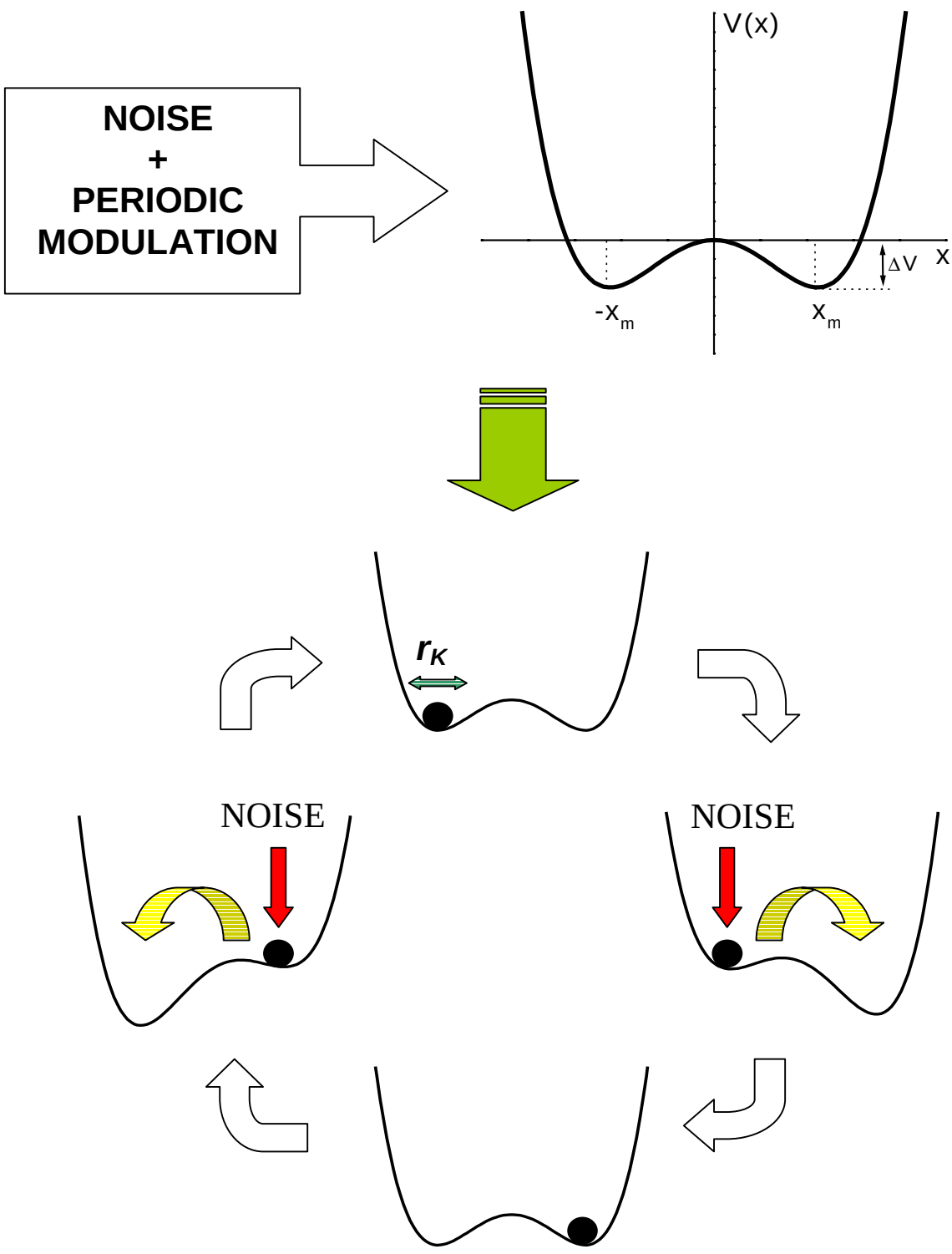

Figure 3.1 *Brief illustration of the stochastic resonance mechanism*

$$T_K = \frac{T_\Omega}{2} \tag{3.6}$$

In this sense, the phenomenon of stochastic resonance can be in general interpreted as a statistical *synchronisation* between noise-induced hopping events and weak periodic driving, achieved by the noise variation.

3.1.2 System Response

As a result of the synchronisation establishment, the periodic component of the system response gets amplified at some optimal noise level. To illustrate this behaviour mathematically the expression for time-dependent system response, (i.e., the solution of equation (3.1)) could be obtained by computing the mean value $\langle x(t) \rangle$. Averaging the stochastic process *x(t)* with initial conditions $x_0 = x(t_0)$ over the ensemble of noise realisations the mean value $\langle x(t) \,|\, x_0, t_0 \rangle$ is calculated, which in asymptotic limit $t_0 \to \infty$ becomes periodic function of time, i.e., $\langle x(t) \rangle_{AS} = \langle x(t + T_\Omega) \rangle_{AS}$ with $T_\Omega = 2\pi/\Omega$. For small amplitudes of the periodic modulation the system response can be written as follows:

$$\langle x(t) \rangle_{as} = \bar{x} \cos(\Omega t - \bar{\phi}), \tag{3.7}$$

where $\bar{x}$ represents noise-dependent amplitude of the periodic component of the system response and could be given by the following approximate expression:

$$\bar{x}(D) = \frac{A_0 \langle x^2 \rangle_0}{D} \frac{2 r_K}{\sqrt{4 r_K^2 + \Omega^2}} \ . \tag{3.8}$$

Here $\langle x^2 \rangle_0$ stands for *D*-dependent variance of the stationary unperturbed system at $A_0 = 0$. [5, 34]. *Figure 3.2* illustrates typical behaviour of the amplitude of the periodic component of the system response in dependence of noise intensity, obtained in our measurement. Two other dependencies, namely signal-to-noise ratio and spectral amplification are intended to provide an essential picture of the behaviour of these stochastic resonance characteristics introduced below in Section 3.2.

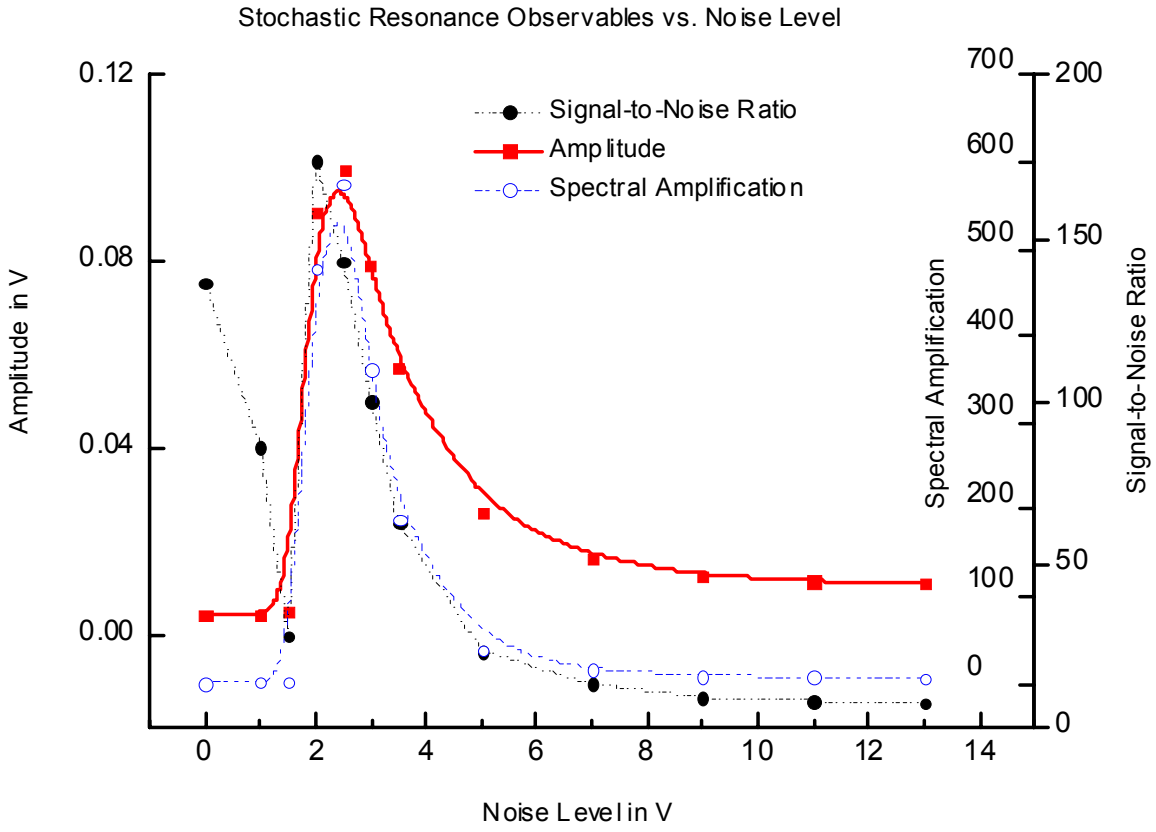

Figure 3.2 *Typical behaviour of the system response characteristics*

As it can be seen, the *periodic response* of the system subject to both weak periodic modulation and noise can be *manipulated* by varying the noise intensity at the system input, since the amplitude of the periodic component $\bar{x}$ depends non-monotonically on the noise strength D. At the increase of the noise the amplitude $\bar{x}$ first increases, reaches the maximum at some optimal noise intensity D_m and decreases again thus demonstrating classical *stochastic resonance effect*. In the view of the above presented physical picture of stochastic resonance as a phenomenon of the system output enhancement established through synchronisation of noise-induced hopping with periodic driving, the value D_m attains following physical meaning. The noise intensity D defines the probability for the system to switch from one potential well into another which is expressed by the noise dependent switching rate of the unperturbed system given by Kramer's rate r_K (see equation (3.4)). Starting with low noise intensity $D << D_m$ the switching events occur very rarely thus making the periodic component of the system output hardly visible since the system behaviour is bounded to the intrawell motion within one potential well.

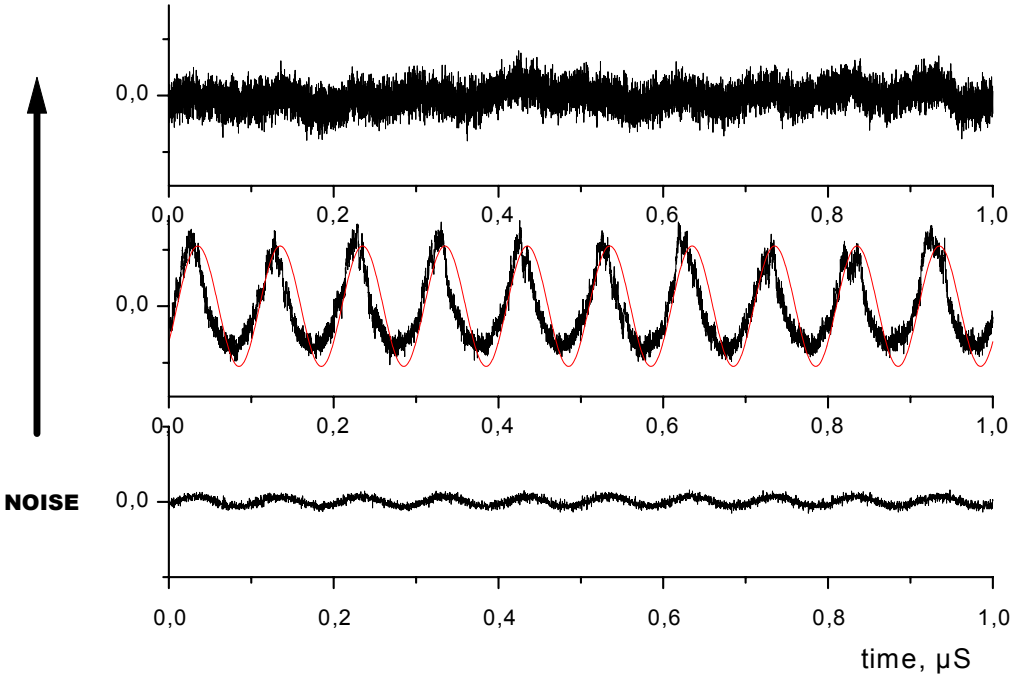

Figure 3.3. *Onset of synchronisation at the increase of the noise intensity*

As the noise is increased, the random switching rate can be tuned by $D = D_m$ so as to fulfil the time matching condition (3.6). At this point the synchronisation between noise induced switching and weak periodic modulation takes place as the probability for the system to switch reaches its maximum (and particle reaches the „best“ opportunity to switch during half period of modulation that tilts the potential). The output signal becomes tightly locked with the periodic input (See *Figure.3.3*). At the further increase of the noise the break of synchronisation sets in for the noise intensities $D >> D_m$, for the system manages to switch many times during each half of the period of the external modulation. This process is illustrated on *Figure 3.3*, where the time series of the output signal is shown for the increased value of the noise intensity *D*.

3.2 Stochastic Resonance Characteristics

Undoubtedly the choice of relevant quantifiers depends on the properties of the system under investigation. Since experimental studies of stochastic resonance cover rather wide range of systems of completely different nature from electronic circuits to neurophysiological applications, there are several distinct methods to characterise the effect. Detailed description of stochastic resonance characteristics used in real experiments and simulations can be found,

for instance, in [34]. We will restrict ourselves to the measures based on the power spectrum for reason of their relevance in relation to our investigations.

3.2.1 Spectral Amplification

According to [13] the spectral amplification is introduced on the basis of the amplitude of periodic component of the output signal as follows. The integrated power P_1 of the delta-like peak at an external modulation frequency $f=\pm\Omega$ of the output power spectrum is

$$P_1 = \pi\bar{x}^2(D). \tag{3.9}$$

The total power of the modulation signal in the absence of noise is

$$P_A = \pi A_0^2. \tag{3.10}$$

The spectral amplification is defined as a ratio between P_1 and P_A:

$$\eta = \frac{P_1}{P_A} = \left[\frac{\bar{x}^2(D)}{A_0}\right]^2. \tag{3.11}$$

3.2.2 Signal-to-Noise Ratio

As mentioned in introduction, stochastic resonance is manifested by an enhancement of weak periodic signals by means of noise. Therefore the study of this effect can be considered as a problem of weak signal extraction from broadband background noise. The corresponding measure widely adopted in radiophysics and electronics is called signal-to-noise ratio (SNR). Here we define the SNR after the papers [13,34] as follows. The output spectral density $S(\omega)$ of the system driven by noise and periodic modulation is represented by superposition of background noise spectral density $S_N(\omega)$ and a number of delta-like spikes centred at $\omega_n = (2n+1)\Omega$, with $n = 0,\pm1,\pm2...$. Considering only first harmonic, for small amplitudes of the external modulation signal the power spectral density of the system output can be separated into two terms, the periodic component with amplitude $\bar{x}(D)$ given by expression (3.8) and noisy background $S_N(\omega)$:

$$S(\omega) = \frac{\pi}{2}\bar{x}^2(D)\left[\delta(\omega-\Omega)+\delta(\omega+\Omega)\right] + S_N(\omega). \tag{3.12}$$

The signal-to-noise ratio measured at the frequency of the periodic modulation is defined by

$$SNR = 2\frac{\lim_{\Delta\omega\to 0}\int_{\Omega-\Delta\omega}^{\Omega+\Delta\omega} S(\omega)d\omega}{S_N(\Omega)}\ . \tag{3.13}$$

The factor 2 reflects the symmetry of power spectral density *S(ω) = S(-ω)*. Writing down the approximate power of background noise $S_N(\omega)$ for the double-well system with relaxation rate $2r_K$ in the form

$$S_N(\omega) = \frac{4r_K\langle x^2\rangle_0}{(4r_K^2+\omega^2)}\ , \tag{3.14}$$

one can obtain the signal-to-noise ratio using equation (3.8)

$$SNR = \pi r_K\left(\frac{A_0\langle x\rangle_0}{D}\right)^2\ . \tag{3.15}$$

According to the expressions for stochastic resonance observables obtained within this approximation, both of them display resonance-like behaviour as a functions of noise intensity. As it will be shown later, the behaviour of signal-to-noise ratio observed in real experiments diverges while developing also a local minimum at low noise levels and therefore expression (3.15) appeals for more detailed consideration. It should be pointed out that at the noise variation, the values of noise intensities that maximise spectral amplification and signal-to-noise ratio do not coincide.

3.3 Stochastic Resonance in Continuous Bistable System

The simplest consideration of stochastic resonance provided in Section 3.1 in the framework of two-state approximation while facilitating the understanding of the effect basics, does not though yield appropriate picture of all effect properties because the system dynamics is reduced only to the switching between two metastable states. The adequate description of the stochastic resonance features is provided within Fokker-Planck approach developed for wide class of continuous bistable systems.

3.3.1 Fokker-Planck Description

As a starting point the motion of overdamped Brownian particle of mass *m* and viscous friction γ in bistable potential *V(x)* is considered. The particle is subject to the source of Gaussian white noise $\xi(t)$ with zero average and autocorrelation function $\langle \xi(t)\xi(s) \rangle = D\delta(t-s)$ and intensity *D* at a temperature Θ and external periodic perturbation, which is characterised by an amplitude A_0 and frequency Ω. The initial phase of periodic forcing is assumed to be equally distributed between *0* and 2π. The system behaviour is described by the Langevin equation ([34]):

$$m\ddot{x} = -m\gamma\dot{x} - V'(x) + mA_0\cos(\Omega t + \varphi) + \sqrt{2\gamma D}\,m\xi(t). \tag{3.16}$$

The statistically equivalent description of this stochastic process is provided by the two-dimensional Fokker-Planck equation for corresponding probability density $p(x, v = \dot{x}, t; \varphi)$

$$\frac{\partial}{\partial t}p(x,v,t;\varphi) = \left\{ -\frac{\partial}{\partial x}v + \frac{\partial}{\partial v}\left[\gamma v + f(x) - A_0\cos(\Omega t + \varphi)\right] + \gamma D\frac{\partial^2}{\partial v^2} \right\} p(x,v,t;\varphi), \tag{3.17}$$

where $f(x) = -V'(x)/m$. Equation (3.16) can be simplified for the high values of friction coefficient γ (overdamped particle) by eliminating the velocity variable. For the system with bistable quartic double-well potential

$$V(x) = -\frac{a}{2}x^2 + \frac{b}{4}x^4 \tag{3.18}$$

with $a>0$, $b>0$, $f(x)$ reads as $f(x) = (ax - bx^3)/m$. Re-scaling the variables as follows

$$\tilde{x} = \frac{x}{x_m}, \qquad \tilde{t} = \frac{at}{\gamma}, \qquad \tilde{A}_0 = \frac{A_0}{ax_m}, \qquad \tilde{D} = \frac{D}{ax_m^2}, \qquad \tilde{\Omega} = \frac{\gamma\Omega}{a}, \tag{3.19}$$

where $\pm x_m = \sqrt{a/b}$ denotes the minima of $V(x)$, the Langevin equation can be written in the following form

$$\dot{x} = x - x^3 + A_0 \cos(\Omega t + \varphi) + \sqrt{2D}\xi(t). \tag{3.20}$$

Here and further on all caps are omitted for convenience. Corresponding Fokker-Planck equation for the probability density reads as follows

$$\frac{\partial}{\partial t} p(x,t;\varphi) = \left\{ -\frac{\partial}{\partial x}\left[x - x^3 + A_0 \cos(\Omega t + \varphi)\right] + D\frac{\partial^2}{\partial x^2}\right\} p(x,t;\varphi). \tag{3.21}$$

By introducing Fokker-Planck operators L_0 in the form of

$$L_0 = -\frac{\partial}{\partial x}(x - x^3) + D\frac{\partial^2}{\partial x^2}, \tag{3.22}$$

which describes the unperturbed dynamics in the re-scaled double well potential $V(x) = -x^2/2 + x^4/4$ with barrier height $\Delta V = \frac{1}{4}$ and L_{ext} as

$$L_{ext}(t) = -A_0 \cos(\Omega t + \varphi)\frac{\partial}{\partial x} \tag{3.23}$$

for periodic perturbation, the Fokker-Planck equation can be re-written in the operator form

$$\frac{\partial}{\partial t} p(x,t,\varphi) = L(t)\,p(x,t,\varphi) \equiv \left[L_0 + L_{ext}(t)\right] p(x,t,\varphi). \tag{3.24}$$

This equation has a periodic drift term in time with the period $T_\Omega = 2\pi/\Omega$. The Fokker-Planck operator in equation (3.24) is invariant for discrete time transitions $t \to t+T_\Omega$, yielding $L(t) = L(t+T_\Omega)$.

3.3.2 Floquet Approach

Applying Floquet theorem [34,44], the solutions of the equations (3.21), (3.24) can be found in form of so-called Floquet solutions, as functions of the following type

$$p(X,t,\varphi) = \exp(-\mu t)\, p_{\mu}(X,t,\varphi)\,, \tag{3.25}$$

where *X(t)* defines the state vector in multidimensional space *X(t)*=**(** $x(t);\dot{x}(t);...$ **)**, μ is Floquet eigenvalue and p_{μ} are the periodic Floquet modes

$$p_{\mu}(X,t;\varphi) = p_{\mu}(X,t+T_{\Omega};\varphi)\,. \tag{3.26}$$

The periodic Floquet modes $\{p_{\mu}\}$ are the eigenfunctions of the Floquet operator

$$\left[L(t) - \frac{\partial}{\partial t}\right] p_{\mu}(X,t;\varphi) = -\mu p_{\mu}(X,t;\varphi)\,. \tag{3.27}$$

Introducing the Floquet modes of the adjoint operator $L^{*}(t)$

$$\left[L^{*}(t) - \frac{\partial}{\partial t}\right] p^{*}_{\mu}(X,t;\varphi) = -\mu p^{*}_{\mu}(X,t;\varphi)\,, \tag{3.28}$$

where the sets $\{p_{\mu}\}$ and $\{p^{*}_{\mu}\}$ are bi-orthogonal and fulfil the following normalisation condition

$$\frac{1}{T_{\Omega}} \int_{0}^{T_{\Omega}} dt \int dX p_{\mu_n}(X,t;\varphi)\, p^{*}_{\mu_m}(X,t;\varphi) = \delta_{n,m}\,, \tag{3.29}$$

one can yield spectral representation of the equations (3.27), (3.28) for the time inhomogeneous transition probability P*(X, t | Y, s)* density, which for $t>s$ can be written as follows

$$\mathrm{P}(X,t \mid Y,s) = \sum_{n=0}^{\infty} p_{\mu_n}(X,t;\varphi)\, p^{*}_{\mu_m}(Y,s;\varphi) \exp[-\mu_n (t-s)] = \mathrm{P}(X,t+T_{\Omega} \mid Y,s+T_{\Omega})\,. \tag{3.30}$$

For large times $\tau = t - s$, $s \to -\infty$ probability P*(X, t|Y, s)* approaches unique asymptotic periodic solution $p_{as}(X,t;\varphi)$ (see eq.(3.25)) of equation (3.21):

$$p_{as}(X,t;\varphi) = p_{\mu=0}(X,t;\varphi), \tag{3.31}$$

which can be expanded into Fourier series, i.e.:

$$p_{as}(X,t;\varphi) = \sum_{m=-\infty}^{\infty} a_m(X) \exp[im(\Omega t + \varphi)]. \tag{3.32}$$

At the next step the corresponding averaged mean values $\langle X(t) \rangle_{as}$ can be evaluated, which are also periodic in time and therefore allow for the representation in the form of Fourier series:

$$\langle X(t) \rangle_{as} = \sum_{n=-\infty}^{\infty} M_n \exp[in(\Omega t + \varphi)]. \tag{3.33}$$

The last expression presents one of the main conclusions of the Floquet theory for the motion of the periodically perturbed Brownian motion. The amplitude of the periodic component of the system response is expressed as a sum of complex-valued amplitudes $M_n \equiv M_n(\Omega, A_0)$, which are nonlinear functions of the modulation amplitude A_0, modulation frequency Ω and the noise intensity.

3.3.3 Expressions for Stochastic Resonance Characteristics

For the purposes of quantitative analysis both measures of stochastic resonance as introduced in Section 3.2 can be expressed using the above mentioned amplitudes of periodic response.

3.3.3.1 Expression for Spectral Amplification

The integrated power of δ-peaks of the *n-th* frequency component of the output spectral density can be expressed in terms of $|M_n|$ ([34]):

$$P_n = 4\pi |M_n|^2. \tag{3.34}$$

If the total power contained in the modulation signal at the system input is given by

$$P_A = \pi A_0^2 , \tag{3.35}$$

then the spectral amplification η at the input signal frequency $\omega = \Omega$ can be written as follows:

$$\eta(A_0, \Omega) = \frac{P_1}{P_A} = 4\left(\frac{|M_1|}{A_0} \right)^2 . \tag{3.36}$$

3.3.3.2 Expression for Signal-to-Noise Ratio

Another characteristic of stochastic resonance frequently used in theoretical investigations, signal-to-noise ratio (SNR) can be also defined through averaged amplitude of the system response.

$$SNR = \frac{4\pi \left| M_1^2 \right|}{S_N(\Omega)} , \tag{3.37}$$

where $S_N(\Omega)$ is the power of noise measured at the modulation frequency.

3.3.4 Results of Simulations

To characterise the behaviour of spectral amplification coefficient η in dependence of system parameters, the course of simulations of stochastic resonance in symmetric double-well potential has been performed in [13] in the framework of Floquet approach as presented briefly above. Here we reproduce main results of these numerical simulations after [34]. *Figure 3.4* shows the spectral amplification η evaluated for three different frequencies as a function of noise intensity. It can be seen that for high frequency Ω the dependence is rather flat and there is practically no power amplification present. At the decrease of the frequency of modulation signal, the maximal value of spectral amplification grows. The position of the maximum shifts towards lower noise intensity values. While obtaining the evident enhancement of the amplitude-frequency characteristic of the system in low frequency range, it is not possible though to get resonance behaviour of spectral amplification coefficient in dependence of increased frequency at a *fixed* noise intensity D. Generally, the spectral amplification in this case shows the behaviour of monotonically decreasing function.

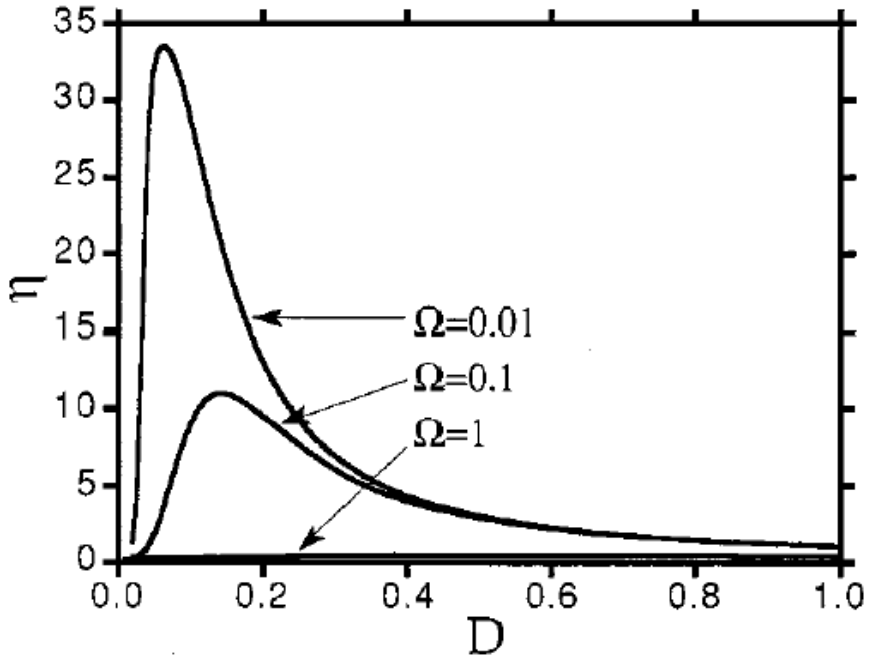

Figure.3.4 *Results of the numerical simulations: dependences of spectral amplification for different frequencies Ω of modulation signal (after [13, 34])*

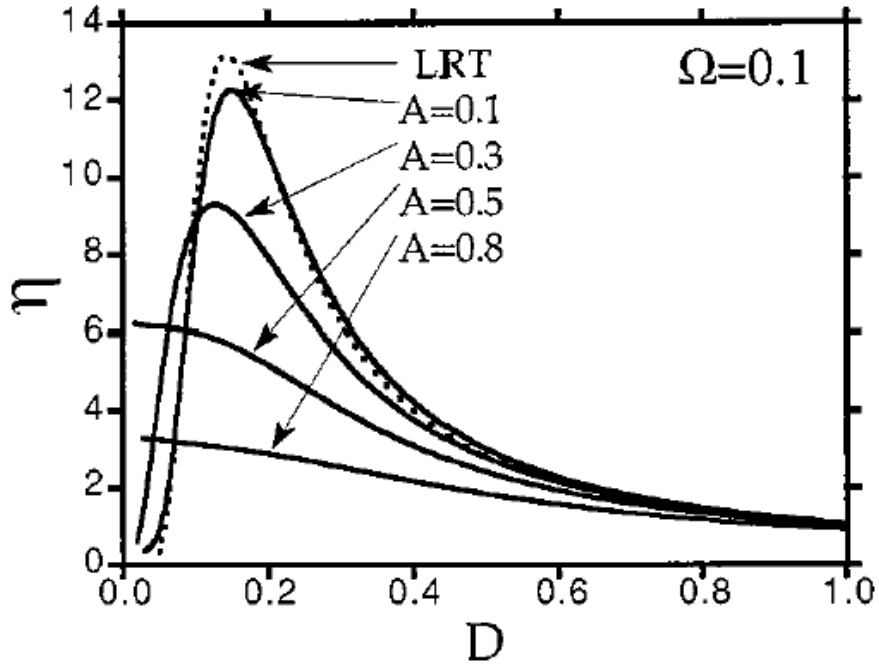

Figure 3.5 *Results of numerical simulations: dependences of spectral amplification for different amplitudes A of the modulation signal. LRT stands for "linear response theory" approximation (after [13, 34])*

The dependence of spectral amplification on noise intensity for several amplitudes of modulation signal is presented on *Figure 3.5*. Here it should be pointed out that on decreasing the amplitude, the location of amplification maximum drifts towards higher noise intensities. With the increase of the amplitude the maximum of the spectral amplification decreases.

3.4 Intrawell Motion Contribution

To characterise adequately the behaviour of signal-to-noise ratio one must undertake a somewhat refined analysis. Returning to the approximate expression for signal-to-noise ratio given by equation (3.15), it can be seen that by scanning the noise intensity, the signal-to-noise ratio undergoes a simple resonance-like dependence with a single maximum reached at some optimum noise strength D_m. Such a behaviour does not though correspond completely to the results of real experiments [10,34,44]. The main distinctive feature observed in these investigations is that the signal-to-noise ratio develops a local minimum at low noise values, as it can be seen for example, from *Figure 3.2*. At the further increase of the noise it reaches the maximum and then decreases again. To provide adequate description of signal-to-noise ratio behaviour, the influence of the intrawell motion which at low noise levels determines in general the system dynamics must be taken into account. To overcome this gap between experiment and theory, the contribution of interwell dynamics in weak noise limit is introduced [34,44] in the framework of linear response theory.

3.4.1 Linear Response Approximation

According to linear response theory, the system response $\langle x(t) \rangle$ to weak external perturbation $A(t) = A_0 \cos(\Omega t)$ in asymptotic limit for large times is given by integral expression [44]:

$$\langle x(t) \rangle_{as} = \langle x(t) \rangle_0 + \int_{-\infty}^{\infty} \chi(t-\tau,) A_0 \cos \Omega \tau d\tau \quad , \tag{3.38}$$

where $\langle x(t) \rangle_0$ is the stationary average of the unperturbed process at $A(t)=0$. The function $\chi(t)$ is called the *response function*. For stationary systems in equilibrium the response function can be expressed through the autocorrelation function of unperturbed system using the fluctuation theorem [34,44]

$$\chi(t) = -\frac{H(t)}{D}\frac{d}{dt}K_{xx}^{(0)}(t), \tag{3.39}$$

where *H(t)* denotes Heaviside step function responsible for the occasional character of response. The approximate expression for correlation function $K_{xx}^{(0)}(t)$ is obtained by expanding it over the eigenvalues λ_n of the Fokker-Planck operator in (3.24). This yields the following equation for the response function:

$$\chi(t) = H(t)\sum g_n \lambda_n \exp(-\lambda_n t). \tag{3.40}$$

Expantion coefficients g_n are calculated by averaging corresponding eigenfunctions and of the unperturbed Fokker-Plank operator [34]
On performing the Fourier transform of $\chi(t)$

$$\chi(\omega) = \int_0^\infty \chi(\tau)\exp(-i\omega\tau)d\tau, \tag{3.41}$$

the spectral representation of response function is derived:

$$\chi(\omega) = \chi'(\omega) + i\chi''(\omega) = \sum_{n=1}^{\infty}\frac{\lambda_n g_n}{\lambda_n + i\omega_n}. \tag{3.42}$$

Using equations (3.40) and (3.38), the expression for the linear response approximation of the system response is obtained:

$$\langle \delta x(t)\rangle = \langle x(t)\rangle_{as} - \langle x(t)\rangle_0 = \frac{A_0}{2}\sum_{n=1}^{\infty}\lambda_n g_n\left[\frac{e^{i\Omega t}}{\lambda_n + i\Omega} + \frac{e^{-i\Omega t}}{\lambda_n - i\Omega}\right]. \tag{3.43}$$

Combining this expression with equation (3.38) yields

$$\langle \delta x(t)\rangle = A_0\left|\chi(\omega)\right|\cos(\Omega t - \phi), \tag{3.44}$$

with phase shift ϕ given by

$$\phi = \arctan\left\{\frac{\chi''(\Omega)}{\chi'(\Omega)}\right\}. \tag{3.45}$$

Both stochastic resonance observables can then be represented through the response function. On comparing the equations (3.33) and (3.44) it follows that the spectral amplitude $|M_1|$ can be written as

$$|M_1| = \frac{A_0}{2}|\chi(\Omega)| \tag{3.46}$$

and therefore the expression for spectral amplification in terms of response function yields [44]

$$\eta = \left(\frac{2|M_1|}{A_0}\right)^2 = |\chi(\Omega)|^2 . \tag{3.47}$$

Analogously, the linear response theory gives for signal-to-noise ratio

$$SNR = \frac{4\pi|M_1|^2}{S_N(\Omega)} = \frac{\pi A_0^2|\chi(\Omega)|^2}{S_N(\Omega)} . \tag{3.48}$$

It should be pointed out that within linear response approximation the noise strength is assumed weak. To describe the bistable dynamics of the system one must take into consideration both characteristic time scales that rule the system behaviour. These time scales are the escape time out of one metastable state into another that corresponds to the interwell dynamics and time that characterises the relaxation within local stable state, i.e., intrawell dynamics. Within the simplest approximation the intrawell motion at small noise strength is characterised by the smallest non-vanishing eigenvalue of unperturbed Fokker-Planck operator L_0

$$\lambda_m = 2r_K = \frac{\sqrt{2}}{\pi}\exp\left(-\frac{1}{4D}\right). \tag{3.49}$$

The approximate expressions for the correlation function and spectral density of the unperturbed system can be written as follows:

$$K_{xx}^0(\tau, D) = \left\langle x^2 \right\rangle_0 \exp(-\lambda_m \tau) \tag{3.50}$$

$$S_N(\omega) = \frac{2\lambda_m \left\langle x^2 \right\rangle_0}{\lambda_m^2 + \omega^2} = \frac{2\sqrt{2}\pi \left\langle x^2 \right\rangle_0 \exp\left(\frac{1}{4D}\right)}{2 + \pi^2 \omega^2 \exp\left(\frac{1}{2D}\right)}. \tag{3.51}$$

To take into account the local interwell dynamics the additional exponential term should be included in the expression for correlation function (3.50), which would describe fast fluctuations within one potential well. Hence the correlation function will describe both interwell and intrawell dynamics:

$$K_{xx}^0(\tau, D) = -g_1 \exp(-\lambda_m \tau) + -g_2 \exp(-\alpha\tau), \tag{3.52}$$

where α is estimated as a second derivation of given potential and for the case of double-well potential is α=2. The expression for power density yields:

$$S_N(\omega) = \frac{2\lambda_m g_1}{\lambda^2 + \omega^2} + \frac{2\alpha g_2}{\alpha^2 + \omega^2} \ . \tag{3.53}$$

The coefficients g_1 and g_2 are defined from correlation function and its derivative at $\tau=0$ and read

$$g_1 = \left\langle x^2 \right\rangle_0 - g_2 \ , \tag{3.54}$$

$$g_2 = \frac{2\lambda_m \left\langle x^2 \right\rangle_0}{\lambda_m + \alpha} + \frac{\left\langle x^2 \right\rangle_0 - \left\langle x^4 \right\rangle_0}{\lambda_m - \alpha}. \tag{3.55}$$

Using the expression for correlation function the estimation for susceptibility taking into account the intrawell dynamics can be written as follows

$$\chi(\omega) = \frac{1}{D}\left(\frac{\lambda_m^2 g_1}{\lambda_m^2 + \omega^2} + \frac{\alpha^2 g_2}{\alpha^2 + \omega^2} \right) - i\omega \left(\frac{\lambda_m g_1}{\lambda^2 + \omega^2} + \frac{\alpha g_2}{\alpha^2 + \omega^2} \right). \tag{3.56}$$

Knowing the susceptibility of the system and power spectral density of the unperturbed system, the expressions for spectral amplification and signal-to-noise ratio can be found according to equations (3.47) and (3.48) [44]:

$$\eta(\Omega, D) = \frac{(g_1\lambda_m)^2\left(\alpha^2+\Omega^2\right)+(g_2\alpha)^2\left(\lambda_m^2+\Omega^2\right)+2g_1g_2\alpha\lambda_m\left(\alpha\lambda_m+\Omega^2\right)}{D^2\left(\alpha^2+\Omega^2\right)\left(\lambda_m^2+\Omega^2\right)}, \tag{3.57}$$

$$SNR = \frac{\pi A^2}{2D^2}\frac{(g_1\lambda_m)^2\left(\alpha^2+\Omega^2\right)+(g_2\alpha)^2\left(\lambda_m^2+\Omega^2\right)+2g_1g_2\alpha\lambda_m\left(\alpha\lambda_m+\Omega^2\right)}{g_1\lambda_m\left(\alpha^2+\Omega^2\right)+g_2\alpha\left(\lambda_m^2+\Omega^2\right)}. \tag{3.58}$$

The dependence of spectral amplification for several different frequencies of periodic modulation is presented on *Figure 3.6* (after [44]). Here the dots correspond to the estimations of amplification coefficient performed without taking into account the intrawell dynamics. Yet using linear response theory does not yield qualitative difference in the behaviour of spectral amplification with the results of Floquet approach described above. On comparing *Figures 3.4, 3.5* and *3.6* it can be assumed that both approaches show good agreement in the region of high amplification values.

On the contrary, the signal-to-noise ratio displays distinct features which are not reflected within general theory of stochastic resonance in double-well potential. The results illustrating the behaviour of signal-to-noise ratio for different frequencies of modulation signal as obtained within linear response approximation are shown on *Figure 3.7* (after [44]). As it is seen, for low frequencies the signal-to-noise ratio at the increase of the noise first develops a local minimum. This point corresponds to the moment where stochastic resonance is "triggered", as the corresponding dependence of spectral amplification starts to grow at approximately the same noise level (compare *Figures 3.6*. and *3.7*). The initial decrease of signal-to noise ratio is contributed by the local intrawell motion. It is clear that for low noise values, the barrier crossing events happen very rarely, hence the system dynamics is limited to the motion within single well. At the further increase of the noise, signal-to-noise ratio increases, reaches its maximum and then slowly falls off. The observed behaviour is in the agreement with experimental results for SNR measured in a variety of different systems where stochastic resonance is studied. With the increase of the frequency the local extrema of signal-to-noise ratio dependence disappear and it becomes a monotonically decreasing

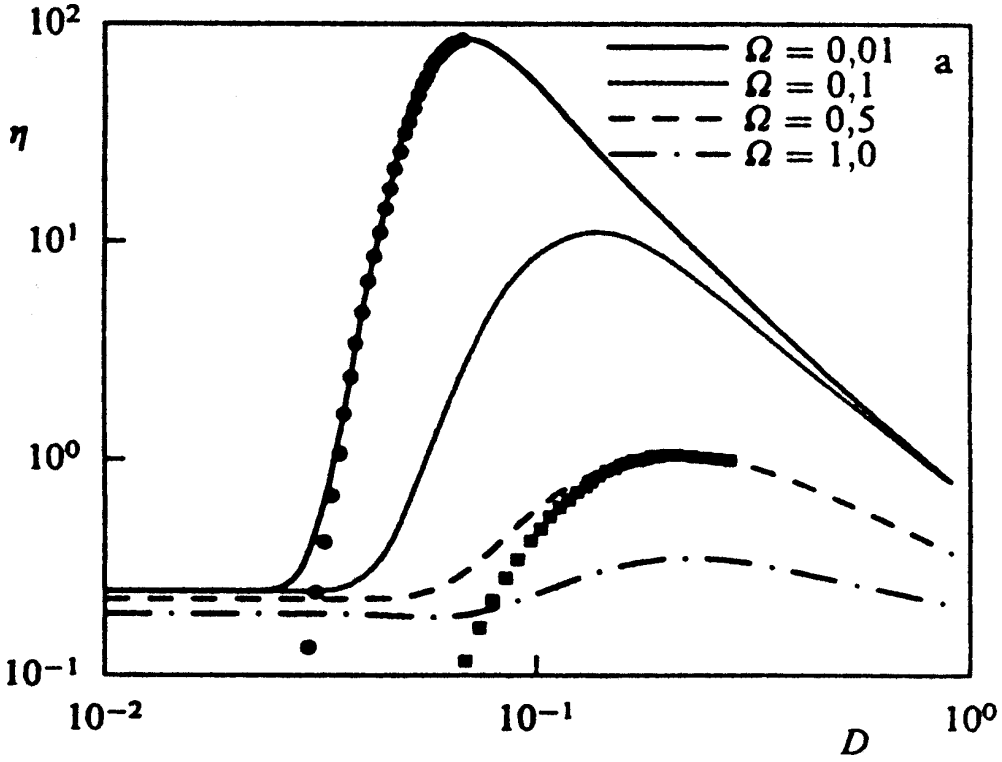

Figure 3.6 *Dependences of spectral amplification on the noise intensity for different frequencies of modulation amplitude obtained in the consideration of intrawell motion contribution. Dots represent estimations that do not take into account the intrawell dynamics [44]*

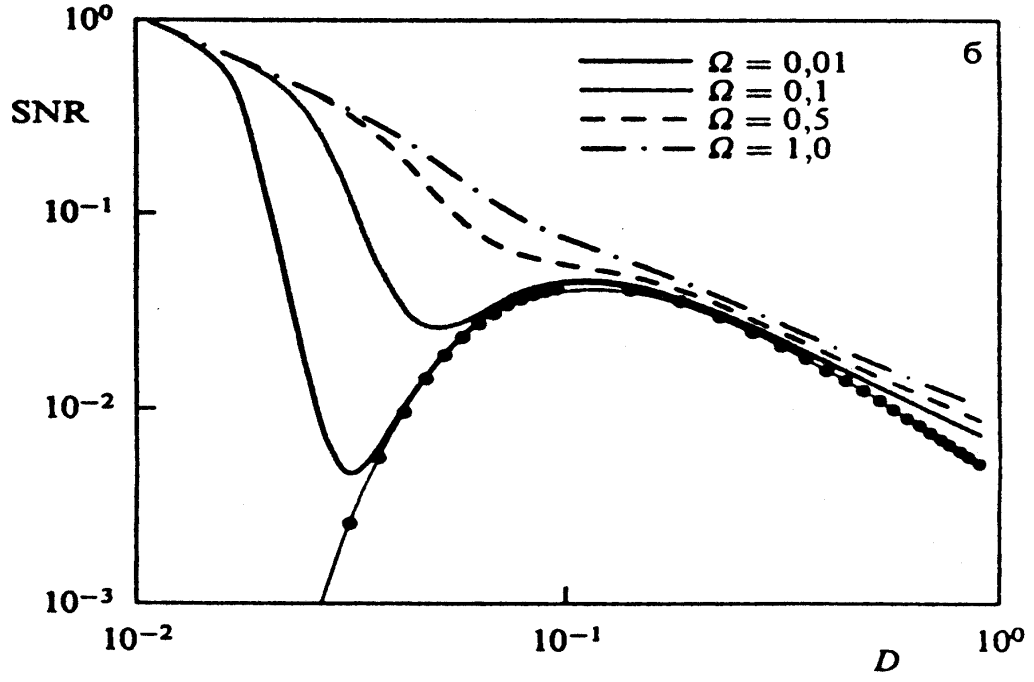

Figure 3.7 *Dependences of signal-to-noise ratio on the noise intensity for different values of modulation frequency, displaying intrawell motion contribution as a local minimum.[44]*

function. The noise intensities that maximise spectral amplification and signal-to-noise ratio do not coincide for the whole frequency range as was already mentioned when introducing corresponding approximate expressions for these characteristics. For low frequencies, the maximum of signal-to-noise ratio is achieved at the noise intensity of approximately D=1/8.
Upon neglecting the intrawell contribution, i.e., setting in the formulas (3.54, 3.55) $g_2=0$, one immediately recovers the expression for signal-to-noise ratio obtained within two-state approximation (3.15):

$$SNR = \pi r_K \left(\frac{A_0 \langle x \rangle_0}{D} \right)^2 . \tag{3.59}$$

3.5 Concluding Remarks

3.5.1 Ferroelectric TGS Crystal as a System Displaying Stochastic Resonance

Triglycine sulphate $(CH_2NH_2COOH)_3H_2SO_4$ (TGS) is a well known one-axis ferroelectric crystal with the second type of phase transition that represents one of the model materials in the physics of ferroelectrics. The ferroelectric phase transition at $\Theta=49\ ^\circ C$ is accompanied by the typical anomalous behaviour of dielectric constant which delivers a sharp value peak at the transition temperature. The temperature dependence of the spontaneous polarisation of TGS is a monotonically decaying function reaching zero value in Curie point [49,51]. At the temperatures below $49\ ^\circ C$ TGS crystal has ferroelectric phase characterised by the two stable states with opposite direction of spontaneous polarisation separated by the energetic potential barrier. Upon applying the electric field of the value exceeding the coercive field of the crystal at a given temperature, the process of the polarisation reversal takes place which is manifested by the typical loop of the ferroelectric hysteresis. While not pursuing the idea of the presentation of all the characteristic ferroelectric properties of TGS, thorough information on which has been gained in the long-run of successful studies, we intend to outline some points important for the stated purpose of study.
As it follows from the Landau's phenomenological theory of phase transitions, below the Curie temperature the thermodynamic potential of the one-axis ferroelectric with second type of phase transition has typical form of double-well potential as shown on *Figure 3.1* and in the vicinity of the curie point can therefore be approximated by the expression (3.2). Clearly, a ferroelectric such as TGS, when imposed to the combined action of external noise and generally periodic modulation, meets the basic requirements for the onset of the stochastic resonance presented in Introduction: a) a nonlinear system with energetic activation barrier or

any form of threshold, b) a weak coherent input signal and c) a source of random noise coupled to the coherent input or embedded in the system.
It is reasonable to assume that once established, stochastic resonance in ferroelectric TGS should be produced by the corresponding behaviour of the spontaneous polarisation, i.e., switching of polarisation direction in coherence with the weak external modulation achieved at some optimal level of noise intensity.

3.5.2 Frequency Scaling

Here we would like to attract reader's attention to a minor but very important detail. As it is explicitly assumed in expression (3.19), the frequency of external modulation among other experimental parameters is scaled against the parameter a of potential barrier $V(x)$ (see eq. (3.18)).Introduced formally in the course of theoretical description of stochastic resonance for a mere computational convenience, this feature in our opinion appeals for more detailed consideration.
As it follows from the proposed scaling property, the frequency of external periodical modulation can be equally varied, from the mathematical point of view, by either direct variation of the frequency of periodic signal, or by changing the height of potential barrier separating two stable states. Since in the present study one has to deal with ferroelectric material, in the last case such a variation can be achieved by the change of the temperature of the ferroelectric, which defines this parameter value.
Having said this, it is straightforward that the expected behaviour of the stochastic resonance observables, displayed at the variation of the frequency of external modulation signal and the temperature of the ferroelectric should be qualitatively similar. Since the behaviour of both signal-to-noise ratio and spectral amplification in dependence on the temperature of the sample will be determined primarily by the temperature dependencies of spontaneous polarisation and dielectric constant, one can expect the following. At lower temperatures it will take higher signals and noise intensities to obtain the effect of the signal amplification. With the increase of the temperature as the system approaches the phase transition point, the maximum system response should decrease and its position move toward lower noise values, which follows from the decay of the spontaneous polarisation with temperature at the simultaneous drastic growth of the sensitivity of the system in the vicinity of phase transition.

Chapter Four

Experimental Results

In order to accomplish the purposes of study as outlined in the Introduction, the series of measurements on the stochastic resonance behaviour in ferroelectric TGS have been conducted. Current chapter presents the results of this experimental investigation. The chapter is organised as follows. First the measurement results concerning the establishment of the stochastic resonance in the system with ferroelectric crystal are presented. The characterisation of the effect performed for the wide range of system parameters such as frequency and amplitude of the modulation signal, temperature of the ferroelectric sample etc. is given in several sections. Each section is followed by the discussion of the observed stochastic resonance behaviour and its peculiarities produced by the physical properties of the system under investigation in particular.

4.1 Signatures of Stochastic Resonance

To establish stochastic resonance in the system with ferroelectric crystal, the parameter space of the system has been scanned. Granted the basic requirements for the onset of the effect are realised experimentally with the help of measurement set-up, one can seek for the appearance of characteristic signatures of the effect, such as synchronisation between the weak modulation signal and noisy system output and typical resonance behaviour of the stochastic resonance measures, e.g., spectral amplification and signal-to-noise ratio.

4.1.1 Synchronisation and Signal Enhancement

As a first step of the current study, the principal possibility of establishing the effect of stochastic resonance has been provided experimentally. In order to meet the above specified general conditions necessary for the onset of the effect, the main system parameters were set as follows before the measurement start.

The ferroelectric sample was stabilised at the temperature of $\Theta=(318\pm0.01)\ K$ well below phase transition point. Periodic (sine) modulation signal plugged at the system input was set to frequency $f=10$ kHz and voltage $U_G=2\text{V}_{\text{RMS}}$ that corresponds approximately to one third of coercive field strength of TGS crystal at given temperature, thus producing no polarisation reversal caused by pure periodic signal. In terms of stochastic resonance requirements it addresses the issue of potential barrier modulated by weak periodic forcing not sufficient to produce deterministic particle switching across the barrier.

To demonstrate the processes taking place in the system during the measurement cycle, time series and power spectra of the electric charge flow registered over capacitor C_0 were measured at the increase of the amplitude of the external noise signal coupled with the periodic modulation from $D=0$ V_{RMS} up to 11 V_{RMS} and its subsequent decrease back down to zero value.

The evolution of time series and power spectra as presented in *Figures 4.1.1* and *4.1.2* for the full cycle of noise variation, allows one to inspect closely the appearance of stochastic resonance in the system under investigation. Let us take a detailed look at the procedure of this measurement performed as follows. At the first step pure sinusoidal signal had been applied to the sample after stabilising the temperature.

Corresponding power spectra and time series are presented in first row of *Figure 4.1.1*. It is clearly seen from the time series that system output is periodical with very low amplitude which indicates that in the absence of noise pure periodic driving is insufficient to cause any polarisation switching in TGS sample at this temperature. Power spectrum contains only first harmonic of driving frequency, with its peak level located approximately *40* dB above the noise. At a next step, the external noise with the amplitude of $D=1\text{V}_{\text{RMS}}$ was added to the system input. While the output signal remains nearly the same at this point, the average noise value in the corresponding power spectrum (second row of *Figure 4.1.1*) grows for about *10* dB, resulting in the decrease of the relative peak value of the first harmonic of system response.

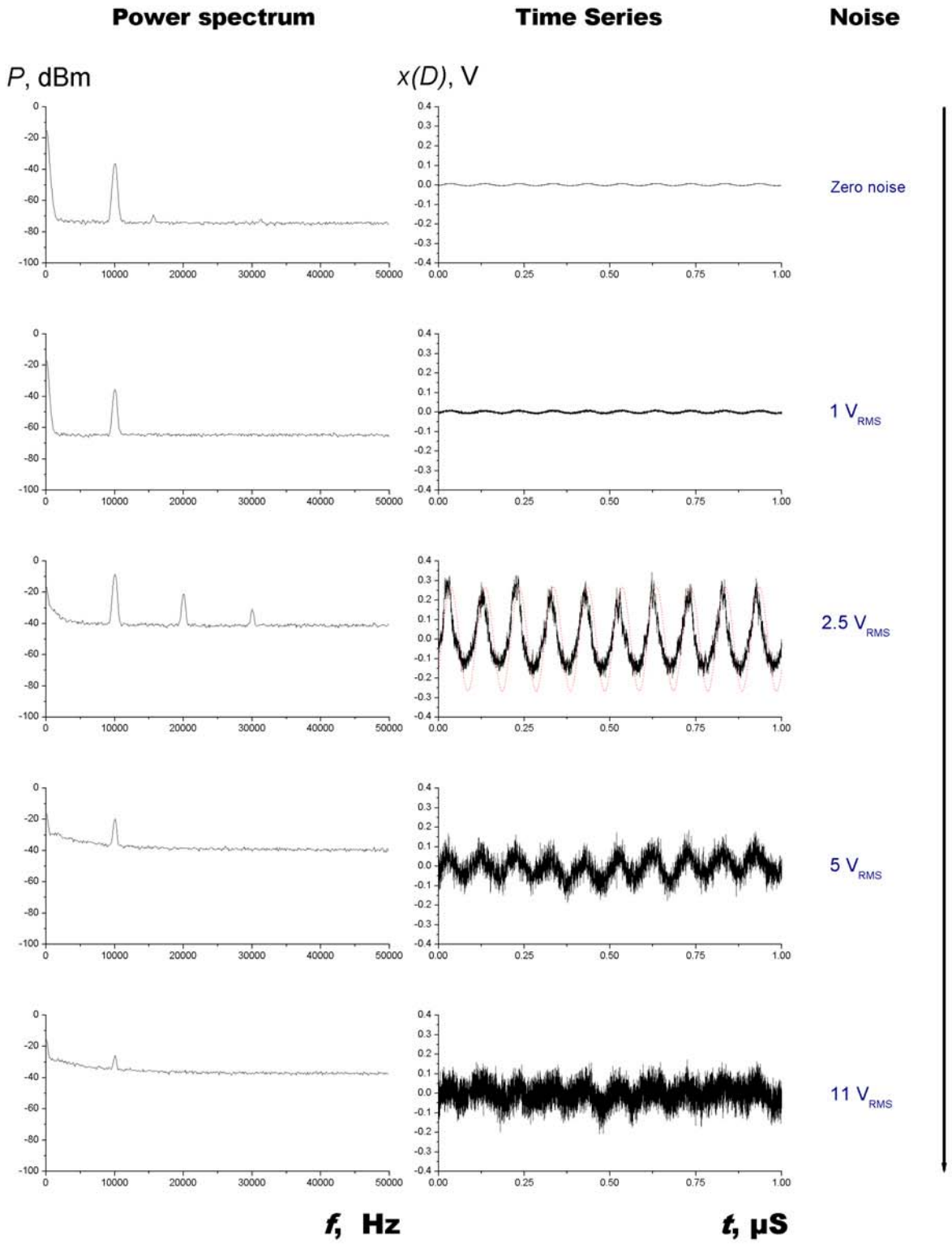

Figure 4.1.1 *Time series and power spectrum of the system response measured at the increase of the noise intensity at the system input*

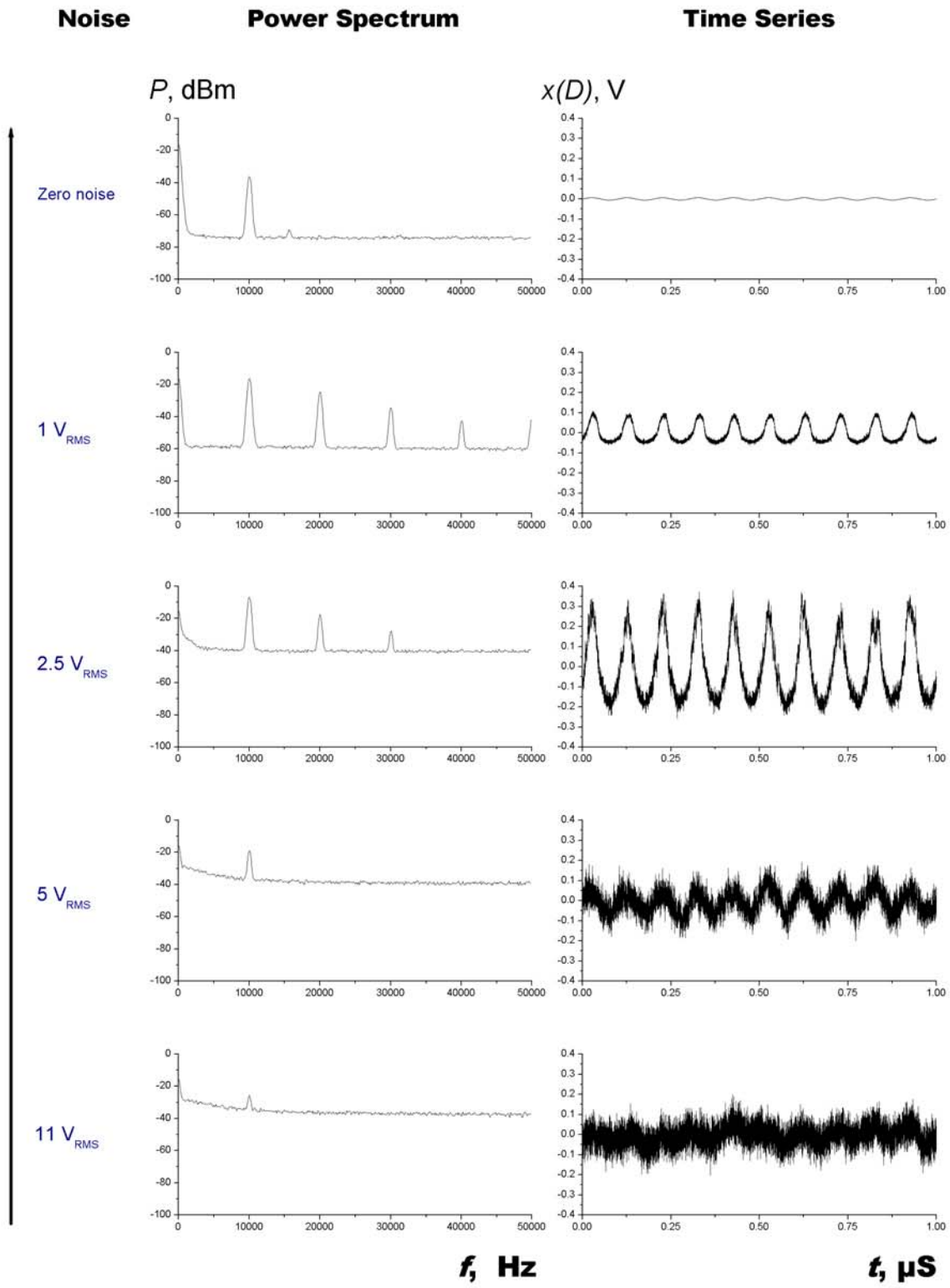

Figure 4.1.2 *Time series and power spectrum of the system response measured at the decrease of the noise intensity at the system input*

The further increase of the input noise value leads to the drastic growth of both output signal and noise. At the noise level of *2.5* V_{RMS} the output signal becomes tightly locked with periodic modulation signal shown with the dot line (see *Figure 4.1.1*, third row). This means that the synchronisation between the input periodic modulation signal and system output takes place as a result of interplay between noise and periodic modulation resulting in a process of „energy pumping“ from broad band noise into the peak at signal frequency. The periodic component of the output signal reaches its maximum as manifested by the absolute peak value of about *–5* dBm with the relative peak approaching practically the initial value of *40* dB. Further increase of the noise leads to the break of synchronisation and consequently to the decrease of the periodic component contribution in the system output. Time series become increasingly noisy followed by continuos decrease of the first harmonic of the power spectrum of system response at growing noise level. At the middle point of measurement cycle which corresponds to the highest noise strength of *11* V_{RMS}, periodic component of the system output becomes hardly visible indicating a drop of about *20 dB* below the maximum peak value in power spectrum. Time series represent only noisy signal with no periodicity detectable (see last row of *Figure 4.1.1*).

After reaching this point, the complete procedure was performed backwards following the same steps of noise variation as for the rate and value of change. The evolution of power spectra and time series is shown on *Figure 4.1.2*. As it follows from the comparative analysis of *Figures.4.1.1* and *4.1.2*, the process run at the decrease of the noise remains quite similar if not the same down to the values of noise approximately equal to those which cause maximisation of signal output during first half-cycle, i.e., in this case *D=2.5* V_{RMS}. The signal evolves from low peak values and noisy time series at *11* V_{RMS} of external noise into the synchronisation region at *2.5* V_{RMS} (see *3*rd row of *Figure.4.1.2*). On the further decrease of the noise though, the signal passes the synchronisation area without loosing the synchronisation down to quite low values of external noise (approx. *1* V_{RMS}), as it can be seen from the second row of *Figure 4.1.2*. Output power spectrum contains up to the 5^{th} harmonic. This sustaining synchronisation is accompanied by the growth of signal output value at simultaneous decrease of the output noise delivering much higher 1^{st} harmonic peak values on the back run. After removing the noise from the system input, the power spectrum and time series of the output signal recover initial values obtained at the start of the measurement.

As it follows from the observed behaviour, at the variation of the noise intensity at the system output, the phenomenon of the statistical synchronisation between the noisy output and input periodic modulation takes place at some “optimal” noise level, which results in the enhancement of the periodic component of the output signal. Such a behaviour is the typical signature of stochastic resonance. The degree of signal optimisation appears to be dependent on the direction of noise variation.

4.1.2 Behaviour of Spectral Amplification

To characterise the process of the onset of stochastic resonance quantitatively the dependencies of spectral amplification and signal-to-noise ratio on the external noise value as introduced in Chapter 3, have been calculated directly from power spectra. Both dependencies reflect very clearly the effect of the amplification of the periodic component of the output signal as a result of synchronisation establishment and consequent "energy pumping" from broad band noise into periodic component of the system output, demonstrating resonance-like behaviour in dependence of external noise intensity by increase as well as by decrease of the noise.

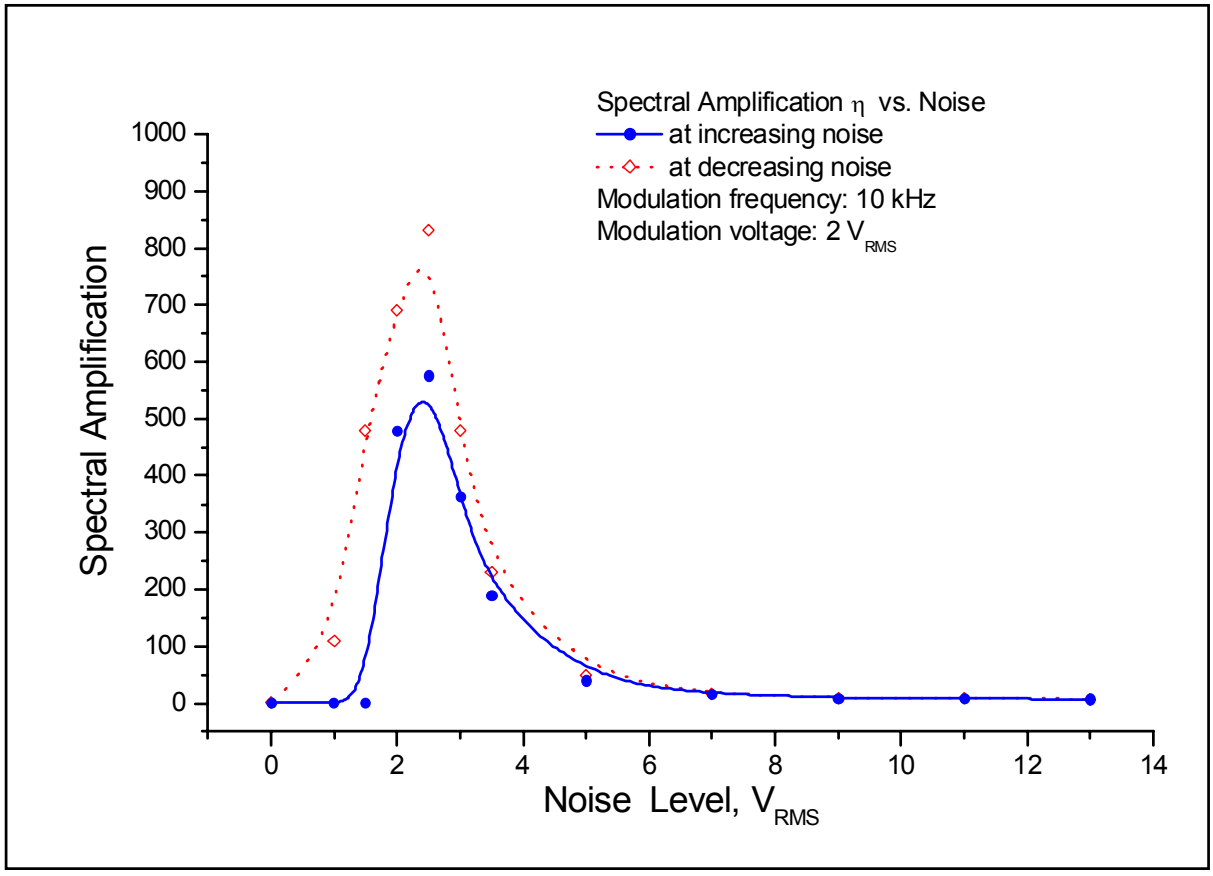

Figure 4.2 *Spectral amplification vs. noise intensity measured at the increase and decrease of the noise*

The dependence of spectral amplification on the noise intensity level for both directions of the noise variation is shown on *Figure 4.2*. The dependence displays typical resonance-like behaviour. Comparing the dependence trajectory obtained at the increase of the noise with the

results of the measurement run for the first half of noise variation cycle (*Figure 4.1.1*) allows one to establish the following facts. Starting with low noise value, the spectral amplification retains low values around *1* due to low value of periodic component of the output signal. It is reflected in power spectrum as well, as the peak value of the first harmonic, which defines the value of spectral amplification (see exact definition in Chapter 3), remains practically unchanged at the level of P=*-35* dBm[4].

As the system steps into stochastic resonance region, where the statistical synchronisation between periodic modulation signal and external noise takes place, as it is reflected in time series of the output signal, this synchronisation leads to the increase of the first harmonic peak value and subsequently to the increase of the spectral amplification. When the stochastic system output becomes tightly locked with the weak modulation signal (shown with red dot line in the third row of *Figure 4.1.1*), and the periodic component of the power spectrum achieves the maximum value by the noise intensity of *2.5* V_{RMS}, the spectral amplification attains its maximum as well. At further increase of the noise intensity, the spectral amplification decreases along with the break of the statistical synchronisation process which is accompanied by the decrease of the first harmonic peak value. As it can be seen, the resonant-like dependence of the spectral amplification on the noise value is *produced* by *the establishment and subsequent break of the synchronisation.*

The behaviour of the spectral amplification during second half cycle of noise variation diverges from that obtained at the increase of the noise intensity. In the present system a peculiarity of the stochastic resonance has been discovered which, to our best knowledge, has been neither described theoretically nor observed experimentally yet in other systems.

As it is shown in *Figure 4.2*, on the decrease of the noise the spectral amplification values undergo a hysteresis, (in general case, as it will be shown later in this chapter, on both scales). While the values of the spectral amplification for both directions of noise variation coincide for the most points on the right shoulder of the dependence, the maximum value of spectral amplification achieved at the decrease of the noise is greater for about 35%. On further decrease of the noise the registered values remain also considerably higher at all measurement steps. As the noise level is driven back to zero value, the final value of spectral amplification equals the initial one.

4.1.3 Behaviour of Signal-to-Noise Ratio

Figure 4.3 presents the dependence of signal-to-noise ratio in the cycle of noise variation. It is worth to mention that though in most applications the values of both characteristics in use, i.e., signal-to-noise ratio and spectral amplification are calculated on the base of the power

[4] Note that the increase of the noise intensity level does not impact noticeably the value of spectral amplification as the relative peak value keeps exceeding 20 dB! These small deviations have been neglected for the sake of convenience in the chosen scale.

spectra of the output signal, they nevertheless display quite a different behaviour in the stochastic resonance region. They are responsible for the characterisation of different stochastic resonance features and complete each other. As value of spectral amplification is defined, generally speaking, by the absolute peak value of the first harmonic, the signal-to-noise ratio reflects the behaviour of the relative peak value during the cycle of noise variation. The dependence of signal-to-noise ratio allows to inspect the behaviour of the system in the weak noise limit, which is not reflected in the dependence of spectral amplification. In the absence of external noise signal-to-noise ratio displays high value due to the very low intensity of internal noise of the system compared to the output signal peak level.

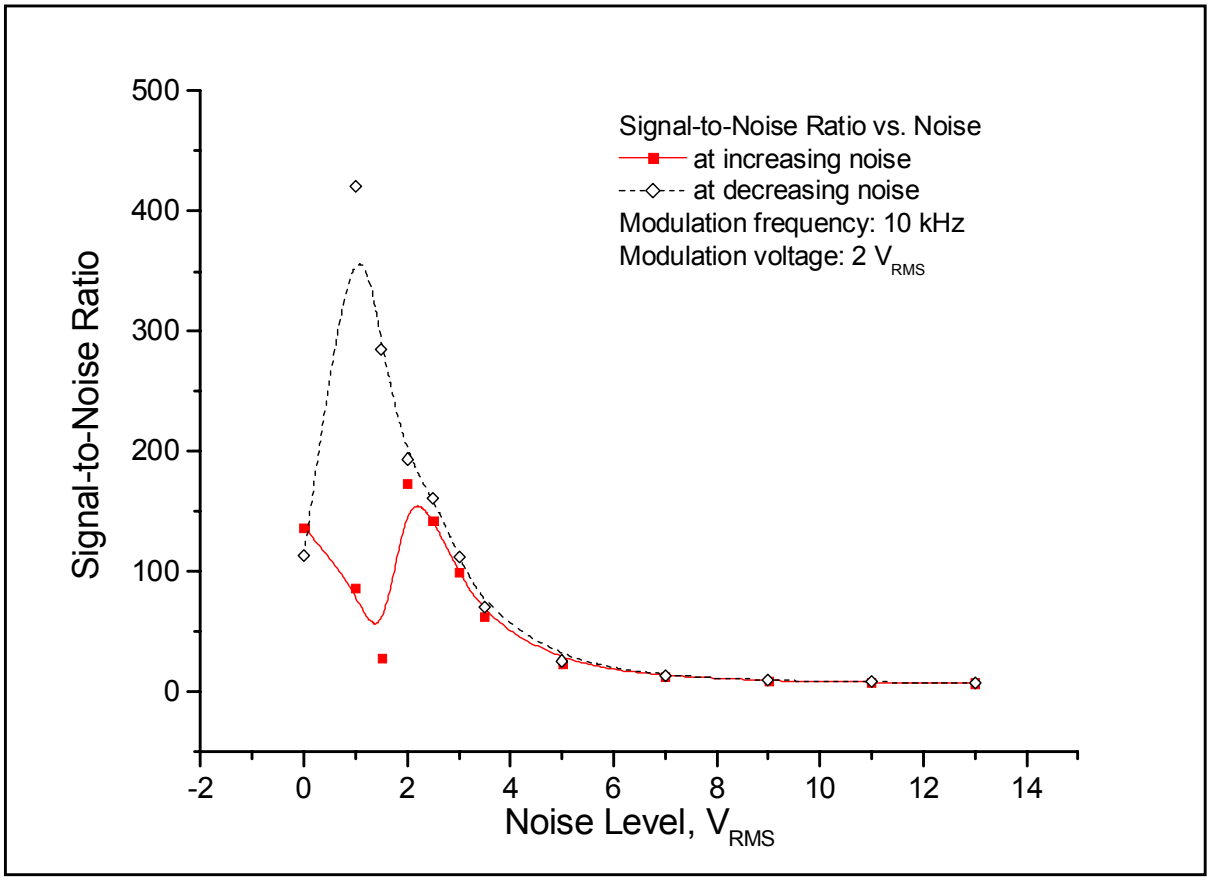

Figure 4.3 *Signal-to-noise ratio vs. noise intensity measured at the increase and decrease of the noise*

At the increase of the noise, the dependence of signal-to-noise ratio on the contrary to that of spectral amplification develops a minimum at a noise level of $D=1.5\ V_{\mathrm{RMS}}$. This happens due to the fact that though external noise of low intensity applied to the system increases yet the noise level of the output signal but is not sufficient to make system switch between its two metastable states. The system dynamics is thus limited to the intrawell motion around

potential minima, and the periodic component of the output signal remains low being determined mostly by the value of weak periodic modulation signal at the input. (Compare with 1st and 2nd rows of *Figure 4.1.1*). This behaviour of signal-to-noise ratio establishes close agreement with the results of theoretical predictions and numerical simulations of the motion of overdamped particle in symmetric quartic double well potential performed in [13,44]. As it has been mentioned in Chapter 3, taking into consideration the interplay of the interwell and intrawell dynamics in the weak noise limit, the results of computation display minimum of the signal-to-noise ratio caused by the contribution of the fluctuations of particle around potential minima, being though not accompanied by the remarkable hopping of the particle between the wells. As the signal-to-noise ratio reaches its minimum, the synchronisation sets in followed by the growth of the periodic component of the system response as manifested in the dependence of spectral amplification and stochastic resonance is "triggered." On the further increase of the noise the dependence of signal-to-noise ratio develops a maximum as well, achieved by the noise amplitude of $D=2V_{RMS}$

It is important to mention that in the actual experiment the values of noise amplitude, which maximise spectral amplification and signal-to-noise ratio do not coincide, as it has been pointed out in [13,34].

Further increase of the noise leads to the decrease of signal-to-noise ratio value, as the periodic component of the output signal and subsequently the relative peak value of first harmonic becomes more and more suppressed by the growing noise level. (*see Figure.4.1.1*). The periodic component of the system response almost vanishes. During the cycle of noise decrease from high values, the signal-to-noise ratio exhibits a hysteretic behaviour as well. In comparison to the spectral amplification dependence, the hysteresis appearing for opposite directions of noise variation is obviously more pronounced for signal-to noise ratio. As it has been described above, on the decrease of the noise the synchronisation, once recovered, is sustained down to very low noise values. Passing the point where signal-to-noise ratio is maximised by the noise intensity of $D=2V_{RMS}$ on the noise increase, the ratio grows furthermore and attains its maximum by the $D=1V_{RMS}$. This is caused by the crossover between the decrease rates of the first harmonic and noise values in the power spectrum. As the first harmonic value reduces, the noise level falls down even faster. This results in an enormous growth of the signal-to-noise ratio (note that in our system we register the power spectrum in dBm scale, therefore the relative peak value of the first harmonic when recalculated in linear scale achieves very high values). Reducing the noise to the zero value, one reaches the initial value of signal-to-noise ratio.

4.1.4 Discussion

The analysis of the results obtained in the course of measurement leads to the following conclusions. Subject to weak periodic modulation signal and external noise, the investigated system displays peculiar behaviour. Upon the continuos increase of the noise at the system input, the statistical synchronisation between the weak input modulation signal and noisy output of the system sets in, accompanied by the enhancement of the periodic component of the system response at some appropriate noise level. This behaviour is reflected in the dependencies of spectral amplification and signal-to-noise ratio, which quantitatively characterise the optimisation of the periodic component of the system output in dependence of the noise value. Both measures display resonance–like trajectories as a function of the noise intensity at the system input.

All the above said peculiarities of the system behaviour point out to the *"resonant"* character of the system response in dependence on *noise intensity* in the system. Therefore one can conclude that the effect of **stochastic resonance** is observed experimentally in the system under investigation, represented by its typical signatures.

In the given experimental configuration, the nonlinear system responsible for the onset of stochastic resonance is represented by the ferroelectric TGS crystal in the ferroelectric phase (below Curie point). Therefore one can assume that the model consideration of the particle in double-well potential corresponds in this particular case to the two metastable states with opposite polarisation direction separated by a potential barrier. The synchronised hopping over the potential barrier is realised as a process of formation and motion of domain walls accompanied by the (partial) polarisation reversal. As it was already mentioned above in Chapter 2, the experimental circuit is configured so as to make the voltage drop across C_0, which is actually measured, proportional to the polarisation of ferroelectric TGS. Therefore the evolution of the corresponding time series and power spectra reflect directly the behaviour of the domain structure of the sample.

As the synchronisation between the weak periodic input and noisy output that leads to the enhancement of the periodic component of the system response takes place upon the noise variation at the system input, the ferroelectric sample obviously undergoes the process of polarisation reversal manifested by the large time series signal (third row of *Figure 4.1.1*). This is also confirmed by the form of power spectrum which contains higher harmonics as in the case of polarisation switching caused by strong electric fields. As one can judge from the time series and power spectrum, at this point the system response becomes not only fully synchronised with the periodic input but appears to be to the great extend periodic itself. Therefore one can assume that the effect of stochastic resonance in ferroelectric TGS is manifested by the *process of polarisation reversal* with the frequency of the weak periodic modulation, produced by the interplay between noise and periodicity. This assumption is also confirmed by the fact that it was not possible to establish any signature of stochastic resonance in the paraelectric phase of TGS where no polarisation reversal exists.

The character of the obtained dependencies of spectral amplification and signal-to-noise ratio confirm the results of theoretical simulations and experimental investigations. The dependence of signal-to noise ratio displays local minimum caused by the increased level of the noise in the system which is not yet sufficient to produce the synchronised hopping over potential barrier (i.e. polarisation switching with the frequency of periodic modulation) thus limiting the system dynamics to the intrawell motion. The values of noise that maximise spectral amplification and signal-to-noise ratio do not coincide, which is also in agreement with theoretical predictions. The observed behaviour of both measures confirms the fundamental character of the effect of stochastic resonance and generality of the corresponding theoretical considerations which appear to be valid for the concrete system under investigation.

4.2 Characterisation of Stochastic Resonance

In order to perform characterisation of stochastic resonance the behaviour of signal-to-noise ratio and spectral amplification has been investigated in dependence of frequency and amplitude of the modulation signal. Obtained results are compared with numerical simulations developed in the framework of Fokker-Planck approach for the description of stochastic resonance presented in Chapter 3.

4.2.1 Frequency Dependences

As the next step in characterisation of stochastic resonance in ferroelectric TGS, the system behaviour in dependence on the value of the frequency of modulation signal has been studied. The other two system parameters responsible for system output, namely temperature of the sample and modulation signal amplitude were kept constant during the measurement. The ferroelectric TGS sample was stabilised at the temperature $\Theta=45$ °C. Periodic modulation voltage was adjusted to $V=0.2$ V_{RMS}, to ensure that there was no polarisation switching produced by modulation signal alone. Then the noise variation from zero up to the highest value allowed by the measurement equipment was performed for each chosen frequency. As the energy of the noise added to the system inevitably transfers into the heat thus affecting the temperature of the sample and consequently, the height of the potential barrier between two metastable states of polarisation, to keep this parameter constant the measurement was performed rather slowly, giving system at each registered point the time to get into equilibrium at stabilised temperature. The chosen frequencies while covering wide frequency range, correspond to the areas where TGS sample is characterised by mobile domain

structure. For the purity of experiment each frequency value was proved so as not to coincide with resonant frequencies of the measurement circuit.

Figure 4.4 presents the results of the spectral amplification measurement for four frequencies of the modulation signal *f=2, 10, 50* and *1 MHz*. As it can be seen, by increasing the frequency, the maximum value of spectral amplification decreases and shifts toward greater values of noise. This behaviour confirms experimentally the results of simulations made in attempt to describe the stochastic resonance behaviour in dependence of modulation frequency of the input signal for the overdamped particle in double well potential, as presented in Chapter 3.

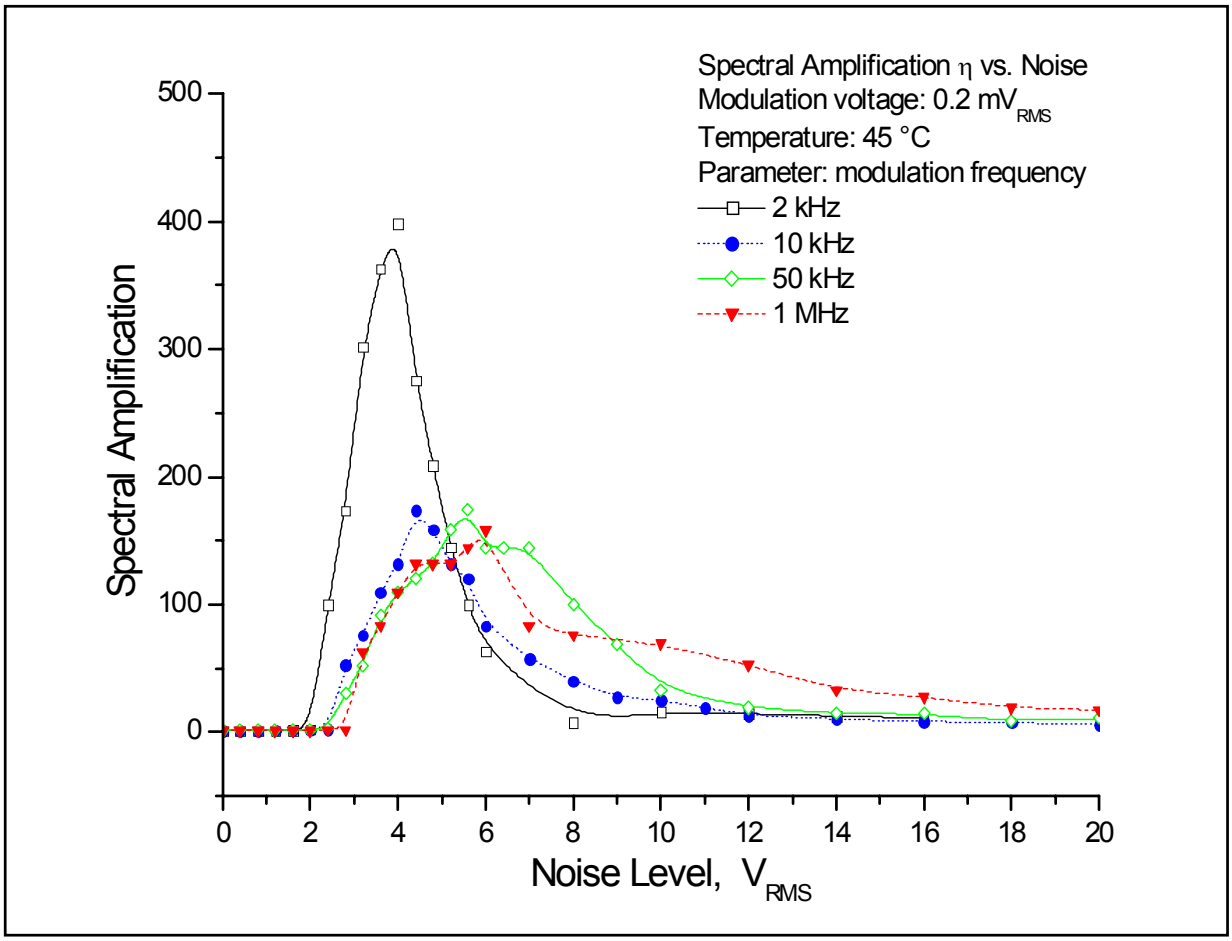

Figure 4.4 *Dependence of spectral amplification on the noise intensity measured for four different frequencies of the modulation signal f=2 kHz, 10kHz, 50 kHz, 1MHz.*

Qualitatively, the observed behaviour can be understood as follows. As the growth of ferroelectric domains (i.e., hopping particles in generic model) is bounded to the finite times of nucleation process, with increasing frequency, fewer and fewer domains manage to switch in coherence with modulation signal, which leads to the decrease of the output signal power in

comparison to low frequency regime. The probability to switch during half period of the modulation is increased by the increase of the noise intensity that in its turn increases the transition rate, shifting the maximum of the system response to the higher values of noise. On the high noise level, the probability for the domain being switched in the anti-phase direction during the period of modulation is increased, which results also in the decline of the signal output. Therefore, one can think of stochastic resonance at high frequencies as a kind of compromise established between two competing processes.

The signal-to-noise ratio has also been measured for the given frequencies. The results are presented on *Figure 4.5*. Exploring the dependencies, one can establish the following facts. For the low noise values for all presented frequencies the signal-to-noise ratio displays a local minimum, which is contributed by the intrawell dynamics of the system. With the increase of the modulation frequency, the relative value of the local maximum in the signal-to noise ratio dependence diminishes, and the dependence trajectory approaches that of the monotonically

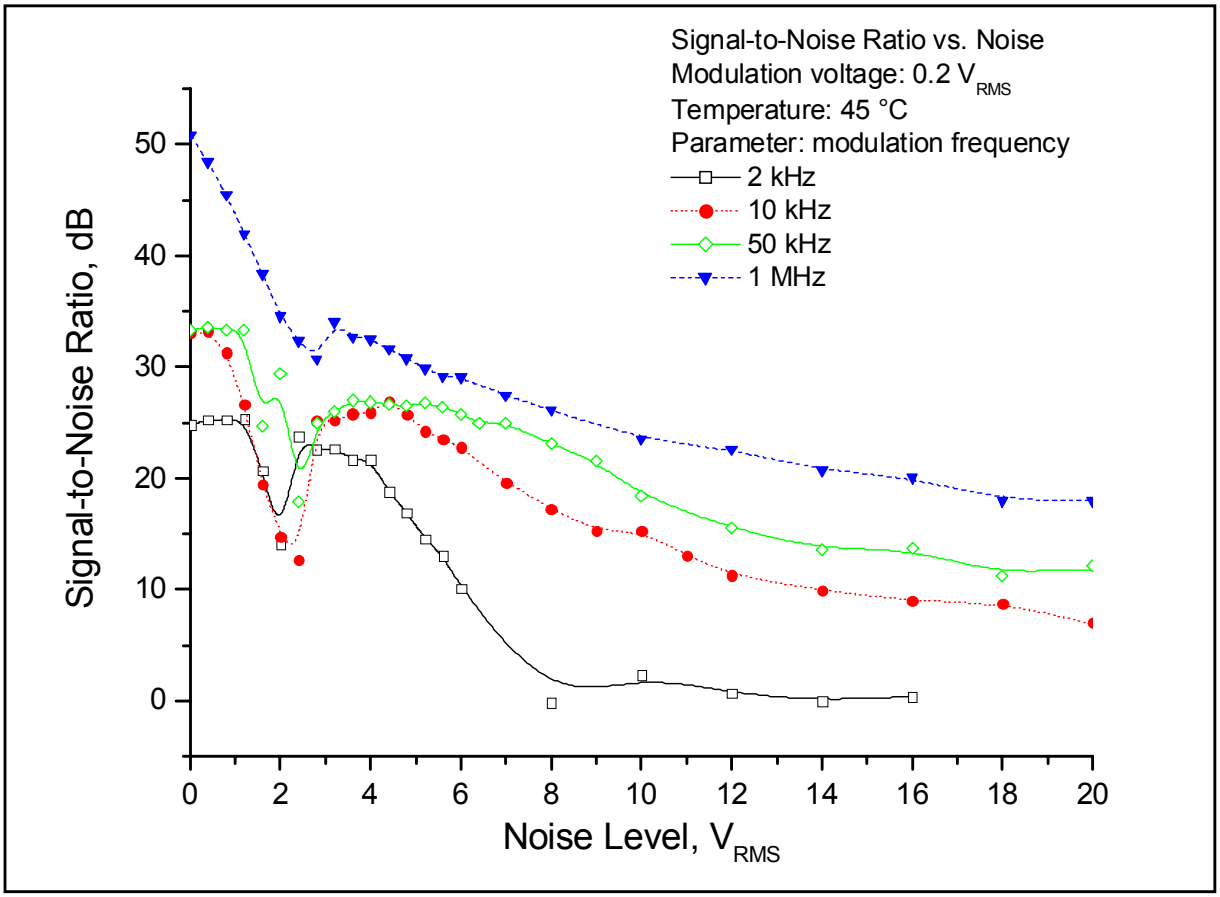

Figure 4.5 *Dependence of signal-to-noise ratio on the noise intensity measured for four different frequencies of the modulation signal f=2 kHz, 10kHz, 50 kHz, 1MHz.*

decreasing function. Due to slow decline of the signal-to-noise ratio values, it is possible to assume that there is no significant frequency dependence of the position of maximum value of signal-to-noise ratio on the noise intensity.
The observed features of stochastic resonance observable proved to be in good qualitative agreement with the results of theoretical investigations for the stochastic resonance behaviour for different frequencies, as presented in Chapter 3, Section 3.3.

4.2.2 Discussion

The obtained results show good qualitative agreement with theoretical predictions considering behaviour of stochastic resonance quantifiers in dependence on the frequency of external modulation signal. Comparing the experimental dependences with the results of numerical simulations, presented in Sections 3.3.4 and 3.4 (see *Figures 3.4-3.7*) of Chapter 3 one can see that the following characteristic properties of the frequency dependence of stochastic resonance have been reproduced successfully in actual experiment.
Upon displaying the obvious enhancement of the amplitude-frequency characteristic of the system at the low frequencies both experimental dependencies of spectral amplification and signal-to-noise ratio follow the simulated behaviour of stochastic resonance and confirm theoretical conclusions which underline low-frequency character of the effect. The dependencies of signal-to noise ratio display a local minimum at the weak noise intensities in the whole investigated frequency range, produced apparently by the motion of domain walls not yet leading to the polarisation switching, which is reflected in theoretical predictions by extending the consideration of the system dynamics with the contribution of intrawell motion.
The resonance-like behaviour of the system response in terms of either spectral amplification and signal-to-noise ratio though divergent for the different frequencies of the measurement has not however been observed at the direct variation of the frequency of modulation signal during the measurement, while keeping other experimental parameters (including noise intensity) constant. It confirms the fact outlined in several works [13,34,42] that stochastic resonance does not represent the case of classical (bona-fide) resonance whereby the enhancement of system response is achieved by locking the natural frequency (or its harmonics) of the system, as it may seem from somewhat misleading terminology. As it follows also from the corresponding results of numerical simulations, the system response shows monotonic decay at the increase of the modulation frequency.

4.2.3 Amplitude Dependences

To investigate the behaviour of the system in dependence on the modulation amplitude value, series of measurements have been performed, varying the amplitude in wide range. The main task of this study was first, to provide as complete characterisation of stochastic resonance in ferroelectric sample as possible by covering wide range of experimental parameters. Secondly, to prove whether theoretical predictions and simulations, performed as a rule for a much simpler system, such as overdamped particle moving in double well potential, can still be considered as valid when it comes to real experiment, where the actual system behaviour is much more complicated. In the course of measurements, the following procedure was performed for each chosen value of modulation amplitude. Granted that the ferroelectric crystal does not yet achieve polarisation switching area if subject to any amplitude value from the proposed parameter variation range in the absence of noise, the full cycle of noise variation has been conducted for each modulation amplitude. The frequency of modulation signal was kept constant at $f=10\ kHz$. The ferroelectric sample was stabilised at the temperature of $\Theta=45\ °C$. *Figures 4.6.1* and *4.6.2* present the dependencies of spectral amplification for the increase and decrease of the noise respectively. As it can be seen, by increasing the noise, the maximum of the spectral amplification increases, and shifts towards lower noise intensities with the increase of the modulation amplitude. The same behaviour is displayed for the decrease of the noise as well. For both directions of noise variation, the character of the dependences gives fair agreement with the results of simulations obtained in the framework of theoretical description (compare with *Figures 3.4-3.7*, Chapter 3). The difference between simulated and experimentally observed dependences is due to the slightly divergent definition of spectral amplification we used in the course of investigation. Having in mind that no absolute signal amplification can be extracted as a result of stochastic resonance as it is reported in the literature ([41]), we scale the power of the first harmonic of the system response over the response amplitude measured in the absence of noise (See Section 2.2, Chapter 2). Such a definition while remaining adequate since the response amplitude in the unperturbed system is proportional to the input amplitude nevertheless leads to the divergent spectral amplification behaviour, as in the actual measurement we practically register scaled response amplitude, which clearly reaches greater values at higher amplitudes of the input modulation (see *Figure 3.5*, Chapter 3)[5].

[5] Note also that in the presented simulation input amplitudes have values less than 1.

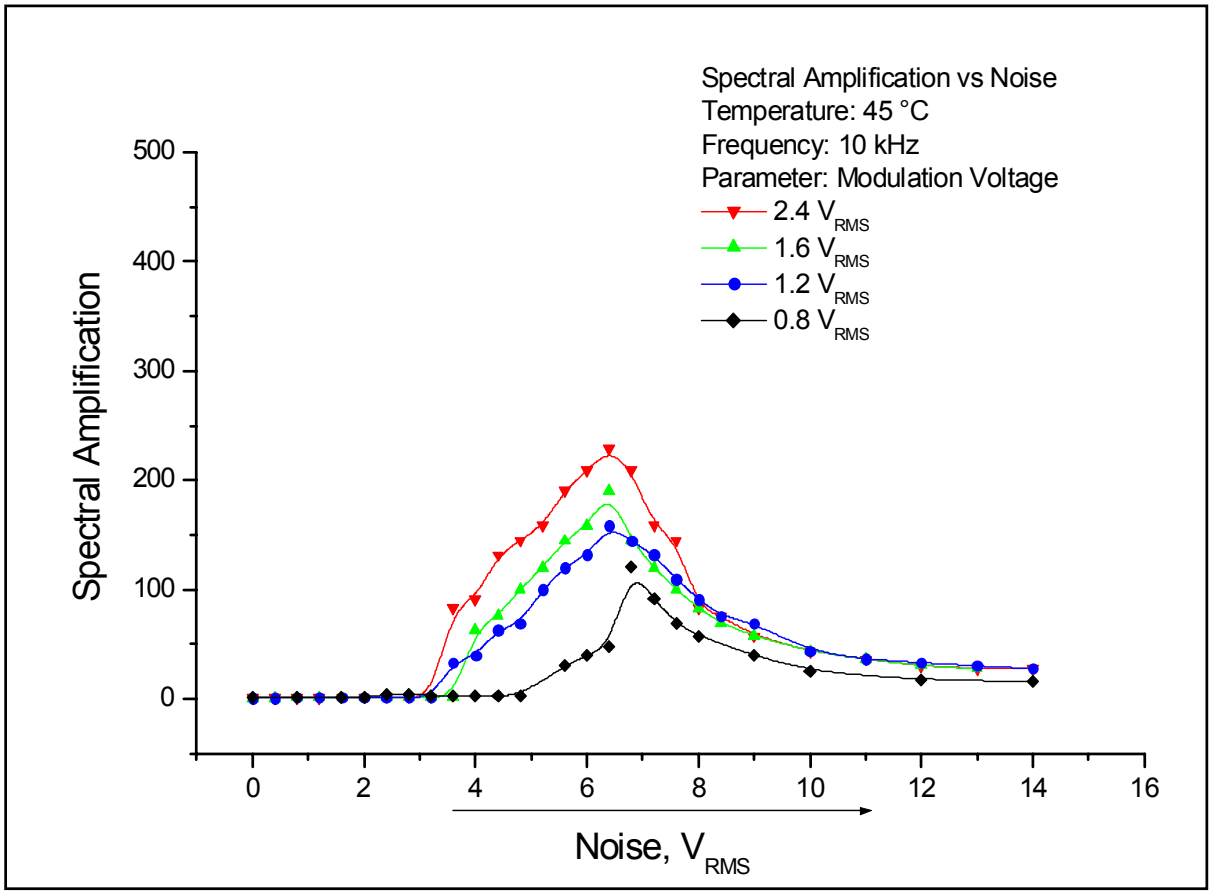

Figure 4.6.1 *Dependences of spectral amplification measured for different amplitudes of the modulation signal at the increase of the noise intensity*

The observed behaviour is intuitively clear. By varying the amplitude of the modulation signal, one changes the energy flow into the system and therefore the probability value of the barrier crossing. At high amplitudes, it is easier for ferroelectric domains to switch in coherence with external modulation, provided the necessary dose of noise is added to the sample. For decreased amplitude of periodic modulation the response of the system is expected to decrease, as it is confirmed by our measurements, because the switching will involve less domains. The lower the amplitude, the fewer domains are reversible due to domains pinning. Furthermore, it inevitably takes then greater values of noise to provide the system with the energy sufficient to produce switching as a result of interplay between noise and coherent signal. Here we would like to draw reader's attention to the point, that our measurements confirm clearly the fact that stochastic resonance is a threshold effect. The value of threshold is set, of course by the system parameters and can be changed. The greater the amplitude of the periodic modulation, the less is the noise intensity, at which system reaches the point where stochastic resonance is „triggered", provided the frequency of external modulation and temperature of the sample are kept constant.

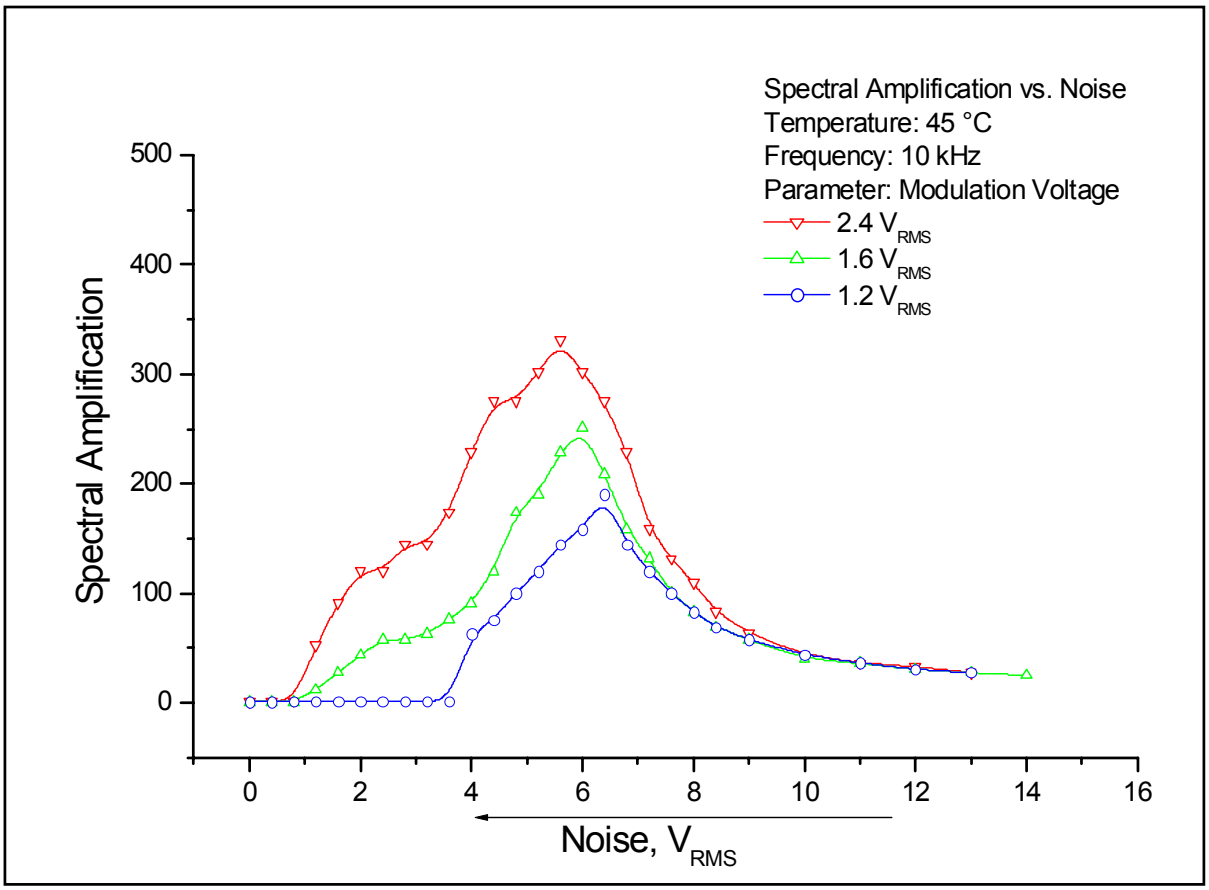

Figure 4.6.2 *Dependences of spectral amplification measured for different amplitudes of the modulation signal at the decrease of the noise intensity*

This fact is reflected, for instance, in *Figure 4.6.1*, as for higher amplitudes of modulation the spectral amplification starts to increase at the lower noise intensities.

The dependence of signal-to-noise ratio demonstrates the similar behaviour as shown on *Figures 4.7.1* and *4.7.2*. By the increase of the noise we observe the local minimum, which, as it has been already mentioned above, appears for low noise level where no polarisation switching is possible. The maximum value of signal-to-noise ratio grows with the increase of the value of amplitude of modulation signal and is established at lower noise level. The difference of initial values of signal-to-noise ratio follows straightforward from the definition of this characteristic as given in Chapter 2, according to which the calculations have been performed. It is obvious that higher initial value of modulation signal (in the absence of noise) leads to the greater relative peak value of the first harmonic which is responsible for signal-to noise ratio value, while the noise variation is the same for all given amplitudes. By the decrease of the noise the dependence of spectral-to-noise ratio displays only maximum achieved by low noise values.

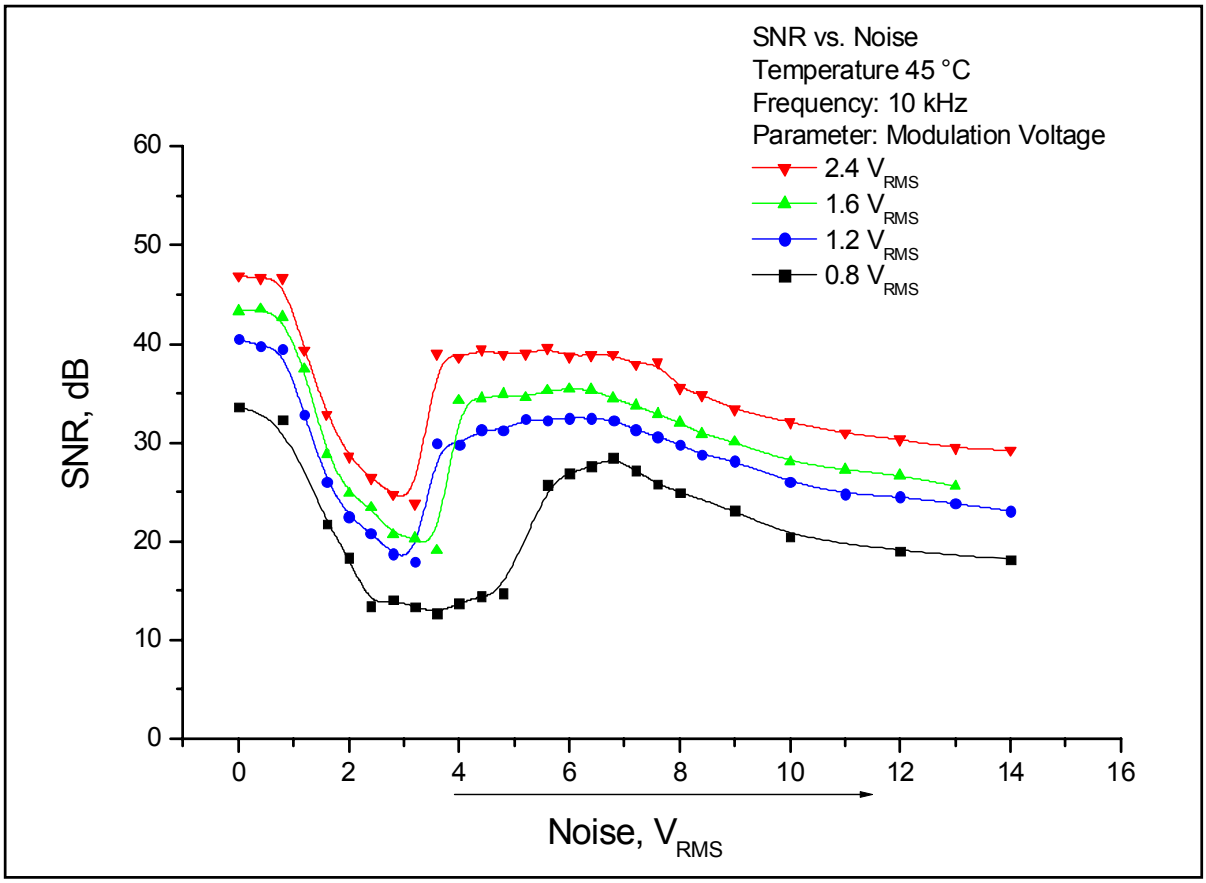

Figure 4.7.1 *Dependences of signal-to-noise ratio measured for different amplitudes of the modulation signal at the increase of the noise intensity*

For all values of the modulation amplitude, both dependencies of spectral amplification and signal-to-noise ratio show clear hysteretic behaviour in dependence on the direction of noise variation. For spectral amplification dependence the difference between the values obtained at the increase and decrease of the noise grows proportionally to the amplitude of the modulation. The gap between the maximal registered values of spectral amplification on the noise intensity scale increases as well. This hysteretic behaviour is more pronounced for the dependence of signal-to-noise ratio. At the decrease of the noise the local minimum of spectral-to noise ratio disappears and maximum is attained for much lower noise intensity.

It should be pointed out that the noise intensity values that maximise spectral amplification and signal-to-noise ratio respectively do not coincide for neither increase or decrease of the noise.

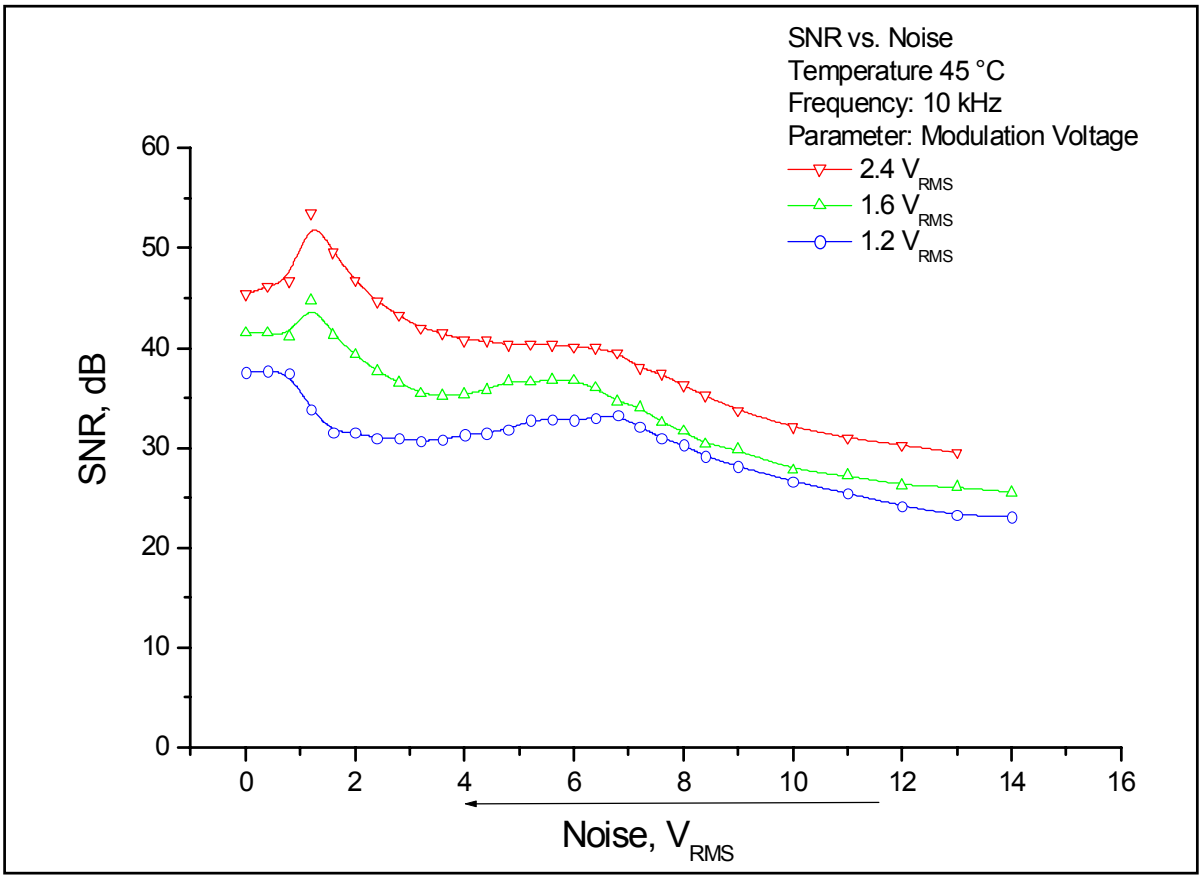

Figure 4.7.2 *Dependences of signal-to-noise ratio measured for different amplitudes of the modulation signal at the decrease of the noise intensity*

4.2.4 Discussion

The behaviour of spectral amplification and signal-to-noise ratio in dependence on the amplitude of the modulation signal observed experimentally proves to be in accordance with theoretical predictions presented in Chapter 3. The system response characteristics attain higher values for greater amplitudes of the modulation signal. The threshold character of stochastic resonance is reflected by the fact that it takes lower noise intensities to "trigger" the signal optimisation, the higher is the amplitude of modulation. The dependence of the behaviour of both stochastic resonance measures on the direction of noise variation is observed. The values of spectral amplification and signal-to noise ratio achieved at the decrease of the noise appear to be much greater than these measured at the increase of the input noise intensity, remaining also relatively high down to very low noise levels thus displaying a hysteretic behaviour. We tend to term this property, that has not yet been described in other systems with stochastic resonance, as "enhanced switching". Having

considered stochastic resonance in ferroelectric above as a process of polarisation reversal with the frequency of external modulation produced by the interaction of noise and periodic signal we seek possible explanation in the nature of domain structure of ferroelectrics. As it is known, in real crystal the ferroelectric domains are always pinned on defects of the crystal structure. Applying high noise intensity to the sample can result in the process of deliverance of domains and lead to more mobile domain structure and consequently, to the increased response to the external perturbations.

The results obtained in the characterisation of stochastic resonance in ferroelectric TGS crystal over broad range of amplitudes and frequencies of the modulation signal show very good qualitative agreement with numerical simulations performed in the framework of Fokker-Planck approach. It allows for the conclusion that this generic theoretical model based on the universal properties of the systems exhibiting stochastic resonance behaviour can be successfully applied for description of this effect in ferroelectrics due to its fundamental character.

Having proved experimentally the theoretical conception developed for continuous bistable systems to be valid for the concrete instance of the system with ferroelectric crystal, the one of purposes of this study has been accomplished.

4.3 Temperature Dependence of Stochastic Resonance Behaviour

Having clarified the main features of stochastic resonance in ferroelectric TGS for different frequencies and amplitudes of the periodic modulation, we next will describe the system behaviour in dependence on the temperature of the ferroelectric sample.

As it has been already mentioned, the actual system behaviour is controlled by the following experimental parameters: the frequency and amplitude of the external modulation signal, the noise intensity and the temperature of the ferroelectric sample. Changing the current parameter values, one affects the characteristic system time scales, which reciprocative competition is responsible for the onset of the stochastic resonance.

The signal parameters and the noise intensity are the external parameters that affect only the velocities of the motions within the system and can be freely varied over the whole appropriate range. The variation of the temperature changes not only the intensity of internal noise of the system, which plays also an important role in the complete picture of stochastic resonance but in the particular case under consideration affects increasingly the structure of the ferroelectric material and consequently all of its properties as well.

Having interpreted the stochastic resonance in ferroelectrics on the basis of the obtained experimental results as a process of the polarisation reversal in coherence with the weak periodic modulation established at the corresponding external noise intensity, it can be next assumed without loss of generality that the properties of the stochastic resonance in dependence on the temperature of ferroelectric sample will be mostly defined by the behaviour of the polarisation of the ferroelectric, which is a decaying function of temperature, and behaviour of corresponding dielectric properties of the material.

In terms of the general model for stochastic resonance presented in Chapter 3, the variation of the temperature of the ferroelectric sample would first of all mean the variation of the form and height of the potential barrier separating two metastable states of the system (i.e., two states with opposite direction of polarisation). Since the presented model is based on the fundamental properties of the effect and does not take into consideration unique properties of the particular systems, the behaviour of the stochastic resonance quantifiers in the dependence on the temperature of the ferroelectric TGS crystal can not be adequately described by means of the proposed theoretical approach. Nevertheless, due to the frequency scaling over the parameters of the potential barrier as featured in numerical simulations performed for the characterisation of the stochastic resonance (see Section 3.4, Chapter 3), at the variation of the temperature of ferroelectric crystal one can expect to observe the behaviour of the effect quantifiers similar to that obtained at the variation of the frequency of the external modulation.

4.3.1 Behaviour of Stochastic Resonance Measures at Different Temperatures of Ferroelectric TGS

In this section first the results of the measurements of signal-to-noise ratio and spectral amplification acquired for different temperatures of the ferroelectric TGS sample are presented. In the course of investigation the same measurement cycles have been performed for three temperatures of ferroelectric TGS sample using different amplitudes of modulation signal. This allows to conduct comparative analysis of the obtained results by varying simultaneously two experimental parameters. The system behaviour observed for temperature $\Theta=45°C$ as shown above has already served to describe the amplitude dependence of stochastic resonance characteristics. *Figures 4.8.* and *4.9* present the results of the measurements of spectral amplification and signal-to-noise ratio obtained at temperatures of ferroelectric sample $\Theta=40\ °C$ and $\Theta=47.5$ ° C respectively.

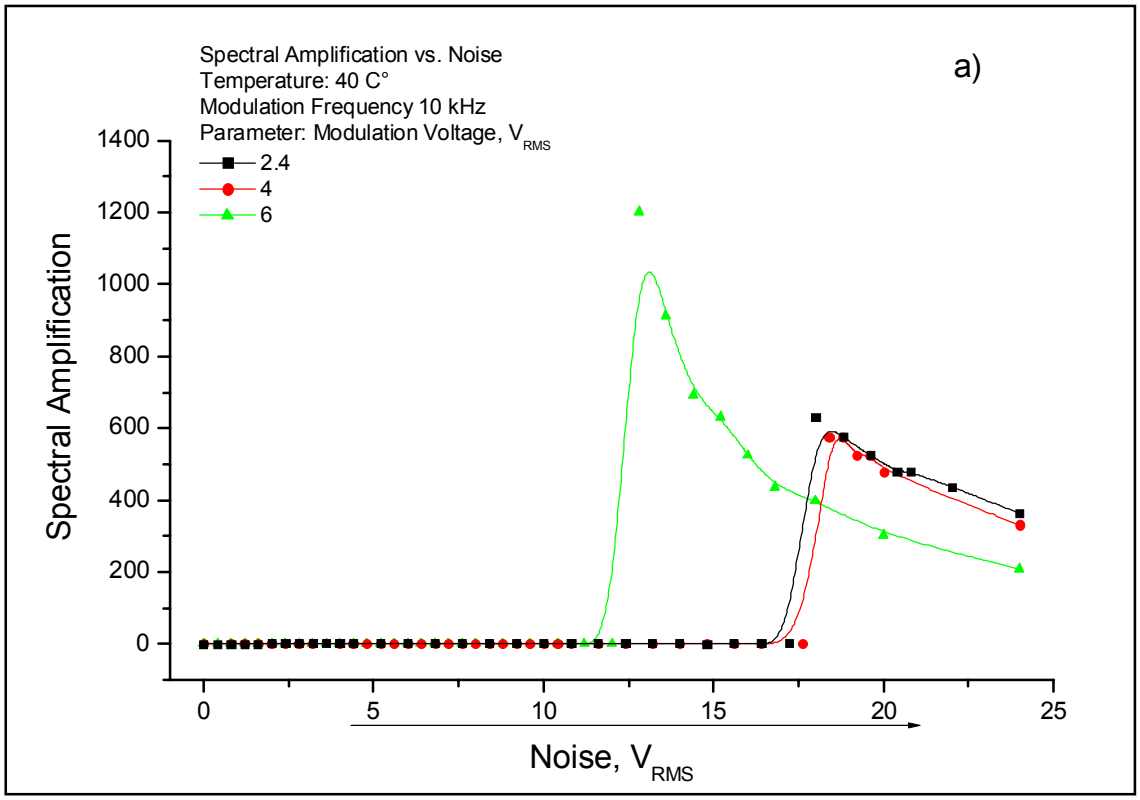

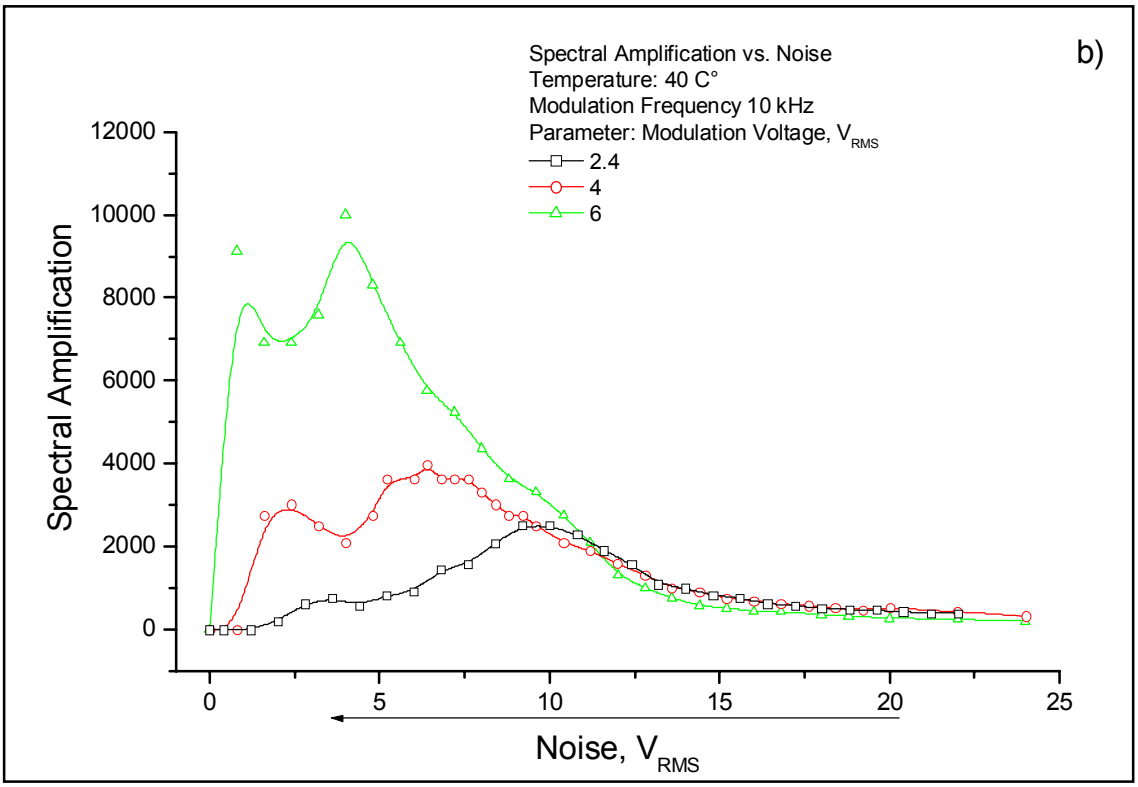

Figure 4.8.1 *Dependences of spectral amplification vs. noise intensity measured for different amplitudes of the modulation signal at the temperature of the ferroelectric sample Θ=40 °C at the* ***a****) increase and* ***b****) decrease of the noise respectively*

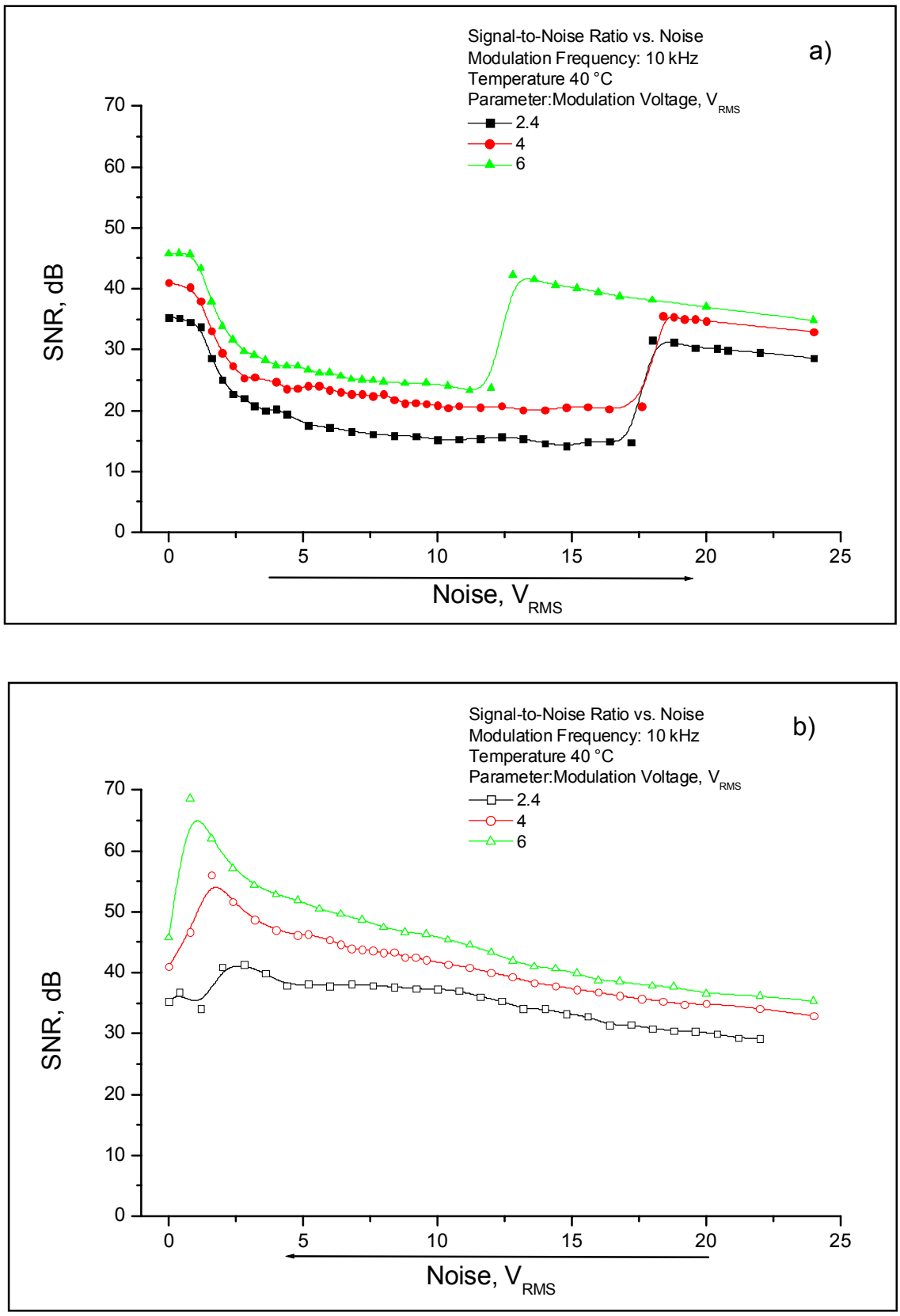

Figure 4.8.2 *Dependences of signal-to-noise ratio vs. noise intensity measured for different amplitudes of the modulation signal at the temperature of the ferroelectric sample Θ=40 °C at the* ***a****) increase and* ***b****) decrease of the noise respectively*

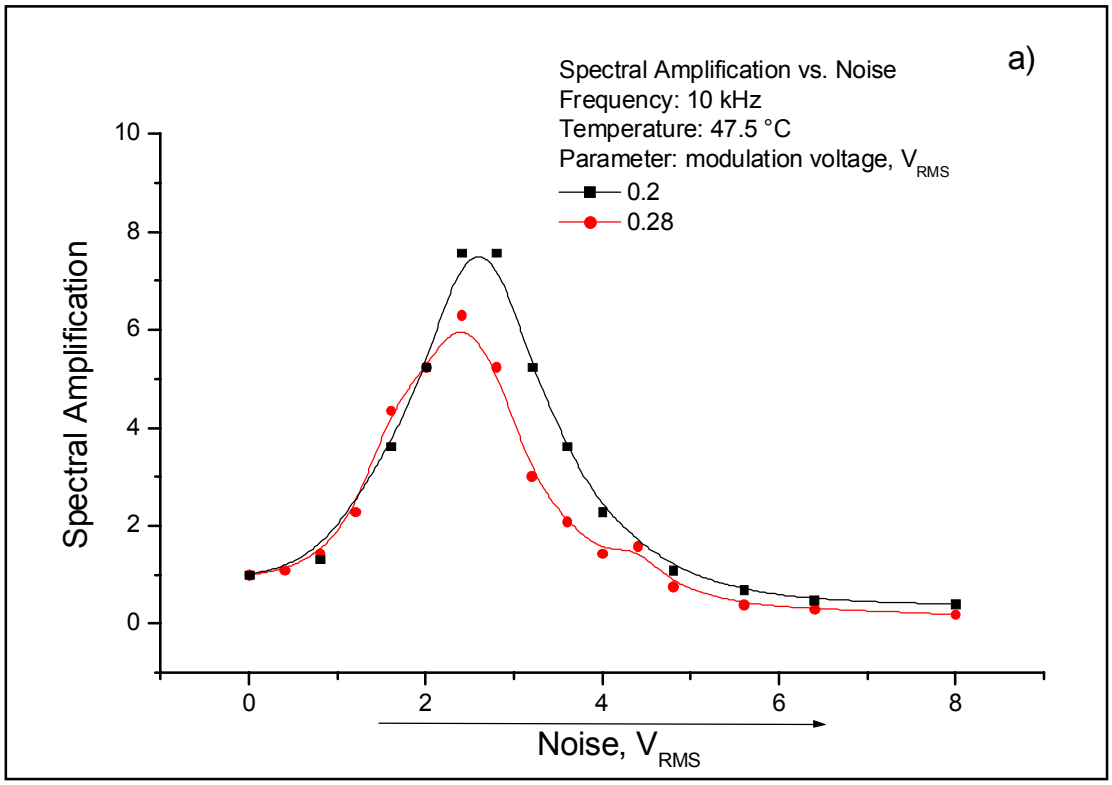

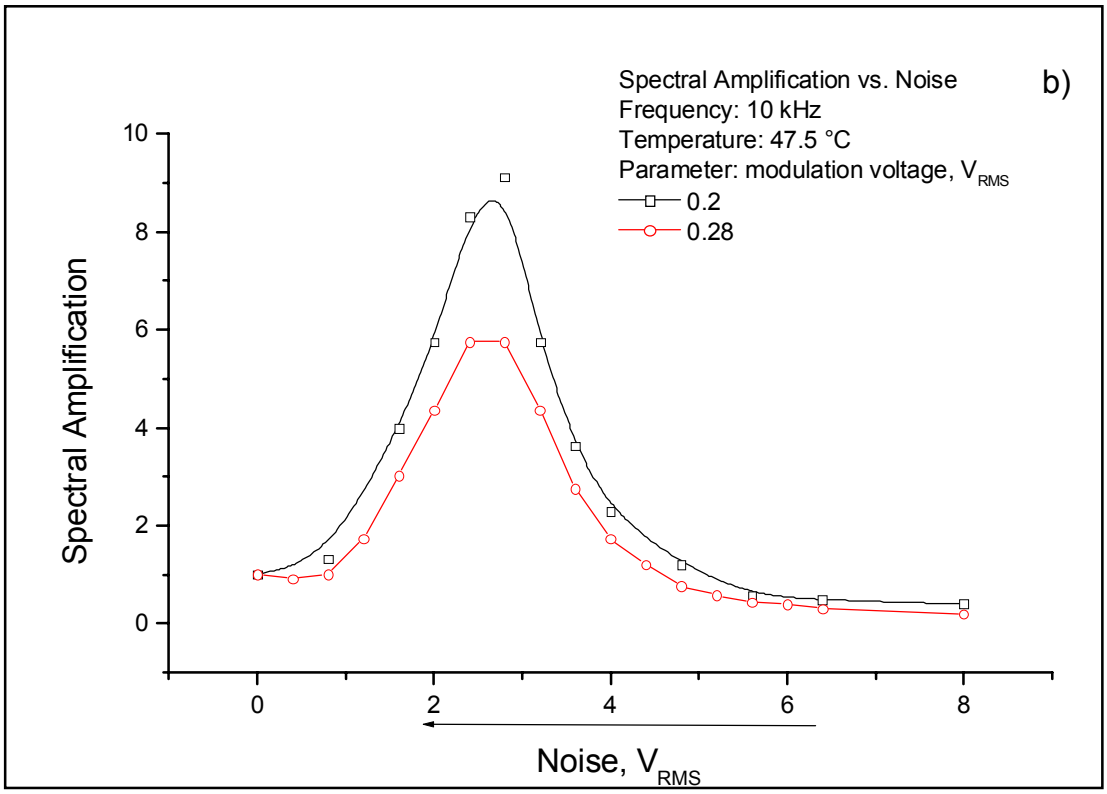

Figure 4.9.1 *Dependences of spectral amplification vs. noise intensity measured for different amplitudes of the modulation signal at the temperature of the ferroelectric sample Θ=47.5°C at the* ***a****) increase and* ***b****) decrease of the noise intensity respectively*

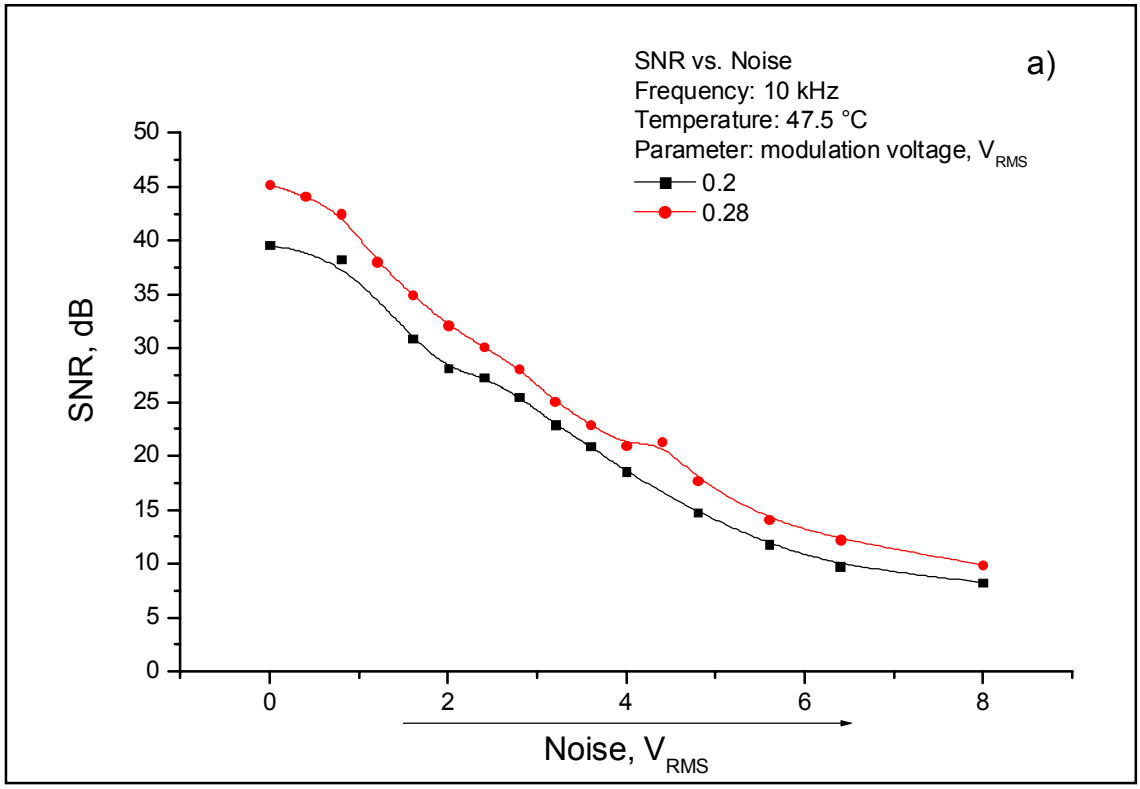

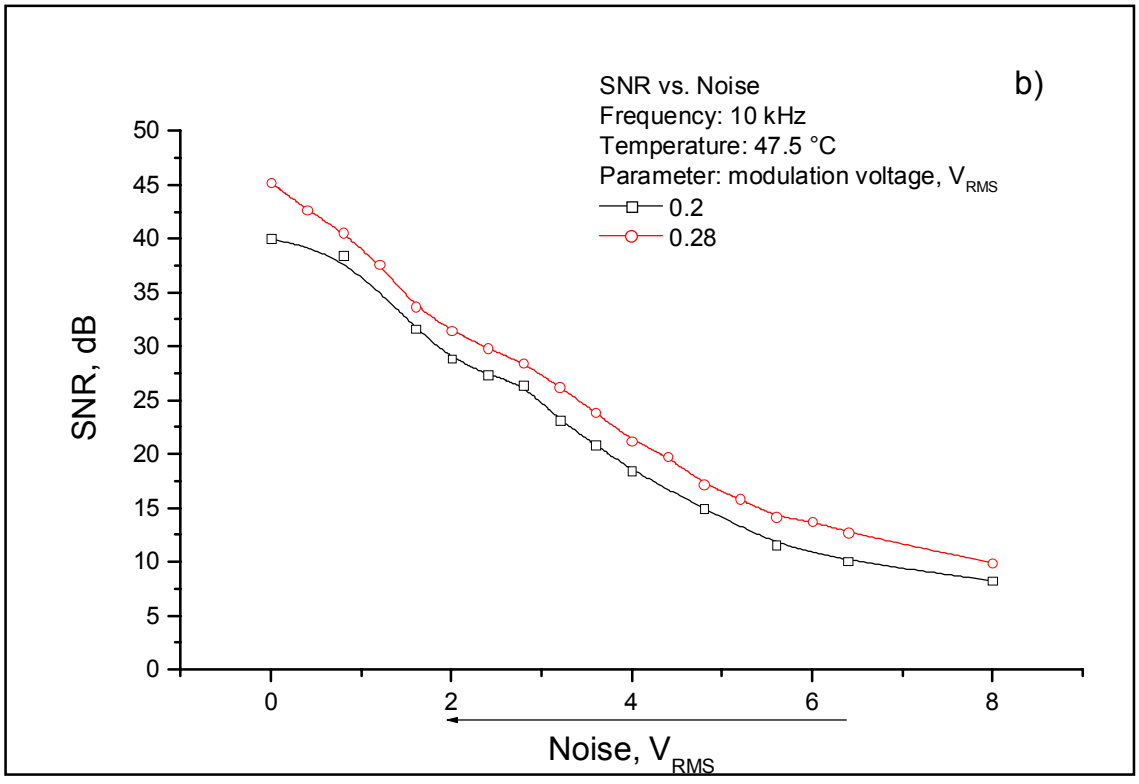

Figure 4.9.2 *Dependences of signal-to-noise ratio vs. noise intensity measured for different amplitudes of the modulation signal at the temperature of the ferroelectric sample Θ=47.5°C at the* ***a)*** *increase and* ***b)*** *decrease of the noise intensity respectively*

As it can be seen, the system behaviour at the temperature of the ferroelectric TGS sample $\Theta=40$ ℃ remains to the great extend similar to that observed for $\Theta=45$ *°C*. With the increase of the modulation amplitude value, the maximum values of both spectral amplification and signal-to-noise ratio increase and shift towards low noise intensities. At the increase of the noise the signal-to-ratio displays wide local minimum which disappears as the direction of noise variation is changed backwards. Both presented characteristics demonstrate hysteresis between the values obtained at decrease and increase of the noise.

On the contrary, the behaviour observed at the temperature of $\Theta=47.5$ ℃ diverges (See *Figure 4.9.1,2*). The spectral amplification still demonstrates comparatively weak maximum. (Note that as the spectral amplification values are converted into linear scale from the peaks in power spectrum measured in dBm scale. Therefore such an increase of spectral amplification, as in this case, that of 6 units of linear scale corresponds to the increase of the peak value of approximately *8* dB only, whereas, for instance, at the temperature of $\Theta=40$ ℃, spectral amplification reaches the values of 1000 and more.). The dependence of signal-to-noise ratio displays no maximum and becomes monotonically decreasing function of noise intensity. No hysteretic behaviour of the values obtained at increase and decrease of the noise is observed either for spectral amplification or signal-to-noise ratio.

4.3.2 Frequency Scaling

To receive an opportunity of comparative analysis of the results presented above in the dependence of the temperature of the ferroelectric sample, one must consider appropriate form of normalisation, as their values diverge in the great range. By varying the temperature of TGS crystal, one changes the height and form of potential barrier which separates two opposite directions of polarisation. As it has been proved above, stochastic resonance in ferroelectric crystal is accompanied by the process of polarisation switching in coherence with weak periodic modulation established every time when the appropriate noise intensity is added to the sample. It is clear that at low temperatures the sample must be driven by much greater periodic and noisy signals to reveal stochastic resonance effect than at temperatures close to the phase transition point where domain structure becomes very sensible even to subtle perturbations and potential barrier can be crossed by very low amplitudes of the external signal already.

Having this in mind, it is necessary to establish an adequate ratio between the value of modulation signal and the height of potential barrier relevant for all temperatures, which would allow to investigate the influence of the barrier height on the stochastic resonance observables, with the rest of experimental parameters being kept constant.

Therefore to perform measurements of signal-to-noise ratio and spectral amplification in dependence on temperature of the sample, the value of modulation amplitude was set such as to obtain the same initial peak level of the first harmonic measured on the system amplitude in the absence of noise for each temperature. This value of modulation amplitude should have not sufficed though to produce polarisation switching of ferroelectric sample, as this is considered to be one of the initial general requirements for classic stochastic resonance. For the sake of the measurement convenience the peak value of the first harmonic was adjusted to $P= -30\ dBm$. The frequency of modulation signal was set to $f=10\ kHz$. Then the cycle of noise variation was performed for each temperature. The results of this measurement are presented on *Figures 4.10.1-4.10.2*. As it can be seen, the values of the modulation amplitude which produce the same first harmonic in the system response differ in two orders of magnitude, being $U_G=6$ and $U_G= 0.28$ V_{RMS} for temperatures $\Theta=45\ °C$ and $\Theta=47.5$ °C respectively.

The values of spectral amplification, measured at increase and decrease of the noise are shown on *Figure 4.10.1.a)* and *b)* respectively for three different temperatures.

It can be seen that with the decrease of the temperature of the measurement that: 1) the threshold value of noise intensity which "triggers" stochastic resonance increases, 2) the maximum value of spectral amplification achieved by the increase of the noise grows and 3) its position shifts toward higher noise intensities. At the decrease of the noise, while the system behaviour still holds true for the above said features, the hysteresis of the spectral amplification values and noise intensities which maximise them is developed as the temperature of the measurements is reduced. At the temperature of $\Theta=47.5\ °C$ which is close to the phase transition of ferroelectric TGS there is no difference in the values measured for the decrease and increase of the noise. At the temperature of $\Theta=45\ °C$ the maximum of spectral amplification observed at the decrease of the noise exceeds that obtained at the increase for about *30%*, with hysteresis of corresponding noise intensities of about $2V_{RMS}$. As the temperature is reduced to *40 °C*, the value of hysteresis grows enormously, reaching at the decrease of the noise over 1000% enhancement of spectral amplification values, while the hysteresis of the noise intensities is spread over more than half of the noise values scale.

The behaviour of signal-to-noise ratio in dependence on the temperature of the ferroelectric sample changes as follows at the increase of the noise. Starting in the same point for all three investigated temperatures due to the measurement condition concerning the equal output power of the periodic component of the system response measured in the absence of noise, the signal-to noise ratio displays local minimum followed by rapid growth of measured values and decays again at the further increase of the noise intensity for the temperatures of the ferroelectric sample $\Theta=40\ °C$ and $\Theta=45\ °C$. The position of the local minimum as mentioned above corresponds to the drastic growth of related spectral amplification dependence and manifests the point where the synchronisation is triggered.

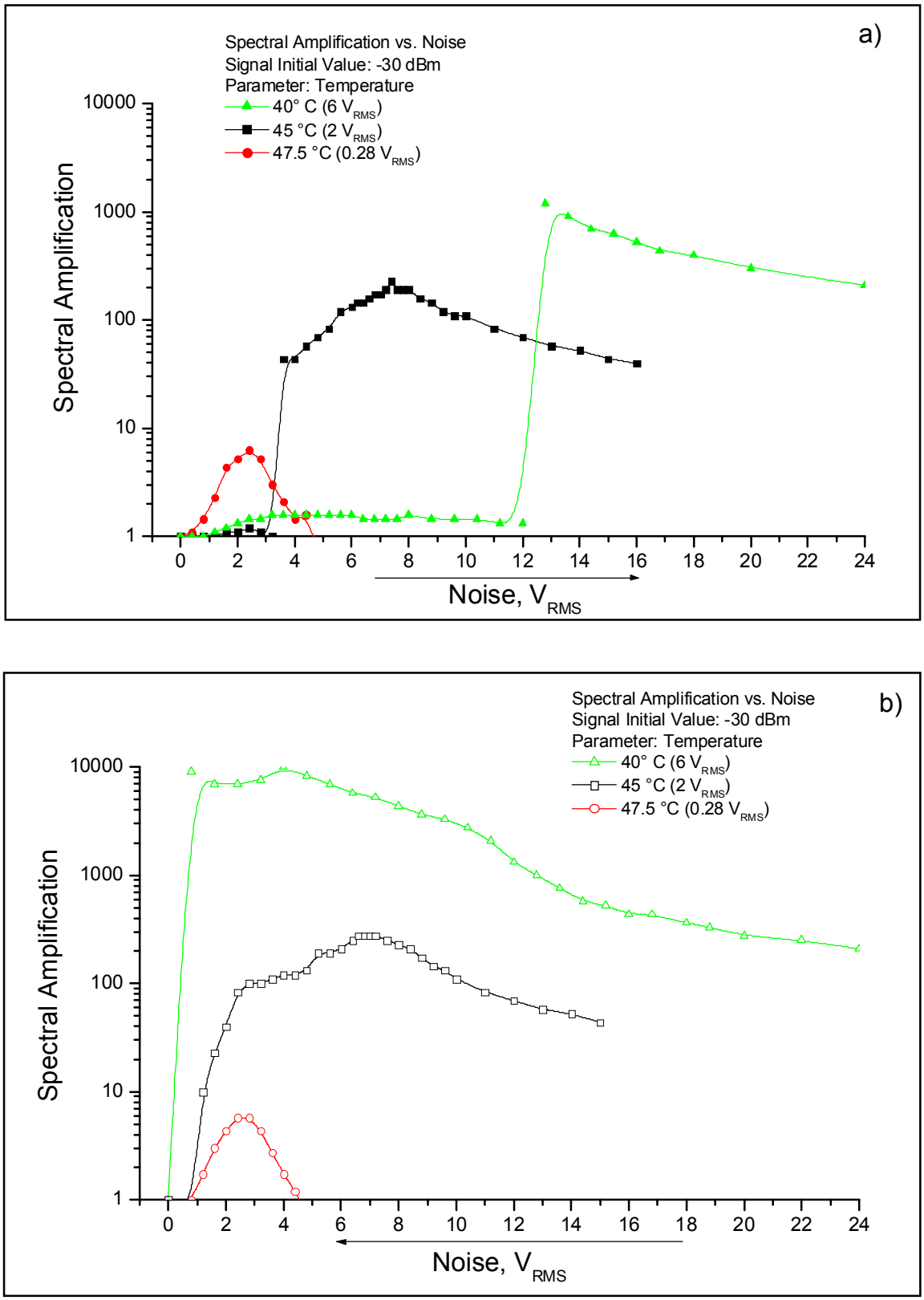

Figure 4.10.1 *Dependences of spectral amplification vs. noise intensity measured for three different temperatures of the TGS sample at the same initial 1st harmonic peak level of P=-30 dBm at the* ***a****) increase and* ***b****) decrease of the noise intensity respectively*

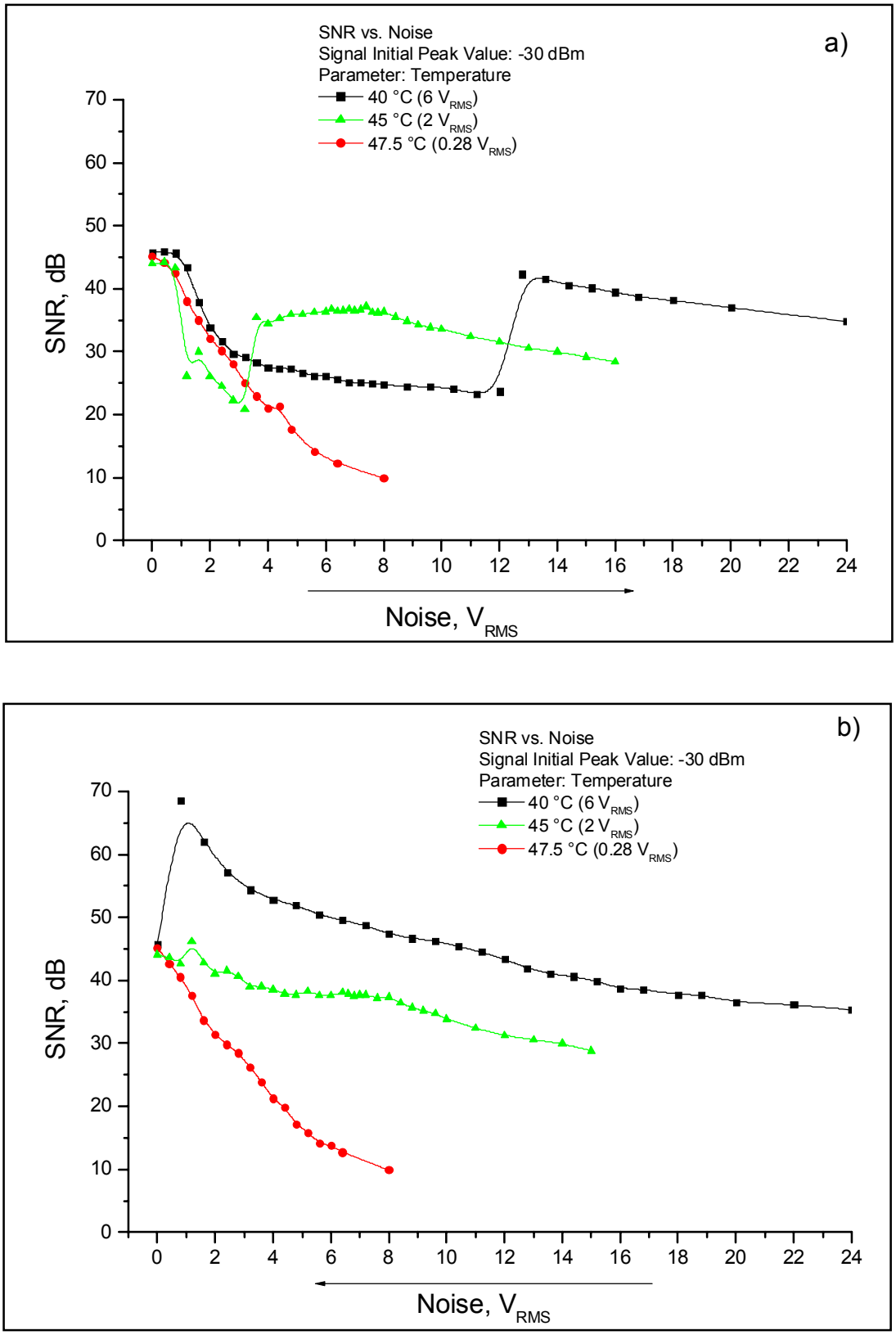

Figure 4.10.2 *Dependencies of signal-to-noise ratio vs. noise intensity measured for three different temperatures of the TGS sample at the same initial 1st harmonic peak level of P=-30 dBm at the* ***a****) increase and* ***b****) decrease of the noise intensity respectively*

In accordance with spectral amplification values, the position of local minimum shifts toward greater noise intensities with the decrease of the temperature of the measurement, and the relative value of the minimum (i.e., the difference between initial and minimal value) decreases. The position of the maximum of signal-to noise ratio dependence shifts towards lower noise intensities at the increase of the temperature, and the value of maximum achieved at the noise variation decreases. On the contrary to the dependencies obtained at the temperatures of $\Theta=40\ ^{\circ}C$ and $45\ ^{\circ}C$ (i.e., relatively far from the phase transition point) the signal-to-noise ratio registered at $\Theta=47.5\ ^{\circ}C$ displays no resonance-like behaviour being a monotonically decreasing function of the noise intensity.

At the decrease of the noise from high values back to zero, the dependencies of signal-to noise ratio measured at $\Theta=40\ ^{\circ}C$ and $45\ ^{\circ}C$ display large hysteresis for both noise intensity and SNR scales in respect to the values registered at the increase of the noise. The hysteresis of the signal-to noise ratio is much pronounced than that of the spectral amplification due to the absence of local minimum of SNR at the decrease of the noise intensity. The value of hysteresis decreases with the increase of the measurement temperature. At the temperature of $\Theta=47.5\ ^{\circ}C$ the hysteresis diminishes as the dependence of signal-to-noise ratio measured at the decrease of the noise completely reproduces that obtained at the increase, and also displays only a monotonic decay as a function of noise intensity.

4.3.3 Discussion

As it follows from the comparative analysis of the behaviour of stochastic resonance observables at different temperatures of the ferroelectric sample, the obtained results appear to be in accordance with the behaviour of corresponding properties of ferroelectric TGS crystal in dependence on temperature. Here we outline the basic features concerning the system behaviour. Clearly, at lower temperatures far enough from the Curie point comparatively high values of both noise intensity and amplitude of the weak periodic modulation are needed to produce the synchronisation between periodic input and system response and subsequently the effect of stochastic resonance. At lower temperatures, according to the known temperature dependencies of spontaneous polarisation and dielectric losses of TGS, subject to the coupled action of periodic modulation and noise, the system delivers also higher values of periodic component of the output signal, taking into consideration the proposed method of scaling. With the decrease of the value of spontaneous polarisation at the temperature increase and simultaneous growth of the dielectric constant, the optimisation of the output signal takes place at the lower noise intensities, as the sensitivity of the sample to the external perturbations is increased. The higher is the temperature, the lower are values of the related measures, both of them being defined by the value of polarisation of the sample.

The observed behaviour confirms the proposal made in Section 3.5 in relation to the frequency scaling property as featured in theoretical approach describing stochastic resonance in continuos bistable systems. As one can see, the behaviour of the stochastic resonance characteristics displayed at the variation of the temperature of the measurement and that of the frequency of weak periodic modulation is qualitatively similar (compare *Figures 4.4,5* and *4.10.1,2*). According to the expressions for the scaled frequency given in chapter three (see eq. (3.19)), seen purely mathematically, the variation of the frequency of the modulation can be „achieved“ either by changing directly the frequency of the external periodic signal or the parameter a of the potential barrier, i.e. the barrier height since $\Delta V = a^2 / 4b$ (see Section 3.4.). In the last case, the potential barrier height is controlled through the temperature of the ferroelectric sample. Corresponding real physical picture may be understood as follows. As well as the increase of the frequency of the modulation signal, the increase of the temperature of the sample (granted the other system parameters are kept constant) affects the motions taking place within the system. As long as the frequency of modulation controls only the velocity of barrier tilting, i.e., acts as an external clock in the system, the variation of the temperature, e.g., increase, leads to 1) the decrease of the potential barrier height which results directly in the increase of the noise-dependent probability for the system to switch between metastable states of polarisation and 2) the increase of the thermal energy of fluctuations within one stable state, i.e., intrawell dynamics contribution.

Therefore the increase of the temperature of the ferroelectric sample at the constant given frequency and amplitude of the modulation will inevitably result in the relative decrease of the periodic component of the system response, as it is shown in presented experimental results, since, on one hand, increased probability to switch will though actualise coherent switching already at lower noise levels, on the other hand, fewer ferroelectric domains find time to switch in phase with external modulation, being permanently switched out of coherence with periodic signal many times during half modulation period. At the temperatures high enough, the potential barrier becomes such low, that it is hardly possible to separate intensive intrawell motion around one stable state from the barrier crossing events taking place at random, which leads to the increase of the actual noise level of the system without contributing to the periodic component of the system output, and as a result of such to the overall decline of signal-to-noise ratio. It is then no longer possible to establish stochastic resonance in the system.

Similarity of the system behaviour at the variation of frequency and temperature, including the disappearance of the stochastic resonance at either high frequencies of modulation or the temperatures of the ferroelectric sample underpins the *statistical* nature of the effect, which is a result of coherent action of noise and periodic components of the system motion, established through the *competition* between characteristic system time scales.

Chapter Five

Conclusions and Outlook

Present work is dedicated to the investigation of the stochastic resonance in ferroelectric TGS. According to the purpose of study outlined in the Introduction, the effect of stochastic resonance has been established in the experimental system with a ferroelectric crystal. Thorough characterisation of the properties of the effect has been conducted for the possible range of parameter variation. It has been checked as well, whether theoretical conceptions developed in the framework of a general theoretical approach for a wide class of continuos bistable systems can be considered valid in the concrete case of ferroelectric crystal as a system displaying stochastic resonance behaviour in the view of the fundamental character of the effect.

Theoretical reasoning for the principle possibility to observe stochastic resonance in ferroelectrics is given in Chapter 3. After introducing the common definition, the basic underlying physical mechanisms along with the methods of the characterisation of the effect are presented. It is shown that stochastic resonance represents a fundamental effect, which is a distinctive characteristic feature of the nonlinear systems independent on their physical nature, where the time scales determining the system behaviour can be controlled through the use of noise. Therefore the theoretical conceptions considering stochastic resonance are based on the corresponding universal properties of nonlinear systems. The theoretical description of the stochastic resonance developed in the framework of Fokker-Planck approach for continuos bistable system presented in Chapter 3 is valid for a wide class of nonlinear systems and can be successfully applied in the particular case of ferroelectric material. Although the theoretical considerations bear rather general character, they allow for accurate predictions

concerning stochastic resonance behaviour in concrete system under investigation in spite of the absence of the special theory of stochastic resonance in ferroelectrics but due to the generality of this phenomenon. Main features of the stochastic resonance to be expected in the experimental study, as resulted from the presented theoretical consideration can be summarised as follows:

- The stochastic resonance appears as an effect of synchronisation between weak input periodic modulation and noisy system output resulting in the enhancement of the periodic component of the system response.

- The corresponding measures of the output signal optimisation such as spectral amplification and signal-to-noise ratio undergo pronounced resonance-like dependence as a function of the input noise intensity. The values of noise which maximise the response amplitude (that stands for amplification) and SNR do not coincide.

- The dependences of both stochastic resonance quantifiers on the amplitude of the periodic modulation are characterised by the increase of the maximum values of the amplification and signal-to-noise ratio at the increase of the amplitude. At the same time, the positions of corresponding maximum values on the noise intensity scale shift toward lower noise levels.

- The spectral amplification reaches greater values when registered at lower frequencies of the periodic modulation, with corresponding maximum amplification being achieved by smaller noise intensities. The Signal-to-noise ratio displays no significant frequency dependence of the position of its maximum values on the modulation frequency. For high modulation frequencies, the local maximum of SNR diminishes and the dependence degenerates into monotonically decreasing function. It should be stressed that at the *direct* continuous variation of the frequency of the periodic modulation, despite obvious enhancement of the amplitude-frequency characteristic of the system in the low frequency range, both stochastic resonance observables display *no resonant-like behaviour* but become *monotonically decreasing* functions of the noise intensity. This property underlines the fact that stochastic resonance is not a bona fide resonance in the original sense.

- The scaling of the modulation frequency among other system quantities over the parameters of the potential performed in the theoretical consideration correlates with the possibility to control the velocities of the processes taking place in the system not only by direct variation of the frequency of the modulation signal but changing the height of the potential barrier, e.g. by the variation of the temperature. As it follows from theoretical

assumptions, corresponding stochastic resonance behaviour should be qualitatively similar to that displayed for different frequency regimes.

These general predictions proved for the wide range of system variables in the series of numerical simulations allow for the comparative analysis of theoretical assumptions and the experimental results obtained for the characterisation of the stochastic resonance in ferroelectrics. The measurement set-up provides the experimental realisation of the requirements for stochastic resonance onset and attains the possibility of the investigation of the effect properties over the wide range of system parameters. The description of the properties and design of the experimental set-up is given in Chapter 2.
The results of the experimental study of the stochastic resonance in ferroelectric TGS crystal, presented in Chapter 4 allow for the following conclusions. The stochastic resonance in ferroelectric TGS appears as a result of (partial) polarisation reversal with the frequency of the weak external modulation signal produced by synchronised action of noise and periodic modulation. The behaviour of the effect measures (i.e. spectral amplification and signal-to-noise ratio) observed in the course of investigations shows very good qualitative agreement with theoretical predictions concerning stochastic resonance properties in dependence on the system parameters as outlined above. Hence the fundamental character of the stochastic resonance as an effect typical for nonlinear system for which the characteristic time scales can be controlled by means of noise is confirmed. Hereby the theoretical conceptions developed for wide class of continuous bistable systems in the framework of general Fokker-Planck approach using universal model assumptions are proved to be valid in the concrete case of ferroelectric material as a system displaying stochastic resonance behaviour. Obtained results of present experimental research admit to conclude that the purposes of this study, i.e., establishment and subsequent characterisation of the stochastic resonance in ferroelectric TGS crystal are successfully achieved.

5.1 Outlook

There is, of course, no need to mention that the study of stochastic resonance in ferroelectrics as presented in this work is yet far from being complete. The performed course of measurements has revealed important issues which appeal for further investigation. In particular, the hysteretic behaviour of the stochastic resonance observables upon the reversal of the direction of noise variation requires prompt attention. Clearly, this new feature of the stochastic resonance, which has not been reported to be observed in other systems and appears to be a specific property of the effect in ferroelectrics is connected directly with the alteration of the domain structure of ferroelectric material as the system goes along the process of the stochastic resonance. Therefore it provides the opportunity to apply a new investigation

technique to the study of ferroelectric domain structure which might bring new and promising results to this complicated matter. Another interesting possibility would be, for instance, to try to extract the information on the thermodynamic potential of the ferroelectric contained in the time series of the output signal since it may result in developing the additional tool in the modelling of the stochastic resonance signatures as well as processes of the polarisation reversal of the ferroelectric itself which still remains an open question.

The results of the conducted investigations confirm the proposal made in the Introduction in relation to the possibility to use presented system with ferroelectric crystal as a model system for experimental study of stochastic resonance. Within the proposed experimental set-up this elegant phenomenon can be realised with delectable convenience in different configurations. It is, for example, of great interest to establish so-called *controlled* stochastic resonance [34], using periodic modulation of the internal system parameters, which delivers much higher signal enhancement and therefore could become very useful in the exploration of weak signals. As the experimental system under consideration can be easily transferred into the nonlinear resonance circuit displaying chaotic behaviour, it is very tempting to discover experimentally stochastic resonance behaviour in the deterministic chaotic system [19,28,32] to provide important empirical information to the understanding of, on one hand, the nature of the effect in this advanced application. On another hand, this would give an insight into the fascinating process of the chaotic oscillations [49] which alone stand for very promising field of research. Besides, the above mentioned proposals while not exhausting the multiple opportunities of study, will contribute to the investigation of the properties of ferroelectric materials, such as domain wall motion, behaviour of the spontaneous polarisation etc., since ferroelectrics serve as a core elements of the described experimental circuits responsible for the system behaviour.

References

1. *R. Benzi, A. Sutera and A. Vulpiani:* "THE MECHANISM OF STOCHASTIC RESONANCE" J. Phys. A: Math. Gen.14L 453, 1981

2. *R. Benzi, G. Parisi, A. Sutera and A. Vulpiani* "STOCHASTIC RESONANCE IN CLIMATIC CHANGE", Tellus, 34,10, 1982

3. *C.Nicolis:* "STOCHASTIC ASPECTS OF CLIMATIC TRANSITIONS - RESPONSE TO A PERIODIC FORCING" Tellus 34, 1, 1982

4. *S. Fauve and F. Heslot:* "STOCHASTIC RESONANCE IN A BISTABLE SYSTEM" Phys. Lett. 97A, 5, 1983

5. *B. McNamara, K. Wiesenfeld and R. Roy:* "OBSERVATION OF STOCHASTIC RESONANCE IN A RING LASER" Phys. Rev. Lett. 60, 2626, 1988

6. *L. Gammaitoni, F. Marchesoni, E. Menichella-Saetta and S. Santucci* "STOCHASTIC RESONANCE IN A BISTABLE SYSTEMS" Phys. Rev. Lett. 62 349 (1989)

7. *B. McNamara and K. Wiesenfeld:* "THEORY OF STOCHASTIC RESONANCE" Phys. Rev. A39 4854 (1989)

8. *P. Jung and P. Hanggi:* "STOCHASTIC NONLINEAR DYNAMICS MODULATED BY EXTERNAL PERIODIC FORCES" Europhys. Lett. 8, 505, 1989

9. *R. F. Fox:* "STOCHASTIC RESONANCE IN A DOUBLE WELL" Phys. Rev. 39A, 4148 (1989)

10. G. *Vemuri and R. Roy:* "STOCHASTIC RESONANCE IN A BISTABLE RING LASER" Phys. Rev. 39A, 4668, 1989

11. *L. Gammaitoni, E. Menichella-Saetta, S. Santucci, F. Marchesoni and C. Presilla:* "PERIODICALLY MODULATED BISTABLE SYSTEMS: STOCHASTIC RESONANCE", Phys. Rev. 40A, 2114, 1989

12. *L. Gammaitoni, F. Marchesoni, E. Menichella-Saetta, M. Punturo and S. Santucci:* "STOCHASTIC RESONANCE: PHENOMENOLOGY AND APPLICATIONS" Non-Equilibrium Statistical Mechanics, World Scientific ed. (1989)

13. *P. Jung and P. Hanggi:* "AMPLIFICATION OF SMALL SIGNALS VIA STOCHASTIC RESONANCE" , Phys. Rev. A44 8032 (1991)

14. *R. F. Fox and Y. Lu:* "ANALYTIC AND NUMERICAL STUDY OF STOCHASTIC RESONANCE" Phys. Rev. E48 3390 (1993)

15. *P. Jung:* "PERIODICALLY DRIVEN STOCHASTIC SYSTEMS", Phys.Rept. 234, 175 (1993)

16. *F. Moss, D. Pierson, D. O'Gorman:* "STOCHASTIC RESONANCE: TUTORIAL AND UPDATE" Int. J. Bifurcation and Chaos 4(6) 1383. [1994]

17. *S. Vohra, L. Fabiny:* "INDUCED STOCHASTIC RESONANCE NEAR A SUBCRITICAL BIFURCATION", Phys. Rev. E50 R2391 (1994)

18. *D.S. Leonard, L.E. Reichl:* "STOCHASTIC RESONANCE IN A CHEMICAL REACTION" Phys. Rev. E49 1734 (1994)

19. *A. Crisanti, M. Falcioni, G. Paladin and A. Vulpiani:* "STOCHASTIC RESONANCE IN DETERMINISTIC CHAOTIC SYSTEMS", J. Phys. A: Math. Gen. 27 L597 (1994)

20. *M.C. Mahato and S.R. Shenoy:* "HYSTERESIS LOSS AND STOCHASTIC RESONANCE: A NUMERICAL STUDY OF A DOUBLE-WELL POTENTIAL", Phys. Rev. E 50, 2503 (1994)

21. *T. Kapitaniak:* "MECHANISM OF NOISE-INDUCED RESONANCE", Physical Review E. 52(1 Part B):1200-1201, 1995 Jul.

22. *L. Gammaitoni, F. Marchesoni and S. Santucci:* "STOCHASTIC RESONANCE AS A BONA FIDE RESONANCE", Phys. Rev. Lett. 74 1052 (1995).

23. *B. Shulgin, A. Neiman, V. Anishchenko:* "MEAN SWITCHING FREQUENCY LOCKING IN STOCHASTIC BISTABLE SYSTEM DRIVEN BY A PERIODIC FORCE", Phys. Rev. Lett. 75, 4157, (1995)

24. *A. Hilgers, M Gremm, J. Schnakenberg:* "A CRITERION FOR STOCHASTIC RESONANCE", Phys. Lett. A 209 313 (1995)

25. *Dubinov A.E., Mikheev K.E., Nizhegorodtsev Y.B., Selemir V.D.:* "ON THE STOCHASTIC RESONANCE IN FERROELECTRICS", Izvestiya Akademii Nauk Seriya Fizicheskaya. 60(10):76-77, 1996 Oct.

26. *Collins J., Chow C., Capela AC., Imhoff T.T.:* "APERIODIC STOCHASTIC RESONANCE", Physical Review A. 54(5):5575-5584, 1996 Nov.

27. *Simonotto E., Riani M., Seife C., Roberts M., Twitty J., Moss F.:* "VISUAL PERCEPTION OF STOCHASTIC RESONANCE", Physical Review Letters. 78(6):1186-1189, 1997 Feb 10.

28. *F. Gassmann:* "NOISE-INDUCED CHAOS-ORDER TRANSITIONS", Physical Review E. 55(3 Part A):2215-2221, 1997 Mar.

29. *Sides SW. Ramos RA. Rikvold PA. Novotny MA.:* "KINETIC ISING SYSTEM IN AN OSCILLATING EXTERNAL FIELD − STOCHASTIC RESONANCE AND RESIDENCE TIME DESTRIBUTIONS"Journal of Applied Physics. 81(8 Part 2B):5597-5599, 1997 Apr 15.

30. *Mahato MC., Jayannavar AM.:* "RELATION BETWEEN STOCHASTIC RESONANCE AND SYNCHRONIZATION OF PASSAGES IN A DOUBLE WELL SYSTEM", Physical Review E. 55(5 Part B):6266-6269, 1997 May.

31. *Bose D., Sarkar SK.:* "NOISY BISTABLE HYSTERESIS WITH MODULATION OF LARGE AMPLITUDE AND HIGH FREQUENCY", Physics Letters A. 232(1-2):49-54, 1997 Jul 21.

32. *Neiman A.., Saparin P.I., Stone L..:* "COHERENCE RESONANCE AT NOISY PRECURSORS OF BIFURCATIONS IN NONLINEAR DYNAMICAL SYSTEMS", Physical Review E. 56(1 Part A):270-273, 1997 Jul.

33. *Mahato M.C., Jayannavar A.M.:* "TWO-WELL SYSTEM UNDER LARGE AMPLITUDE PERIODIC FORCING − STOCHASTIC SYNCHRONIZATION, STOCHASTIC RESONANCE AND STABILITY", Modern Physics Letters B. 11(19):815-820, 1997 Aug 20.

34. *Gammaitoni L., Hanggi P., Jung P. Marchesoni F.:* "STOCHASTIC RESONANCE" [Review], Reviews of Modern Physics. 70(1):223-287, 1998 Jan.

35. *Mahato M.C., Jayannavar A.M.:* "SOME STOCHASTIC PHENOMENA IN A DRIVEN DOUBLE-WELL SYSTEM", Physica A. 248(1-2):138-154, 1998 Jan 1.

36. *Hess S.M., Albano A.M.:* "MINIMUM REQUIREMENTS FOR STOCHASTIC RESONANCE IN THRESHOLD SYSTEMS", International Journal Of Bifurcations And Chaos, 8(2):395-400, 1998 Feb.

37. *Godivier X., Chapeaublondeau F.:* "STOCHASTIC RESONANCE IN THE INFORMATION CAPACITY OF A NONLINEAR DYNAMIC SYSTEM", International Journal Of Bifurcations And Chaos, 8(3):581-589, 1998 Mar.

38. *Tretyakov M.V.:* "NUMERICAL TECHNIQUE FOR STUDYING STOCHASTIC RESONANCE", Physical Review A. 57(4):4789-4794, 1998 Apr

39. Fakir R.: "NONSTATIONARY STOCHASTIC RESONANCE", Physical Review A. 57(6):6996-7001, 1998 Jun.

40. *Sides S.W., Rikvold P.A., Novotny M.A.:* "STOCHASTIC HYSTERESIS AND RESONANCE IN A KINETIC ISING SYSTEM", Physical Review A. 57(6):6512-6533, 1998 Jun.

41. *Galdi V., Pierro V., Pinto I.M.:* "EVALUATION OF STOCHASTIC RESONANCE-BASED DETECTORS OF WEAK HARMONIC SIGNALS IN ADDITIVE WHITE GAUSSIAN NOISE", Physical Review A. 57(6):6470-6479, 1998 Jun.

42. *Choi M.H., Fox R.F., Jung P.:* "QUANTIFYING STOCHASTIC RESONANCE IN BISTABLE SYSTEMS – RESPONSE VS. RESIDENCE TIME DISTRIBUTION FUNCTIONS", Physical Review A. 57(6):6335-6344, 1998 Jun.

43. *Kim Y.W., Sung W.:* "DOES STOCHASTIC RESONANCE OCCUR IN PERIODIC POTENTIALS", Physical Review A. 57(6):R6237-R6240, 1998 Jun.

44. *V.S. Anishenko, A.B. Neiman, F.Moss, L.Shimansky-Geier:* "STOCHASTIC RESONANCE: NOISE ENHANCED ORDER", Uspehi Fizicheskih Nauk 169 (1), 1999 Jan (In Russian)

45. *Yu. L. Klimontovich:* "WHAT ARE STOCHASTIC FILTRATION AND STOCHASTIC RESONANCE", Uspehi Fizicheskih Nauk 169 (1), 1999 Jan (In Russian)

46. *R.-P. Kapsch:* "UNTERUCHUNGEN DES EINFLUSSES SCHWACHER, FAST RESONANTER BZW. RESONANTER STÖRUNGEN AUF NICHTLINEARE DYNAMISCHE SYSTEME AM BEISPIEL DES DIELEKTRISCH NICHTLINEAREN SCHWINGKREISES", Ph.D thesis, Halle 1994

47. *R-P. Kapsch, M. Diestelhorst, H. Beige:* "SMALL SIGNAL AMPLIFICATION CAUSED BY THE NONLINEAR DIELECTRIC PROPERTIES OF TGS", Ferroelectrics, Vols.208-209, 1998

48. *M. Diestelhorst, K. Drozhdin:* "STOCHASTIC RESONANCE IN FERROELECTRIC TRIGLYCINE SULFATE", Ferroelectrics, Vol.238, 2000

49. *H. Beige, M. Diestelhorst, R. Forster, T. Krietsch*: "CHAOS NEAR STRUCTURAL PHASE TRANSITIONS", Phase transitions 37, 1992, 213

50. *M.E. Lines, A.M. Glass:* "PRINCIPLES AND APPLICATIONS OF FERROELECTRICS AND RELATED MATERIALS", Clarendon Press Oxford 1977

51. *J.C. Burfoot:* "FERROELECTRICS. AN INTRODUCTION TO THE PHYSICAL PRINCIPLES", Princeton 1967

52. *B.A. Strukov, A.P. Levaniuk:* "PHYSICAL PRINCIPLES OF THE FERROELECTRICITY IN CRYSTALS", Moscow, 1983 (in Russian)

53. *M. Diestelhorst.* Personal remarks

54. *Gammaitoni et al.*, http://www.pg.infn.it/sr/

An dieser Stelle möchte ich allen zum Entstehen dieser Arbeit beigetragenen Personen meinen herzlichen Dank aussprechen.
Besonders danke ich Herrn Dr. M. Diestelhorst, für die mir erwiesene Ehre, mein Freund und Mentor zu sein, für seine Engelsgeduld und Teufelsakribie und für Spaß, das mir Physik - teilweise nur seiner Bemühungen wegen, - machte.
Den Kollegen der Fachgruppe „Nichtlineare Dynamik/Ferroelektrizität“ – besonders den Herrn Dr. R.-P. Kapsch, A. Tille, E. Fuchs, – danke ich für ihre Hilfe, und vor allem für die freundliche und offene Atmosphäre, in der die Zeit lustig und unbemerkt verflog.
Ich danke Herrn Prof. Dr. H. Beige für die Möglichkeit, in der Fachgruppe „Nichtlineare Dynamik/Ferroelektrizität“ des Fachbereiches Physik der Martin-Luther-Universität Halle-Wittenberg zu promovieren.
Herrn Dr. D. Lorenz danke ich für die Freundschaft,
und meinen Eltern – für Alles.

Konstantin Drozhdin

Ich versichere, daß ich die vorliegende Arbeit selbständig angefertigt habe. Ich habe keine anderen Quellen und Hilfsmittel als die angegebenen benutzt und den benutzten Werken inhaltlich oder wörtlich entnommene Stellen als solche gekennzeichnet.

Konstantin Drozhdin

Halle, den 28.11.2001

Lebenslauf

Name:	Konstantin Drozhdin
geboren:	12. Juli 1973 in Woronesh

Ausbildung:

1980-1990	Schulausbildung an der 58sten Oberschule in Woronesh mit Spezialisierung für Mathematik und Physik
1990-1996	Studium der Physik an der physikalischen Fakultät der Saatsuniversität zu Woronesh
1997-2000	Doktorand in der Fachgruppe „Nichtlineare Dynamik/Ferroelektrizität“ an der Martin-Luther-Universität Halle-Wittenberg

Konstantin Drozhdin